

FMH606 Master's Thesis 2024

Modeling and simulation of oil recovery through advanced multi-lateral wells with CO₂-WAG injection

Ismail Hossain Rafi

Faculty of Technology, Natural sciences and Maritime Sciences
Campus Porsgrunn

Course: FMH606 Master's Thesis, 2024

Title: Modeling and simulation of oil recovery through advanced multi-lateral wells with CO₂-WAG injection.

Number of pages: 96

Keywords: Enhanced oil recovery, advanced multi-lateral well, OLGA, ECLIPSE, WAG injection, CO₂-WAG injection, Algebraic controller.

Thesis ID: MT-03-24

Participant: Ismail Hossain Rafi

Supervisors: Britt M. E. Moldestad and Ali Moradi

Project partner: Equinor and SINTEF

Summary:

The oil industry has been an important source of conventional energy. The enhanced oil recovery (EOR) method is one of the most efficient methods in the oil recovery process. Using an advanced multi-lateral well model in the oil recovery process created an exceptional benchmark. In this study, simulation was conducted for both the WAG injection and CO₂-WAG injection using FCDs in an advanced horizontal well in the OLGA and ECLIPSE simulator. CO₂-WAG injection has a better oil production rate than WAG injection because of the miscibility characteristics of CO₂ with oil. CO₂-WAG injection can be simulated only for advanced horizontal wells in the ECLIPSE simulator by the solvent model. The solvent model can not be used for the multisegment well model.

Preventing early water and gas breakthroughs is challenging in the oil recovery process. To overcome this issue inflow control technologies like ICD, AICD, and AICV are introduced. This study result showed that AICD and AICV have a better choking effect on low viscous fluids like water and gas delaying their early breakthrough in the pipe. Before the water breakthrough, the AICD and AICV valve was fully opened for oil production. A new mathematical model was implemented in the algebraic controller to control the valve opening of AICD. AICD valve opening gets closed better with the increasing rate of water cut.

Optimizing the water/CO₂ injection ratio for the CO₂-WAG injection EOR is also an important factor for better oil recovery. In this study, CO₂-WAG injection EOR was simulated for several water/CO₂ injection ratios and the result showed the ratio of 1.5 has the optimum oil production considering the water production as well. In conclusion, the CO₂-WAG injection and the WAG injection EOR are successfully simulated for both the advanced horizontal well and the multi-lateral well using the inflow control devices in the OLGA and ECLIPSE simulator.

Preface

This report presents the master's thesis conducted during the spring of 2024 at the University of South-Eastern Norway (USN), Porsgrunn, as a requirement for attaining a Master of Science degree at USN.

This work primarily aimed to utilize OLGA and ECLIPSE software to perform simulations of advanced inflow control technologies such as ICD, AICD, and AICV in oil production. This research is part of the ongoing "Digiwell project" conducted in collaboration with Equinor and SINTEF.

Prof. Britt Margrethe Emilie Moldestad and Ph.D. scholar Ali Moradi supervised this work. Their continuous guidance and mentorship significantly enhanced my knowledge and skills throughout the project.

I sincerely thank Prof. Britt M. E. Moldestad and Ali Moradi, who served as my supervisors, for their invaluable time and guidance in evaluating the work and providing valuable advice.

I would also like to thank the dedicated staff at the USN library and the IT department for their consistent assistance whenever needed. Finally, also grateful to Equinor and SINTEF for allowing young professionals to learn and gain knowledge in the industry to shape their future.

Porsgrunn, 15th May 2024

Ismail Hossain Rafi

Contents

1 Introduction	13
1.1 History and Statistics	13
1.2 Modern technology	14
1.3 Task description	15
1.3.1 Objectives	15
1.3.2 Outline	15
2 Literature review	16
2.1 Water-alternating gas (WAG) injection	17
2.2 CO ₂ enhanced oil recovery (EOR).....	17
2.2.1 Miscible CO ₂ -EOR	17
2.2.2 CO ₂ properties for EOR	19
2.2.3 Immiscible CO ₂ -EOR	20
2.3 Advanced well technology	20
2.4 Flow control technology	21
2.4.1 Inflow control device (ICD)	21
2.4.2 Autonomous inflow control device (AICD)	22
2.4.3 Autonomous inflow control valve (AICV)	23
3 Theoretical background	24
3.1 Reservoir rock properties	24
3.1.1 Porosity (ϕ)	24
3.1.2 Permeability (k).....	25
3.1.3 Relative permeability (k_r)	26
3.1.4 Wettability	27
3.1.5 Capillary pressure (P_c)	27
3.1.6 Saturation of fluid	28
3.2 Reservoir fluid properties	28
3.2.1 Classification of crude oil	28
3.2.2 Reservoir fluids	29
3.2.3 Black oil model	29
3.2.4 Gas-oil ratio (GOR)	30
3.2.5 Water cut (WC)	30
3.3 Mathematical models for inflow control devices.....	31
3.3.1 Passive inflow control device (ICD)	31
3.3.2 Autonomous inflow control device (AICD)	31
3.3.3 Valve opening control with Algebraic controller for AICD	31
3.3.4 Autonomous inflow control valve (AICV)	33
3.4 Multisegment well model	34
3.5 Solvent model	35
3.5.1 Todd-Longstaff model	35
4 Development of the OLGA/ECLIPSE model	37
4.1 Well model in OLGA	37
4.1.1 Flow component set-up	38
4.1.2 Case definition	39
4.1.3 Compositional setup	40
4.2 Reservoir model in ECLIPSE	40

4.2.1 PUNQ-S3 reservoir model construction	40
4.2.2 PUNQ-S3 reservoir rock and fluid properties	41
4.2.3 Water and CO ₂ injection	42
4.2.4 PUNQ-S3 reservoir permeability.....	43
4.2.5 Initial conditions	43
4.3 Multisegment well model in ECLIPSE	44
5 Results and discussion	45
5.1 Horizontal well with FCDs in OLGA and ECLIPSE	45
5.1.1 Oil production	45
5.1.2 Water production.....	46
5.1.3 Liquid production	47
5.1.4 Water cut variations	49
5.1.5 Performance analysis of algebraic controller for AICD.....	49
5.1.6 Fluid and gas saturations.....	51
5.2 CO ₂ -WAG vs WAG	53
5.2.1 Oil production	53
5.2.2 Water production.....	54
5.2.3 Water cut and GOR	55
5.3 Multilateral wells with different FCDs	56
5.3.1 Oil production	56
5.3.2 Water production.....	56
5.3.3 Water cut	57
5.4 Water/CO ₂ injection ratio for CO ₂ -WAG injection	58
5.5 Discussion.....	60
5.5.1 Simulation in OLGA/ECLIPSE	60
5.5.2 Simulation in ECLIPSE	60
5.5.3 Future task recommendation	61
6 Conclusion.....	62
References.....	63
Appendix A: Thesis task description	68
Appendix B: ECLIPSE data file for PUNQ-S3 reservoir model.....	71
Appendix C: Known variables for algebraic controller.....	95
Appendix D: OLGA model with OPENHOLE/ICD and AICD.....	96

List of Figures

Figure 1.1: Global consumption of gas, coal, and oil	13
Figure 1.2: Global oil consumption by countries from 1965 to 2022.....	13
Figure 1.3: Recovered and expected oil production in Norway	14
Figure 2.1: Classifications of oil recovery methods	16
Figure 2.2: Simple diagram of WAG injection method.....	17
Figure 2.3: Sustainable EOR methods over the period.....	18
Figure 2.4: CO ₂ -WAG injection method	18
Figure 2.5: Density behavior of CO ₂ in different pressure and temperature	19
Figure 2.6: Water and gas breakthrough in heel section.....	20
Figure 2.7: Classification of multi-lateral wells.	21
Figure 2.8: Channel-type ICD with its flow pattern	21
Figure 2.9: Nozzle-type ICD with its flow pattern	21
Figure 2.10: Orifice-type ICD with its flow pattern	22
Figure 2.11: Flow pattern in AICD.....	22
Figure 2.12: AICD mounted on sand screen joints.....	22
Figure 2.13: AICV mounted on a production pipe	23
Figure 2.14: Flow path of oil through AICV	23
Figure 3.1: Rock formation in a reservoir.....	24
Figure 3.2: Types of pores in a reservoir	25
Figure 3.3: Permeability relation with porosity in reservoir.....	25
Figure 3.4: Core sample test for Darcy's law	26
Figure 3.5: Relative permeability curve for water-wet rock (left) and oil-wet rock (right)	27
Figure 3.6: Water wet, mixed-wet and oil wet in pore spaces.....	27
Figure 3.7: Effect of capillary pressure in capillary tubes and porous medium	28
Figure 3.8: Crude oil classification by API gravity	29
Figure 3.9: Phase diagram of Black oil model.....	30
Figure 3.10: Pressure drops in laminar and turbulent flow restrictors.....	33
Figure 3.11: A simple schemetic of a multi-segment well model	34
Figure 3.12: MSW model for an advanced horizontal well.....	35
Figure 3.13: Dispersed zone in a grid block displacing oil by solvent.....	36

Figure 4.1: Cross sectional and side view of a production pipe in annulus.....	37
Figure 4.2: Fluid flow path through reservoir and annulus in a packer	37
Figure 4.3: Schematic of a single zone in a production pipe	38
Figure 4.4: OPENHOLE/ICD (left) and AICD (right) setup in OLGA for a single production zone.....	39
Figure 4.5: PUNQ-S3 reservoir fluid saturation in XY plane	41
Figure 4.6: Positioning of Production pipe and injectors into reservoir.....	42
Figure 4.7: Porosity and permeability in X, Y and Z direction.	43
Figure 4.8: Initial water, oil, and gas saturation in the PUNQ-S3 reservoir.....	44
Figure 5.1: Oil production rate for OPENHOLE, ICD, and AICD.	45
Figure 5.2: Accumulated oil production for OPENHOLE, ICD, and AICD.....	46
Figure 5.3: Water production rate for OPENHOLE, ICD, and AICD.....	46
Figure 5.4: Accumulated water production for OPENHOLE, ICD, and AICD.	47
Figure 5.5: Liquid production rate for OPENHOLE, ICD, and AICD.....	48
Figure 5.6: Accumulated liquid production for OPENHOLE, ICD, and AICD.....	48
Figure 5.7: Water cut in OPENHOLE, ICD, and AICD.....	49
Figure 5.8: Valve opening vs oil volume fraction for the algebraic controller in different phases of fluid.....	50
Figure 5.9: Valve opening with algebraic controller in toe (Controller 18) and heel section (Controller 1).	50
Figure 5.10: Valve opening of the algebraic controller according to GVF.	51
Figure 5.11: Oil saturation for OPENHOLE, ICD, and AICD after 3500 days.	52
Figure 5.12: Water saturation for OPENHOLE, ICD, and AICD after 3500 days.....	52
Figure 5.13: Gas saturation for OPENHOLE, ICD, and AICD after 3500 days.	53
Figure 5.14: Oil production rate and total oil production for CO ₂ -WAG injection and WAG injection.....	54
Figure 5.15: Water production rate and total oil production for CO ₂ -WAG injection and WAG injection.	54
Figure 5.16: Water cut for CO ₂ -WAG injection and WAG injection.....	55
Figure 5.17: GOR for CO ₂ -WAG injection and WAG injection.....	55
Figure 5.18: Oil production rate and total oil production in multi-lateral well for all the FCDs.	56
Figure 5.19: Water production rate and total water production in multi-lateral wells for all the FCDs.	57
Figure 5.20: Water cut for OPENHOLE, ICD, AICD, and AICV in multi-lateral well.....	57

Figure 5.21: Oil production for different water/CO ₂ injection ratios.	58
Figure 5.22: Water production for different water/CO ₂ injection ratios.....	58
Figure 5.23: Error message generated in ECLIPSE.....	60

List of tables

Table 2.1: Properties of CO ₂ in critical condition.....	19
Table 3.1: Classification of reservoir fluid and its characteristics.....	29
Table 4.1: Technical data of the wellbore and the production pipe.	38
Table 4.2: Technical data for OPENHOLE, ICD, and AICD.....	39
Table 4.3: Integration data for simulation in OLGA for OPENHOLE, ICD, and AICD.	39
Table 4.4: Compositional setup in OLGA.	40
Table 4.5: PUNQ-S3 reservoir grid dimensions.	41
Table 4.6: PUNQ-S3 rock and fluid properties	41

Nomenclature

Symbols	Expressions	Unit
Φ	Porosity	%
Q	Volumetric flow rate of water through the medium	m^3/s
V_b	Bulk volume of the reservoir rock	cm^3
V_{gr}	Grain volume	cm^3
V_p	Pore volume	cm^3
A	The cross-sectional area of the core plug	m^2
T	Temperature	$^{\circ}\text{C}$
$\frac{dP}{dL}$	Pressure gradient over the section	Pa/m
μ	Dynamic viscosity	$\text{Pa}\cdot\text{s}$
k_r	Relative permeability	
k_e	Effective permeability	
k	Absolute permeability	d
k_{rw}	Relative permeability of water	
k_{ro}	Relative permeability of oil	
k_{rg}	Relative permeability of gas	
k_{rwcw}	Maximum relative permeability of water	
S_{wc}	Irreducible water saturation	
S_{orw}	Residual oil saturation	
S_w	Water saturation	
S_o	Oil saturation	
S_g	Gas saturation	
S_n	Saturation of nonwetting hydrocarbon	
P_c	Capillary pressure	Pa
P_{nw}	Pressure in non-wetting phase	Pa
P_w	Pressure in wetting phase	Pa
γ_o	The specific gravity of oil	
ρ_o	Oil density	kg/m^3
ρ_w	Water density	kg/m^3

ρ_g	Air density	kg/m^3
V_g	Volume of gas	m^3
V_o	Volume of oil	m^3
\hat{C}_u	Conversion value	
\dot{Q}_o	Volumetric oil flow	m^3/s
\dot{Q}_w	Volumetric water flow	m^3/s
\dot{Q}_g	Volumetric gas flow	m^3/s
\dot{Q}_l	Volumetric liquid flow	m^3/s
ΔP_f	Frictional pressure	Pa
L	Wellbore length	m
ρ	Fluid density	kg/m^3
v	Flow velocity	m/s
d	The diameter of the wellbore pipe	m
μ_m	Mixture effective viscosity	
μ_{oe}	Effective viscosity of oil	
μ_{ge}	Effective viscosity of gas	
ω	Todd-Longstaff mixing parameter	
C_D	Discharge coefficient	
ρ_{mix}	Density of the fluid mixture	kg/m^3
μ_{mix}	Viscosity of the fluid mixture	
α_{oil}	Volume fractions of oil in the fluid mixture	
α_{water}	Volume fractions of water in the fluid mixture	
α_{gas}	Volume fractions of gas in the fluid mixture	
ΔP	Pressure drop over the restrictor	Pa
k	Geometrical constant	

Abbreviations

NCS	Norwegian Continental Shelf
IOR	Improved Oil Recovery
EOR	Enhanced Oil Recovery
AMW	Advanced Multi-lateral Well
FCD	Flow Control Devices
ICD	Inflow Control Devices
AICD	Autonomous Inflow Control Devices
RCP	Rate Controlled Production
AICV	Autonomous Inflow Control Valves
WAG	Water Alternating Gas
GI	Gas Injection
WF	Water Flooding
FWL	Free Water Level
PVT	Pressure-Volume-Temperature
API	American Petroleum Institute
MSW	Multi-Segment Well
GOR	Gas-Oil Ratio
GLR	Gas-Liquid Ratio
WC	Water Cut

1 Introduction

1.1 History and Statistics

The history of oil goes before the modern era when it was used as a material for construction and to light lamps. The very first well oil was drilled in China in 347 AD [1]. From then crude oil became one of the biggest conventional energy sources creating a large business industry. Technological development is continuous for more efficient recovery of crude oil. The first modern oil well was drilled in the year of 1857 in the town of La Brea, Trinidad [2]. Figure 1.1 shows the consumption rate of three major fossil fuels from 1965 to 2022. Oil is one of the most consumed energy sources shown in the chart.

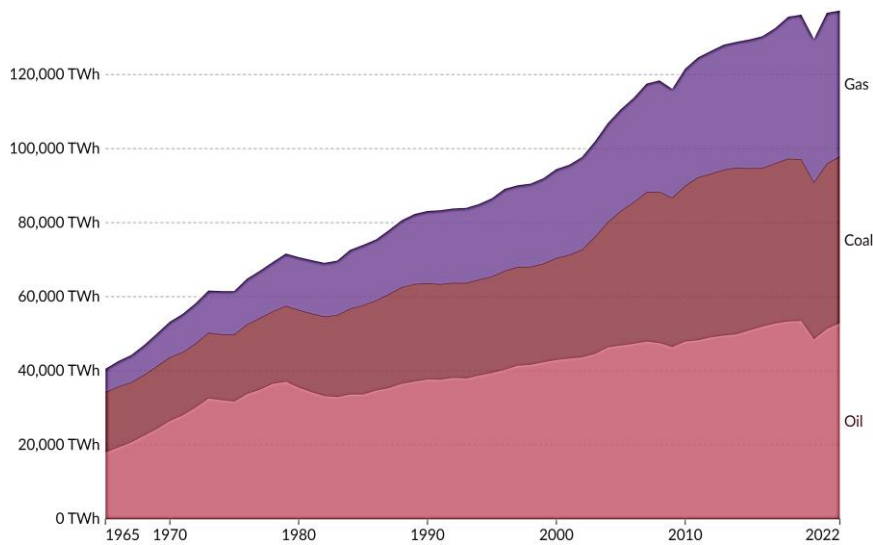


Figure 1.1: Global consumption of gas, coal, and oil [2].

Figure 1.2 shows the global oil consumption rate from 1965 to 2022 in different regions of the world.

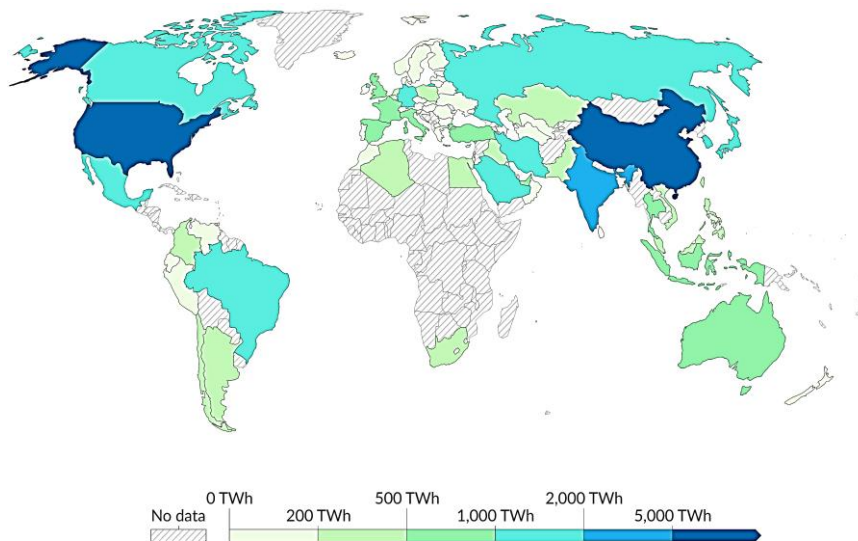


Figure 1.2: Global oil consumption by countries from 1965 to 2022 [2].

Norway is one of the largest oil producers in Europe and in the history of the last 50 years, Norway has produced and sold 55% of the recoverable resources from the Norwegian Continental Shelf (NCS). It also indicates the future potential to produce more oil in the upcoming 50 years [3]. Figure 1.3 shows the history of recovered oil and the expected oil production till 2028 [3].

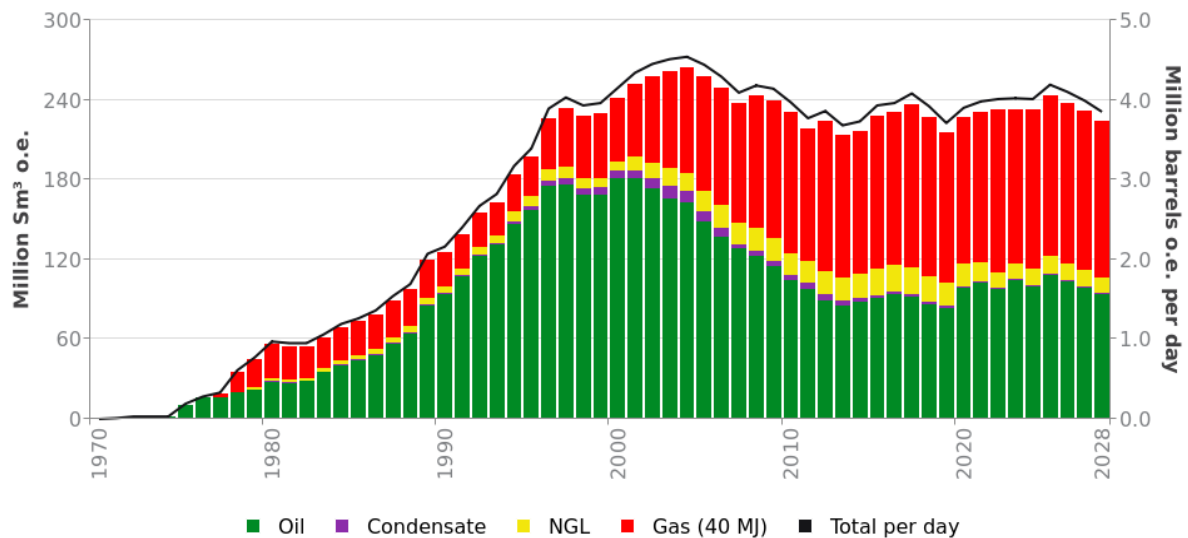


Figure 1.3: Recovered and expected oil production in Norway [3].

1.2 Modern technology

Producing oil from the reservoir has always been a challenging task. Reducing the production rate of unwanted water and gas has been the major obstacle to the maximum recovery of oil. Because of early breakthroughs of water and gas, the reservoir needs to be shut down though a considerable amount of oil can be recovered. To prevent this phenomenon, flow control devices such as ICD, and AICD are developed. These two inflow control devices can prevent early water and gas breakthroughs and increase the reservoir life. Further technology development introduced AICV considering the choking effect for low viscous fluids like water and, gas [4].

Using the multi-lateral well is one of the most economical and sustainable solutions for maximum oil recovery. Because of the geological complexity in some parts of a reservoir, it is very difficult to recover oil. Multi-lateral wells can be a solution to those geological complex zones. Advanced multi-lateral wells are vastly used in the Norwegian Continental Shelf (NCS) and in the last two decades more than hundreds of multi-lateral wells have been drilled for oil production [5].

1.3 Task description

1.3.1 Objectives

1. Literature study on Enhanced oil recovery (EOR) with CO₂-WAG injection, WAG injection, and advanced multi-lateral wells (AMW).
2. Development of oil models for the simulation of oil recovery through advanced horizontal wells.
 - Performance of the horizontal well using different types of flow control devices (FCD) in OLGA multiphase flow simulator coupled with ECLIPSE. The heterogenous PUNQ-S3 reservoir was designed in ECLIPSE.
 - The mathematical development for valve opening control with the algebraic controller for autonomous inflow control device (AICD) in OLGA.
 - Performance analysis between enhanced CO₂-WAG and WAG oil recovery in ECLIPSE for PUNQ-S3 reservoir.
 - Performance analysis of CO₂-WAG injection for different water/CO₂ injection ratios.
3. The performance of advanced multi-lateral wells (AMW) model with different types of FCDs for the simulation of oil recovery in ECLIPSE.

1.3.2 Outline

This study contains six chapters. The first chapter contains the study background and overview of the oil recovery process. Chapter Two discusses the literature study and overview. Chapter Three contains a theoretical study related to the study. Chapter Four describes the simulation setup for the oil model and Chapter Five discusses the result analysis and discussion. Finally, Chapter Six concludes the study of this thesis.

2 Literature review

Oil recovery can be classified into three methods illustrated in Figure 2.1. Initially, oil can be extracted from the drilling of a well from the surface to the underground reservoir. Pressure from the reservoir drives the oil through the well bore and then can be extracted by using some mechanical devices such as a mechanical pump or any electric-driven multistage submersible pump. This process continues till the surface pressure exceeds the reservoir pressure. This process is known as Primary oil recovery. Potentially only 5% to 15% of oil can be recovered using the primary oil recovery method [6]. Injecting water or gas to move the remaining reservoir oil to the production pipe is commonly known as the secondary oil recovery method. In this method 20% to 40% of the total volume of oil in the reservoir is extracted which can extend the life of the production of a reservoir [7]. This method is also known as improved oil recovery (IOR). Further oil production can be increased by using enhanced oil recovery or tertiary oil recovery methods. Combinations of chemicals, thermal energy, or infusion of microbials are some examples of this method. Reservoir rock and fluid properties, capillary pressure within the porous medium, relative permeability, interfacial tension, and wettability can be alternated in enhanced recovery methods [8].

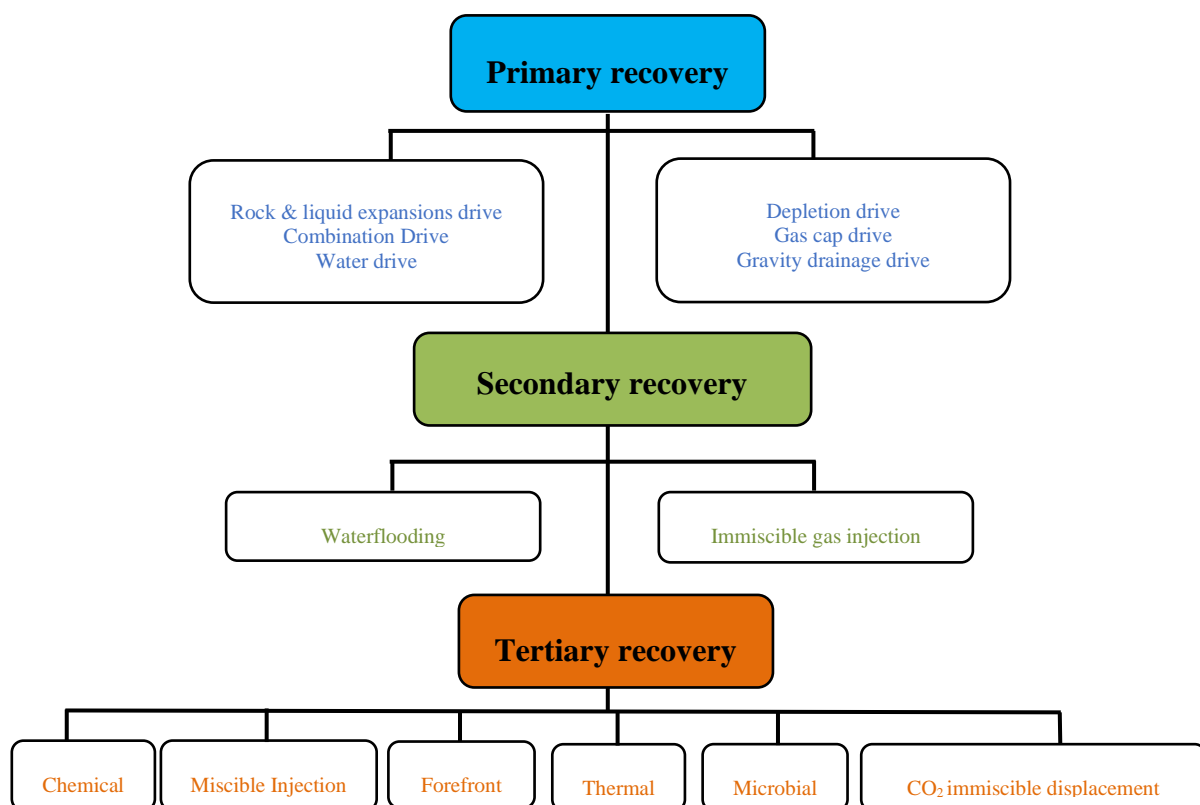


Figure 2.1: Classifications of oil recovery methods [6].

2.1 Water-alternating gas (WAG) injection

One of the most used methods to enhance the extraction of the remaining oil from the reservoir is the water alternating gas injection method. Because of its good performance in hydrocarbon reservoirs, the oil and gas industry is very much interested in water alternating gas injection as a reasonably advanced technology. The primary objective of the WAG projects is to combine the advantages of gas injection (GI) and waterflooding (WF) to manage mobility and reduce the issue of viscous fingering, resulting in enhanced oil recovery [9]. In this way, injected gas pushes the oil from the porous medium and makes it easier to use the waterflooding process to drive oil toward the production pipe. Figure 2.2 illustrates the process of the WAG injection method in a reservoir where two-phase zonal isolation can be seen, with one WAG zone and a miscible zone. Residual oil is driven from the WAG zone to the miscible zone and finally, oil is recovered by the production pipe [10].

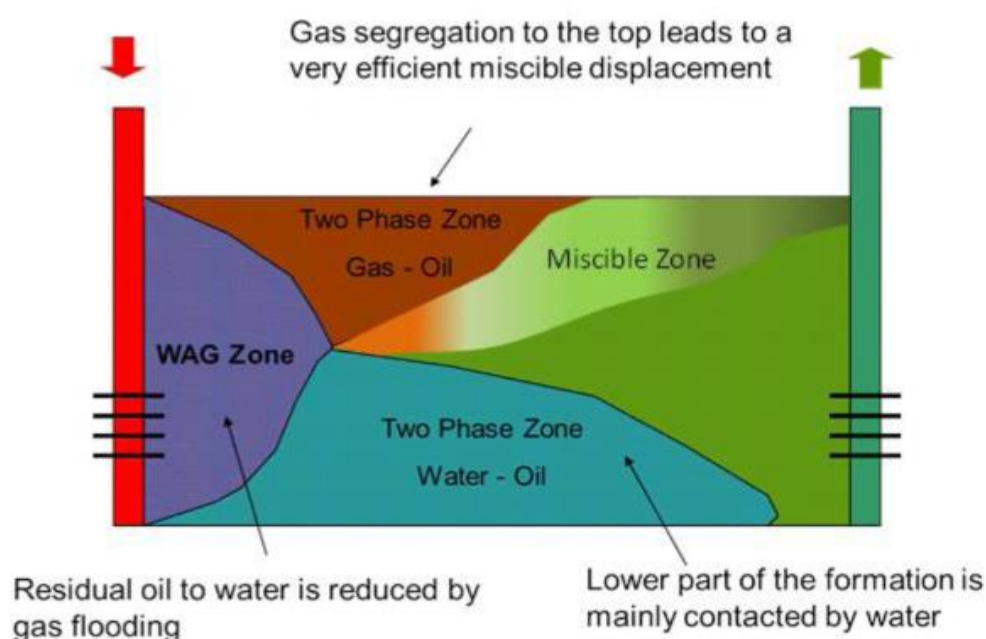


Figure 2.2: Simple diagram of WAG injection method [10].

The WAG injection process can be done using natural gas, N_2 , and CO_2 gas. In terms of the WAG injection process, production efficiency can be hampered by thermodynamic conditions of Water flooding (WF) and gas injection. For this reason, major challenges can be classified for many field applications such as early breakthrough, loss of injectivity, corrosion and asphaltene, and hydration formation [9].

2.2 CO_2 enhanced oil recovery (EOR)

2.2.1 Miscible CO_2 -EOR

One of the most advanced techniques used in enhanced oil recovery is miscible CO_2 injection. CO_2 EOR was first experimented in the early 1970s in West Texas. More than 5% of oil production in the USA comes from this technique [11]. Figure 2.3 shows that CO_2 EOR is becoming more popular in the 21st century because of oil production improvement for oil

reservoirs and its positive environmental impact on minimizing carbon emissions. Controlling carbon emissions to nature is one of the most alarming events nowadays [12].

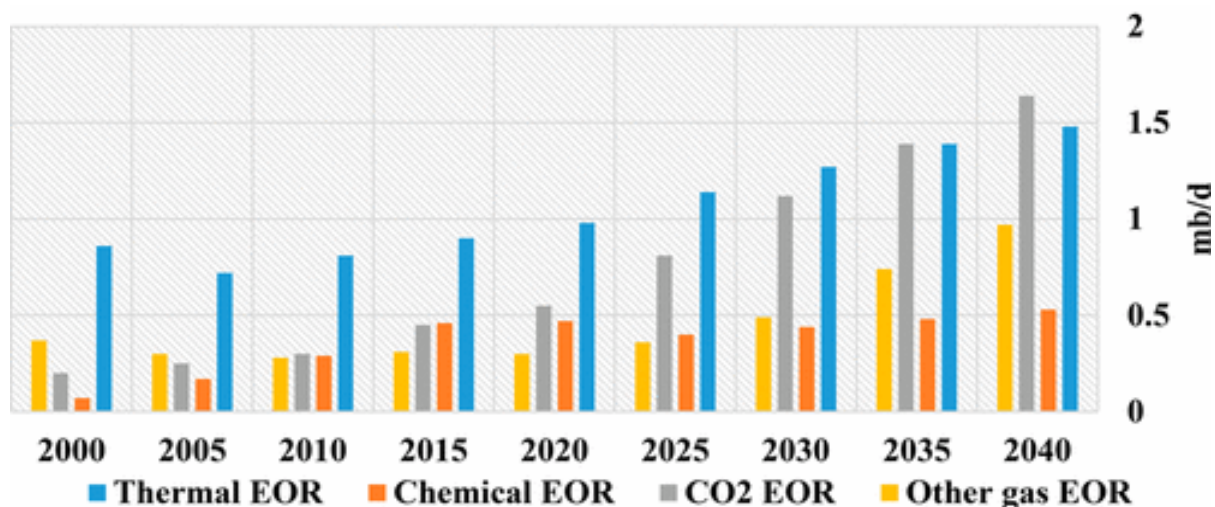


Figure 2.3: Sustainable EOR methods over the period [12].

In this technology, CO₂ acts as a solvent and is mixed with the remaining oil in the reservoir. The homogeneous mixture of oil and gas can easily be recovered to the surface. Also, CO₂ is economically viable to use [13]. Figure 2.4 illustrates the miscible process of CO₂ EOR with simultaneous injection of water and gas, where CO₂ is being dissolved in the crude oil and as a result, the viscosity of oil reduces because of CO₂ swelling. Using alternated water flooding helps the low viscous CO₂ not to surpass way ahead of the driven oil which can result in fingering problem [13].

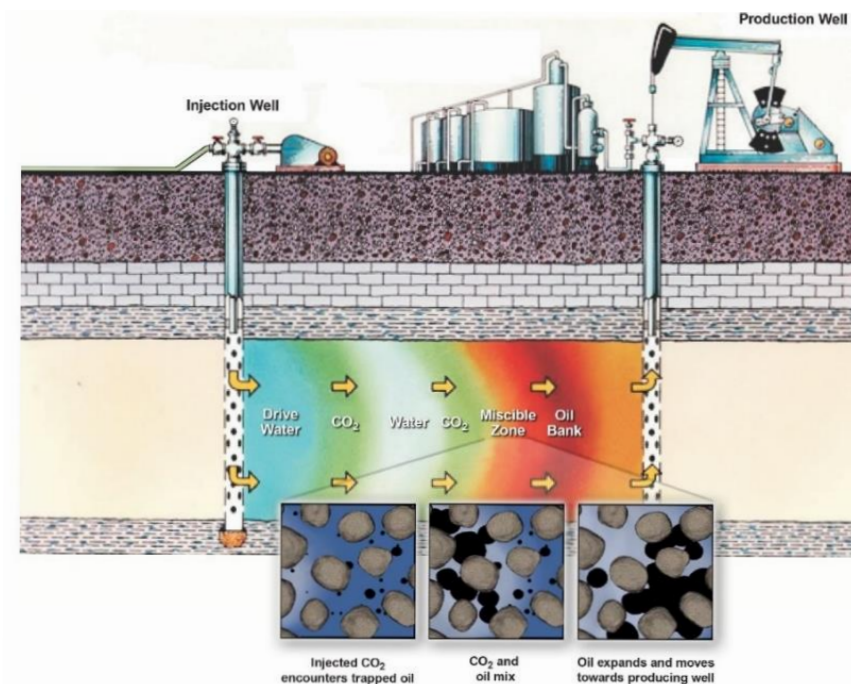


Figure 2.4: CO₂-WAG injection method [13].

2.2.2 CO₂ properties for EOR

CO₂ is non-combustible in nature and is also a color and odorless gas. The molecular weight is 44.01 gm/mole which is denser than air. Figure 2.5 shows the behavior of CO₂ in a density vs temperature plot. Below the critical temperature and pressure, CO₂ is either in the gas phase or in the liquid phase. With increasing pressure, it goes into the supercritical region [14].

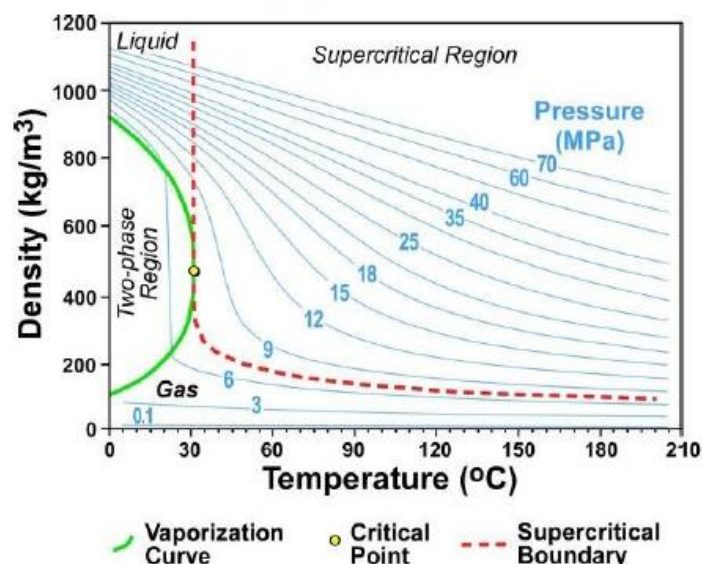


Figure 2.5: Density behavior of CO₂ in different pressure and temperature [14].

According to this plot, the critical properties of CO₂ are given below-

Table 2.1: Properties of CO₂ in critical condition [15].

Parameter	Value
T _C	31.05 ° C
P _C	73.9 bar

Variations in pressure, temperature, and composition of oil are responsible for oil swelling. Swelling means the solubility of CO₂ in residual oil. It is a vital factor as the residual oil saturation is inversely proportional to the swelling factor [16].

CO₂ reduces the oil viscosity and interfacial tension because of dissolving in oil. However, the total viscosity reduction depends on the initial viscosity. Interfacial tension reduction increases the relative permeability of oil in the relative permeability curves [16]. Also, gravity segregation can be reduced due to the less density difference between oil and water as a result of CO₂ dissolvent [16].

2.2.3 Immiscible CO₂-EOR

When CO₂ is injected below miscible pressure into the reservoir, it is known as immiscible CO₂ EOR. CO₂ injection pressure and reservoir temperature are considered two of the most important factors which enable the dissolving of CO₂ in oil and as a result, the impact can be seen in the productivity of the immiscible CO₂ injection process [17]. Because of the increasing temperature in the reservoir, the mobility of gas molecules increases, for which the solubility of CO₂ decreases. Higher activity of gas molecules tends to get separated from the oil solution rather than dissolve in it. For higher recovery purposes lower reservoir temperature and higher injection pressure but below miscible pressure is a requirement [17]. On the other hand, in the heavy oil recovery process, it is quite difficult to reach miscible displacement, hence immiscible CO₂ technique is recommended for heavy oil reservoirs [18].

2.3 Advanced well technology

For maximum oil recovery, some considerations are needed such as, more contact with the reservoir, preventing early gas, and water breakthrough, and minimization of the heel-toe effect. For better reservoir contact long horizontal wells and multi-lateral wells can be the perfect options. Pressure drop in long horizontal pipes occurs because of fluid friction in the production pipe and pressure drop has a proportional relation to flow rate, fluid density, diameter, and length of well. As a result, the pressure drop is increased in longer pipes with increasing pressure differences in the heel and toe sections. This early water and gas breakthrough can be found in the heel section which is shown in Figure 2.6 [4]. The different permeability of a heterogeneous reservoir is another reason for uneven oil production.

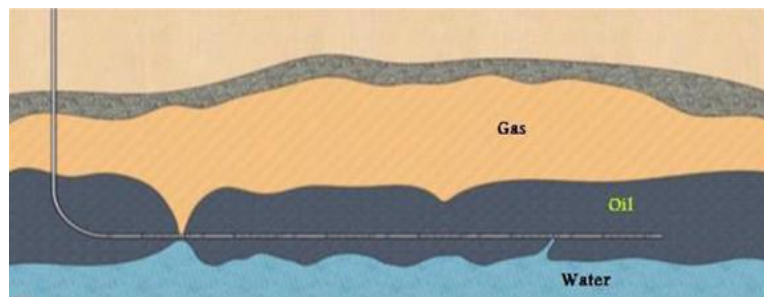


Figure 2.6: Water and gas breakthrough in heel section [4].

Multi-lateral wells are the most famous in advanced well technology as more reservoir contact can be gained. From the main wellbore, multiple branches are extracted in the reservoir either at the same depth or at different depths. Lateral extends and respective depths are the two key factors in designing multi-lateral wells. Numerous combinations can be found using these factors to have more reservoir contact [19]. Figure 2.7 shows the basic designs of multilateral wells. Stacked dual lateral can be designed in the same vertical plane in the same direction or a different direction. In the same horizontal plane, laterals can be designed and if the laterals are in opposite directions, it can be named as gullwing. Herringbone patterns or fishbone pattern laterals are different types where multiple laterals are drilled out from one single horizontal wellbore.

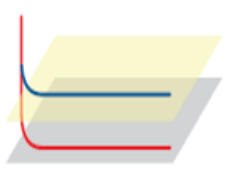
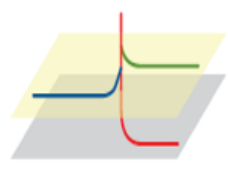
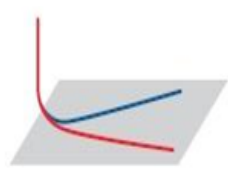
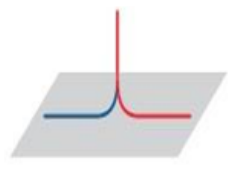
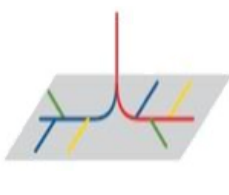
				
Dual lateral (stacked)	Dual opposed and stacked opposed triple lateral	Dual lateral (planar)	Dual lateral (planar opposed)	Herringbone pattern (planar opposed dual lateral)

Figure 2.7: Classification of multi-lateral wells [19].

2.4 Flow control technology

To prevent the early water and gas breakthrough, flow control devices were developed such as inflow control devices (ICD) and autonomous inflow control devices (AICD). These devices enhance reservoir life and improve oil recovery. A brief description of flow control devices is given in the next subchapters.

2.4.1 Inflow control device (ICD)

ICD can be referred to as a flow balancing device which is a part of the sandface completions hardware to delay the early water and gas breakthrough. It seeks to decrease annular flow and balance the inflow profile of the horizontal well at the cost of a small additional pressure drop [20]. ICD is classified into three categories such as channel-type ICD, nozzle-type ICD, and orifice-type ICD [21]. Channel type ICD has some helical paths with pre-determined diameter and length which specific differential pressure can be imposed at a specified flow rate [21]. Figure 2.8 also illustrates its flow pattern.

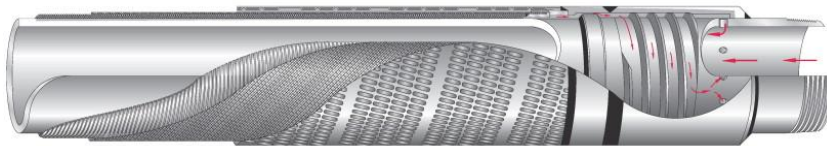


Figure 2.8: Channel-type ICD with its flow pattern [21].

In terms of nozzle-type ICD, fluid passes through some preconfigured nozzles where extra pressure resistance is generated. Pressure drop is highly sensitive to the density of fluid and not dependent on the viscosity [20]. Figure 2.9 shows the flow pattern for nozzle-type ICD.

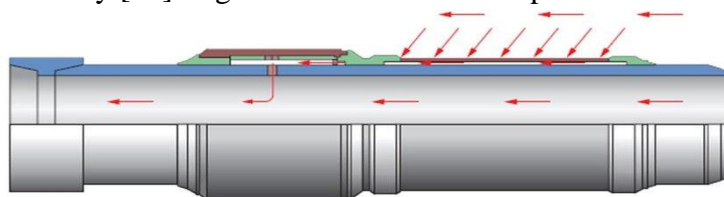


Figure 2.9: Nozzle-type ICD with its flow pattern [47].

Orifice-type ICD is designed with different numbers of open orifices to adjust the differential pressure. Each orifice is designed with pre-determined diameter and flow characteristics [21]. Figure 2.10 shows its flow pattern.

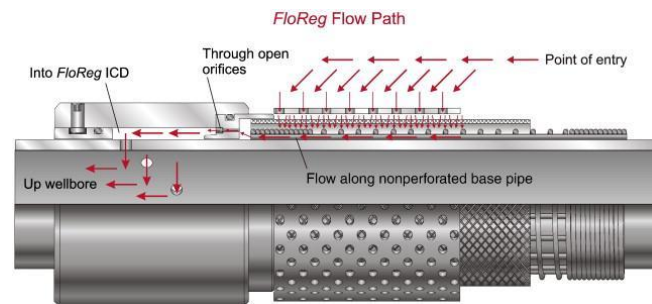


Figure 2.10: Orifice-type ICD with its flow pattern [48].

2.4.2 Autonomous inflow control device (AICD)

The main objective of the traditional ICD was to maintain the uniform flow in production zones balancing completion pressure differences with the reservoir pressure differential. Maximized oil production can be gained by maintaining equal flow which delays the influx of undesirable fluids. For conventional ICD it is not possible to regulate a flow when a breakthrough of low-viscosity fluids occurs. To maintain this phenomenon autonomous inflow control device (AICD) was developed. This device minimizes the output from zones with undesirable fluid to increase the oil production rate [22].

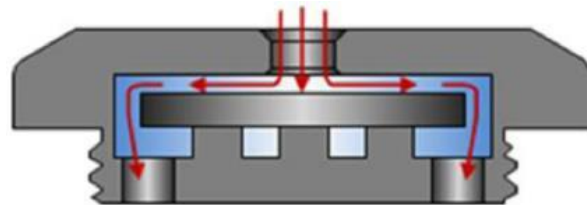


Figure 2.11: Flow pattern in AICD [23].

Figure 2.11 illustrates the streamlining of fluid through the Rate Controlled Production (RCP) valve which obstructs the flow stream of low viscous fluid. Because of the high inlet fluid velocity, pressure drops on the other side of the valve. Then the total force acts on the disc and it moves towards the inlet to prevent the fluid flow with less flow area. [23].

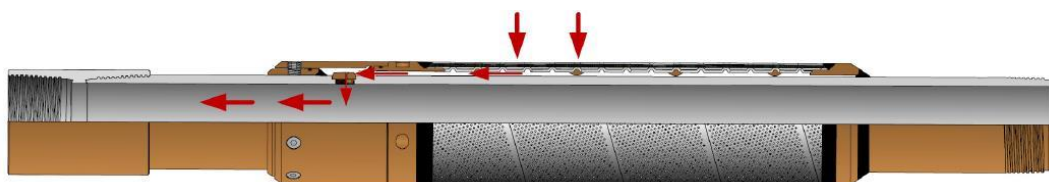


Figure 2.12: AICD mounted on sand screen joints [23].

RCP valves are mounted on sand screen joints which is shown in Figure 2.12. Reservoir fluids pass through the sand screen filter via annulus to reach the inflow control housing where AICD is installed. Then fluid passes through the AICD to enter into the production well and rises to the surfaces along with the output from other screens. Filter section and AICD housing consist same outside diameter ensuring the optimized AICD screen design [23].

2.4.3 Autonomous inflow control valve (AICV)

To enhance the oil recovery the most modern inflow control technology invented is the AICV. Early water and gas breakthrough is prevented for a longer time most efficiently by the choking effect of AICV. It is mounted in the same way as the ICD along the production pipe. Figure 2.13 shows the AICV mounted on the production pipe.

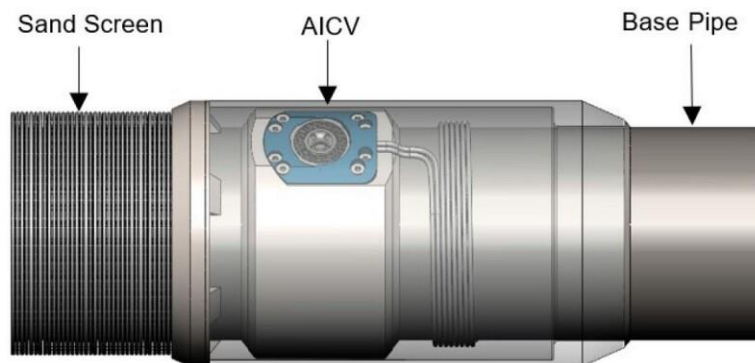


Figure 2.13: AICV mounted on a production pipe [24].

In a heterogeneous reservoir thin oil layer is found between a gas cap and the underlying aquifer. For this kind of oil field, the AICV is the best solution for oil recovery. In a study, it was found that AICV has a higher oil production rate of 48.7% than conventional ICD and sand screens. AICV has also less cumulative gas production of 22.5% and 26.7% compared to ICD and sand screens respectively [24].

In the AICV there are two flow restrictors, one is laminar and the other is turbulent flow restrictors. Turbulent flow restrictor consists of a thin orifice plate and laminar flow restrictors is a spiral piping element [4]. Figure 2.14 shows the oil flow to the production pipe in the AICV.

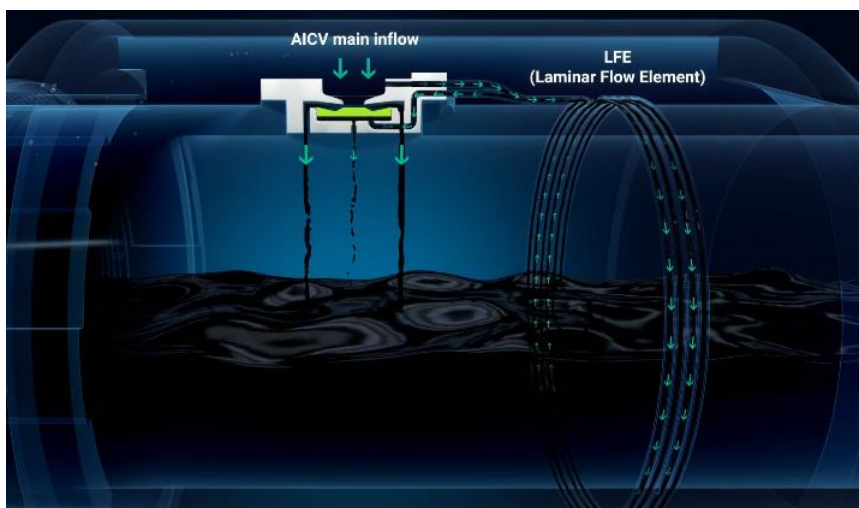


Figure 2.14: Flow path of oil through AICV [49].

3 Theoretical background

Simulating an oil well requires a clear understanding of the theoretical background. In this chapter fundamental principles and mathematical formulations are discussed including the main parameters of a reservoir rock and fluid and mathematical derivations of the flow control devices (FCDs).

3.1 Reservoir rock properties

In the first place, mineral composition, particle size, orientation, cementation level, and compaction influence the properties of rock. Only eight major elements are present in the minerals that make up the majority of the rock in the earth's crust: O, Si, Al, Fe, Ca, Na, Mg, and K. The qualities of rocks are influenced by their grain size and orientation. For example, a rock with tiny grain size and good alignment would have low porosity. Then, permeability and porosity will be related, but this does not imply that high porosity would have high permeability. Additionally, cementation and porosity will be related. Cementation increases and porosity decreases with increasing deepness. Figure 3.1 shows the formation of rocks below the surface and the fluid positioning according to their density [25].

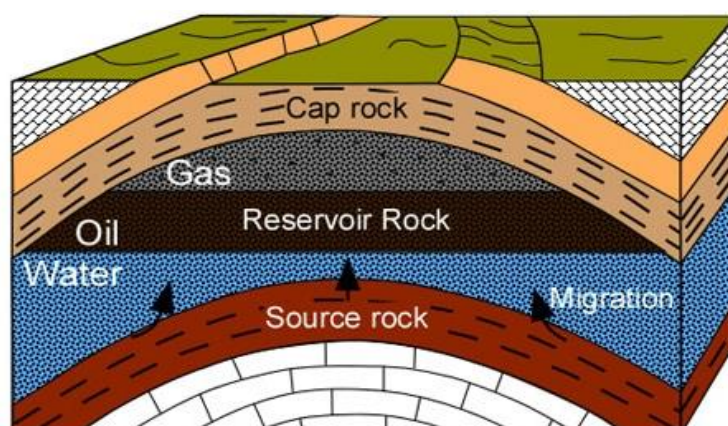


Figure 3.1: Rock formation in a reservoir [25].

3.1.1 Porosity (ϕ)

Reservoirs with sandstone and limestone which are formed from sand grains and carbonate particles have frequent irregularities in shape. As a result, void space created among those grains is known as pore space and is occupied by liquid or gas. Porosity can be defined as the ratio of pore volume to the bulk volume of a reservoir and the mathematical expression is shown in Equation 3.1 [26]:

$$\phi = \frac{V_b - V_{gr}}{V_b} = \frac{V_p}{V_b} \quad (3.1)$$

Where Φ is the porosity, V_b is the bulk volume of the reservoir rock, V_{gr} is the grain volume and, V_p is the pore volume.

Different types of pores can be found in the porous medium of a reservoir. Figure 3.2 illustrates the types of pores in a reservoir rock such as dead-end, isolated and interconnected pores [27].

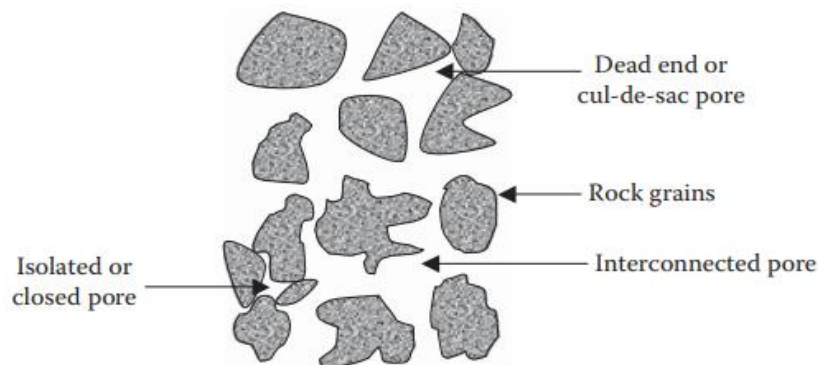


Figure 3.2: Types of pores in a reservoir [27].

3.1.2 Permeability (k)

The ability to flow the fluids through pores of rocks is defined as permeability. Figure 3.3 displays the permeability in a reservoir according to the rock porosity. When only one fluid flows through a permeable zone it is called absolute permeability (k) whereas effective permeability (k_e) is defined when more than one fluid flow is found. In this case, the permeability of each fluid decreases because of the presence of multiple fluid flows [28].

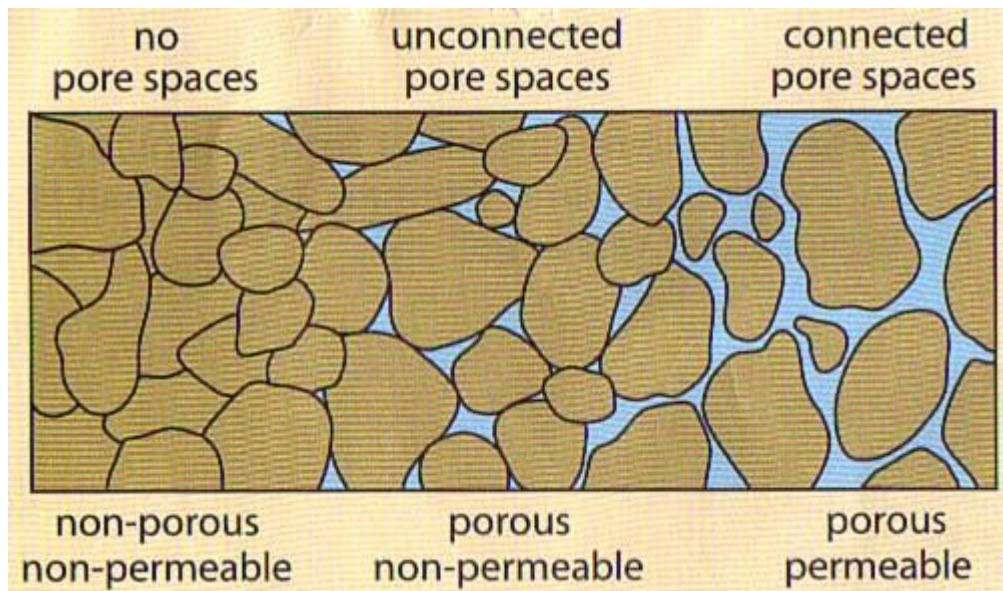


Figure 3.3: Permeability relation with porosity in reservoir [28].

A French civil engineer, Henry Darcy, developed an equation for fluid to interpret absolute permeability in a porous medium which is commonly known as Darcy's law. He conducted a simple test with a core sample which is shown in Figure 3.4 that leads to a mathematical formula mentioned in equation 3.2 [26]:

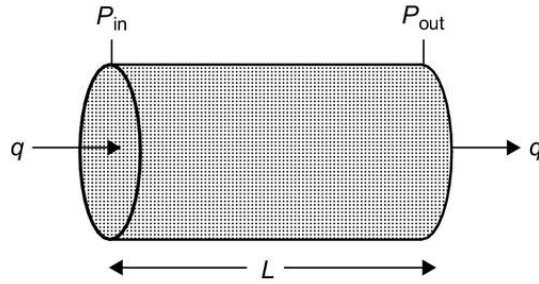


Figure 3.4: Core sample test for Darcy's law [26].

$$v = \frac{q}{A_c} = -\frac{k}{\mu} \frac{dp}{dl} \quad (3.2)$$

Where k is the permeability, v is the fluid velocity, q is the flow rate, l is the length of the core sample, μ is the viscosity of the fluid, $\frac{dp}{dl}$ is the pressure gradient, A_c is the cross-sectional area of core volume.

3.1.3 Relative permeability (k_r)

In most cases, the reservoir can be found with multiphase fluid as the reservoir rocks are saturated with at least two fluids, for example, oil and water or oil and gas or gas, oil, and water. Thus, the concept of effective permeability is generated. Relative permeability can be defined as the ratio of effective permeability to absolute permeability and the mathematical formula is given in the below equation 3.3 [27]:

$$k_r = \frac{k_e}{k} \quad (3.3)$$

For oil, water, and gas the effective permeability can be written as k_{eo} , k_{ew} and k_{eg} respectively and the relative permeability as k_{ro} , k_{rw} and k_{rg} .

Figure 3.5 illustrates the relation between relative permeability and saturation curves for water-wet and oil-wet rock. S_{wc} is denoted by irreducible water saturation and S_{orw} is denoted residual or critical oil saturation. In the case of water-wet reservoir rock, below S_{wc} water is not mobile because of capillary forces and the relative permeability is zero. Below S_{orw} oil is not mobile, and the relative permeability is also zero. In water-wet cases, the rock surfaces get wet with water, and oil located at the center of the pores is surrounded by the water which works as a lubricator. In the case of an oil-wet reservoir the pore surfaces are wetted by oil and

the center of pores is occupied by the water. Generally, S_{wc} is lower in an oil-wet reservoir rock than water-wet reservoir rock [29].

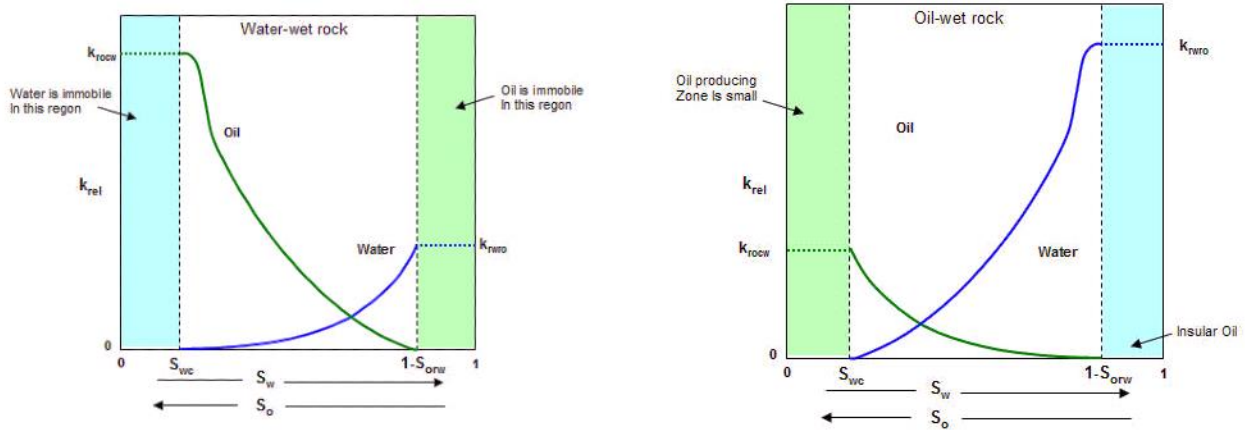


Figure 3.5: Relative permeability curve for water-wet rock (left) and oil-wet rock (right) [29].

3.1.4 Wettability

Wettability is commonly known as the tendency of any fluid to adhere to or spread over a solid surface or particles. Wettability is considered a key factor in reservoir engineering as capillary pressure, relative permeability, and distributions of fluids within the reservoir rocks are highly influenced by it [27]. In oil-wet conditions, rocks adhere to oil, and pores are occupied by water. In water-wet conditions, rocks adhere to water, and pores are occupied by oil. When small pores are occupied by water-wet and on the other hand large pores are occupied by oil can be defined as mixed wet. Figure 3.6 shows the wettability state of water-wet, mixed-wet, and oil-wet [30].

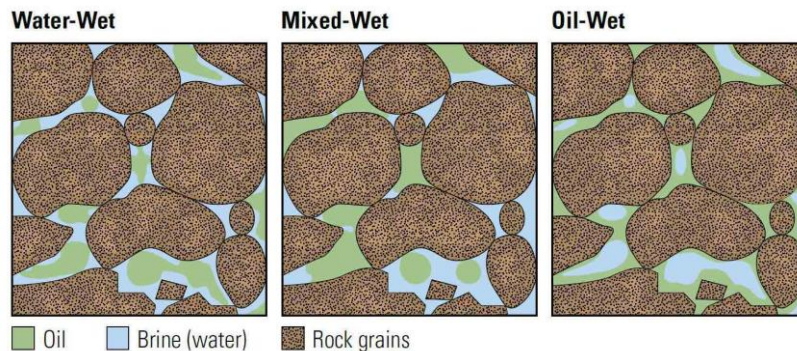


Figure 3.6: Water wet, mixed-wet and oil wet in pore spaces [30].

3.1.5 Capillary pressure (P_c)

The pressure difference between the interface of two immiscible fluids on a curved surface is defined as the capillary pressure. Equation 3.4 represents the equation for capillary pressure [26]:

$$P_c = P_{nw} - P_w \quad (3.4)$$

Figure 3.7 illustrates the change of water level in different capillary tubes over the free water level (FWL) and the same events are also found in the reservoir porous medium [31].

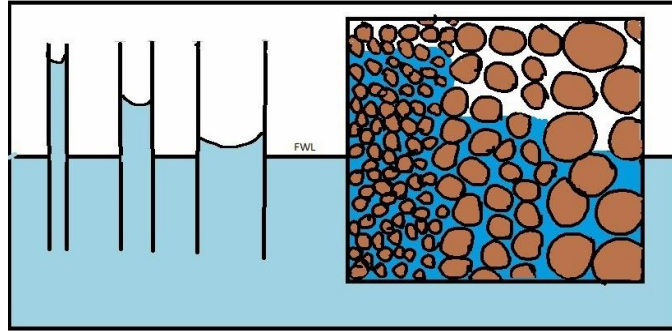


Figure 3.7: Effect of capillary pressure in capillary tubes and porous medium [31].

3.1.6 Saturation of fluid

Fluid saturation can be defined as the ratio between the volume of a fluid phase to the pore volume of a sample in a reservoir and it is denoted by S [27]. Equation 3.5 is the mathematical representation of fluid saturation-

$$\text{Fluid saturation } (S) = \frac{\text{Total volume of the fluid phase}}{\text{Pore volume}} \quad (3.5)$$

For oil, water, and gas it can be denoted as S_o , S_w and S_g respectively.

3.2 Reservoir fluid properties

Some important physical properties of reservoir fluid are essential for reservoir simulation. In this subchapter, some of these properties are described.

3.2.1 Classification of crude oil

Specific gravity (γ_o) most commonly used to classify according to financial perspective or price. Specific gravity is expressed in equation 3.6 as the ratio of oil density and water density at standard conditions at the temperature of 60°F [27].

$$\gamma_o = \frac{\rho_o}{\rho_w} \quad (3.6)$$

Another gravity scale known as API (American Petroleum Institute) or °API, is also used in oil and gas industry and is expressed as [27]:

$$^{\circ}API = \frac{141}{\gamma_o} - 131.5 \quad (3.7)$$

The API gravity classification of crude is shown in Figure 3.7 [32].



Figure 3.8: Crude oil classification by API gravity [32].

3.2.2 Reservoir fluids

Generally, fluids in a reservoir are found in two phases, gas, and liquid. Besides solid phases can be found such as wax, asphaltene, and hydrates. For having a clear concept of characterization according to the phase behavior and properties reservoir fluids can be classified from an engineering point of view. Table 3.1 shows the classification and the fluid characteristics [27]:

Table 3.1: Classification of reservoir fluid and its characteristics [27].

Reservoir fluid	API gravity (°)	Viscosity (cP)	Color of stock tank liquid
Black oils	15-40	2 to 3-100 and up	Dark, often black
Volatile oils	45-55	0.25-2 to 3	Brown, orange, or green
Gas condensates	greater than 50	In the range of 0.25	Light-colored or water white
Wet gases	greater than 50	In the range of 0.25	Water white
Dry gases	No liquid is formed and named as dry	0.02-0.05	

3.2.3 Black oil model

For petroleum reservoir simulation the black oil model is widely used. Mainly it is assumed that heavy component (oil) and light component (gas) are responsible for keeping the composition of hydrocarbon constant and no mass transfer can be found between these two phases. The black oil model consists of the following equations [33]:

- Conditions of thermodynamic equilibrium
- Equation of state
- Darcy's law for the volumetric flow rates
- Mass conservation equation for each component

Figure 3.9 illustrates the typical phase behavior of the black oil model. Vertical line 1-3 represents the pressure declination in a constant temperature. Above the bubble point (between 1-2) the reservoir is in an undersaturated state which means that the reservoir can absorb more gas. Bubble gas starts forming at point 2 and below point 2 oil becomes saturated with gas. At point 3 more gas comes out of the oil and in this state, the reservoir pressure cannot drive fluids to the surface. A large percentage of the oil phase is recovered at the surface from a black oil reservoir [34].

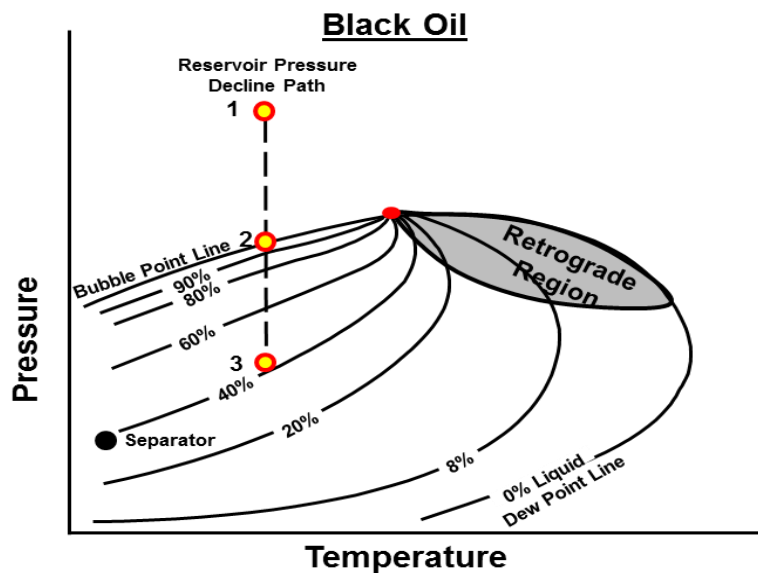


Figure 3.9: Phase diagram of Black oil model [34].

3.2.4 Gas-oil ratio (GOR)

The solution gas-oil ratio is considered an important parameter to characterize an oil. It can be defined as the ratio between the volume of gas to the unit volume of oil at standard pressure and temperature. The mathematical expression of GOR is [35]:

$$GOR = \frac{V_g}{V_o} \quad (3.8)$$

3.2.5 Water cut (WC)

Water cut can be defined as the ratio volumetric flow rate of produced water to the volumetric flow rate of total liquid produced. It can also be represented as the percentage [36]:

$WC = \frac{\dot{Q}_w}{\dot{Q}_l} = \frac{\dot{Q}_w}{\dot{Q}_w + \dot{Q}_o} \times 100\%$	(3.9)
---	-------

3.3 Mathematical models for inflow control devices

3.3.1 Passive inflow control device (ICD)

In Chapter 2, it is mentioned that to prevent the early water and gas breakthrough passive ICD was developed, and the mathematical formula is expressed as follows [37]:

$$\dot{Q} = C_D A \sqrt{\frac{2\Delta P}{\rho}} \quad (3.10)$$

Where \dot{Q} is the volume flow rate of the fluid through the ICD, ΔP is the pressure drop over the ICD, ρ is the fluid density, A is the cross-sectional area of the ICD nozzle, C_D is the discharge coefficient.

3.3.2 Autonomous inflow control device (AICD)

AICD is the improved version of ICD with the characteristics to delay the water and gas breakthroughs and partially close for low-viscosity fluids like water and gases. The empirical equation that describes the behavior of the RCP-type AICDs is as follows [37]:

$$\Delta P = a_{AICD} \cdot \left(\frac{\rho_{mix}^2}{\rho_{cal}}\right) \cdot \left(\frac{\mu_{cal}}{\mu_{mix}}\right)^y \cdot \dot{Q}^x \quad (3.11)$$

Where \dot{Q} is the volume flow rate of the fluid through the AICD, ΔP is the pressure drop over the AICD, ρ_{mix} is the density of the fluid mixture, μ_{mix} is the viscosity of the fluid mixture.

a_{AICD} , x and y in the equation are user input parameters that depend on the AICD design and the fluid properties, while ρ_{cal} and μ_{cal} are calibrating parameters. ρ_{mix} and μ_{mix} are calculated as mentioned below:

$$\rho_{mix} = \alpha_{oil}\rho_{oil} + \alpha_{water}\rho_{water} + \alpha_{gas}\rho_{gas} \quad (3.12)$$

$$\mu_{mix} = \alpha_{oil}\mu_{oil} + \alpha_{water}\mu_{water} + \alpha_{gas}\mu_{gas} \quad (3.13)$$

Where α_{oil} is the volume fraction of oil in the mixture, α_{water} is the volume fraction of water in the mixture, α_{gas} is the volume fraction of gas in the mixture.

3.3.3 Valve opening control with Algebraic controller for AICD

Valve opening control is one of the most important functions of a flow control device. In this study the AICD valve opening was controlled by logical mathematical expression in equation 3.14 from the relation of equation 3.7 and equation 3.9. Taking consideration of both water cut (WC) and gas-oil ratio (GOR), the mathematical expression for the algebraic controller is calculated.

For ICD:

$$\Delta P_{ICD} = \dot{C}_u \frac{\rho_{mix} \dot{Q}_{ICD}^2}{2\gamma^2 A^2 C_D^2} \quad (3.14)$$

$$\Rightarrow \dot{Q}_{ICD} = \gamma A C_D \sqrt{\frac{2\Delta P_{ICD}}{\rho_{mix} \dot{C}_u}} \quad (3.15)$$

For AICD:

$$\Delta P_{AICD} = a_{AICD} \cdot \frac{\rho_{mix}^2}{1000} \cdot \left(\frac{1}{\mu_{mix}}\right)^y \cdot \dot{Q}_{AICD}^x \quad (3.16)$$

$$\Rightarrow \dot{Q}_{AICD} = \left(\frac{1000 \cdot \Delta P_{AICD} \cdot \mu_{mix}^y}{a_{AICD} \cdot \rho_{mix}^2}\right)^{\frac{1}{x}} \quad (3.17)$$

Here \dot{Q} is the flow rate, ΔP is the pressure drops, A is the cross-sectional area of the fluid flow, C_D is the discharge coefficient, \dot{C}_u is the unit conversion value.

$$\rho_{mix} = \alpha_{oil} \rho_{oil} + \alpha_{water} \rho_{water} + \alpha_{gas} \rho_{gas}$$

$$\mu_{mix} = \alpha_{oil} \mu_{oil} + \alpha_{water} \mu_{water} + \alpha_{gas} \mu_{gas}$$

$$\alpha_{oil} + \alpha_{water} + \alpha_{gas} = 1$$

α_{oil} , α_{water} , α_{gas} are the volume fractions of oil, water, and gas in the mixture.

Now, matching $\Delta P - \dot{Q}$ curves of ICD and AICD at ΔP_{match} and \dot{Q}_{match} points we can get-

$$\Delta P_{ICD} = \Delta P_{AICD} = \Delta P_{mix} \quad (3.18)$$

$$\dot{Q}_{ICD} = \dot{Q}_{AICD} \quad (3.19)$$

From equation 3.15 and 3.17 we can get-

$$\gamma = \frac{\left(\frac{1000 \cdot \Delta P_{mix}}{a_{AICD}}\right)^{\frac{1}{x}} \cdot \mu_{mix}^{\frac{y}{x}} \cdot \rho_{mix}^{\frac{x-4}{2x}}}{A C_D \sqrt{\frac{2\Delta P_{mix}}{\dot{C}_u}}} \quad (3.20)$$

$$\Rightarrow \gamma = \beta \cdot \mu_{mix}^{\frac{y}{x}} \cdot \rho_{mix}^{\frac{x-4}{2x}} \quad (3.21)$$

$$\Rightarrow \gamma = \beta \cdot \left\{ \alpha_{oil} \mu_{oil} + \alpha_{water} \mu_{water} + \alpha_{gas} \mu_{gas} \right\}^{\frac{y}{x}} \cdot \left\{ \alpha_{oil} \rho_{oil} + \alpha_{water} \rho_{water} + \alpha_{gas} \rho_{gas} \right\}^{\frac{x-4}{2x}} \quad (3.22)$$

In the OLGA model, two transmitters are used to take the values of oil volume fraction (α_{oil}) and (α_{water}) as an input variable from the wellbore. Equation (3.22) is put as an expression option in the algebraic controller in OLGA. To implement α_{oil} , α_{water} as input variables into the equation (3.22) they are introduced as unknown variables X1 and X2 in the algebraic controller. The expression in the algebraic controller is as follows:

$$\Rightarrow \gamma = \beta \cdot \left\{ X1 \cdot \mu_{oil} + X2 \cdot \mu_{water} + (1 - X1 - X2) \cdot \mu_{gas} \right\}^{\frac{y}{x}} \cdot \left\{ X1 \cdot \rho_{oil} + X2 \cdot \rho_{water} + (1 - X1 - X2) \cdot \rho_{gas} \right\}^{\frac{x-4}{2x}} \quad (3.23)$$

Here $\alpha_{oil} = X1$, $\alpha_{water} = X2$ and $\alpha_{gas} = 1 - X1 - X2$

All the known parameters are given in Appendix C.

3.3.4 Autonomous inflow control valve (AICV)

As it is mentioned in Chapter 2 that the AICV has pipe shaped laminar flow restrictors and turbulent flow restrictors in series, Figure 3.10 shows how the AICV performs according to the pressure drops.

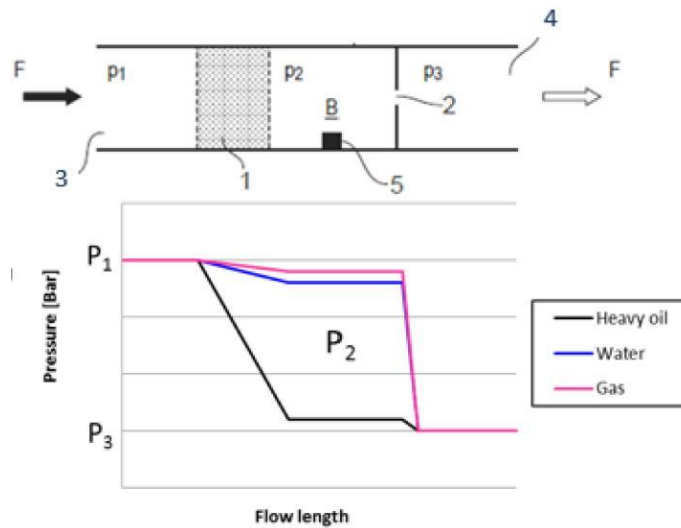


Figure 3.10: Pressure drops in laminar and turbulent flow restrictors [4]

Pressure drops in the laminar flow restrictors is expressed in the equation (3.24) and turbulent flow restrictors are expressed in the equation (3.25).

$$\Delta P = \frac{32\mu\rho vL}{D^2} \quad (3.24)$$

$$\Delta P = k \frac{1}{2} v^2 \quad (3.25)$$

Here ΔP is the pressure drop over the restrictors, μ is the fluid viscosity, ρ is the fluid density, v is the fluid velocity, L is the laminar restrictor length, D is the laminar restrictor diameter, and k is the geometrical constant.

3.4 Multisegment well model

Multisegment well (MSW) model is a unique feature of the ECLIPSE simulator to simulate the advanced horizontal well and multilateral wells with inflow control devices. The wellbore can be divided into more segments as much as required. The more segments the more accurate simulation. Figure 3.11 shows a simple schematic of a multi-segment well model. Each segment contains one segment node and one flow path connecting to a neighboring segment. All the connected segments are directed to the wellhead which is considered an outlet [38].

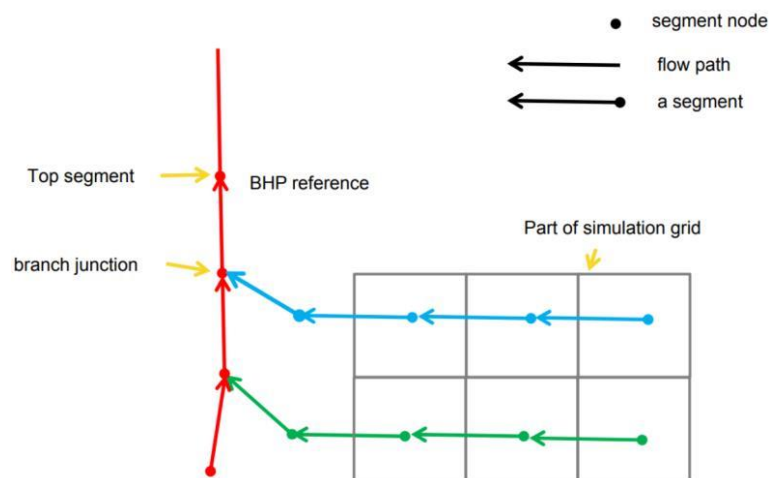


Figure 3.11: A simple schematic of a multi-segment well model [38].

Figure 3.12 illustrates an MSW model for an advanced horizontal well where tubing and annulus are considered as different branches. The control valve is considered an inflow control device that connects the annulus to the production tubing. Fluid flows from the reservoir to the annulus and then passes to the production tubing. Finally, the total flows to the outlet through production tubing. The full model is designed by connecting the annulus, valve, and tubing segments [39].

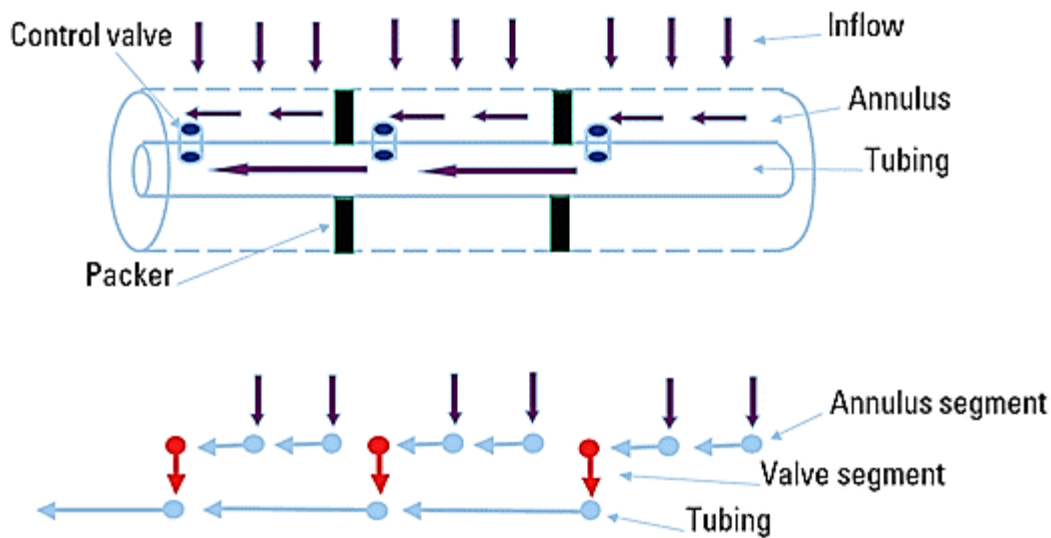


Figure 3.12: MSW model for an advanced horizontal well [39].

3.5 Solvent model

For the CO₂-WAG miscible EOR method in ECLIPSE, the solvent model can be used as it is a miscible flood modeling case. The model was suggested by M. Todd and W. Longstaff and is known as the Todd-Longstaff model [40]. Optionally it can be a four-component system of reservoir gas, oil, water, and solvent injected from the surface or a three-component water, oil, and solvent gas or oil/solvent system. Injected gas is considered a solvent and assumed to be miscible with the reservoir oil in full proportion and a single hydrocarbon phase will exist [40]. In this chapter, the solvent model is briefly described with different parameters.

3.5.1 Todd-Longstaff model

M. Todd and W. Longstaff considered a grid block like Figure 3.13 where a dispersed zone of mixing of oil and solvent for both stable and unstable 2D fluid flow can be seen. If the dispersion area is comparatively large to the grid size, then it can be assumed that oil and solvent are completely mixed with the same effective density and viscosity. If the dispersion zone is too small, it is to be considered that the effective fluid properties of solvent and oil are of their pure component. and the actual fluid properties can be expected in the limit of the mixing zone. Reflecting on this, K. S. Lee and E. L. Claridge of Shell Development Co. suggested equation (3.26) and equation (3.27) which describe the effect of partial mixing on effective viscosities. ω is the Todd-Longstaff mixing parameter which ranges between 0 to 1 [41].

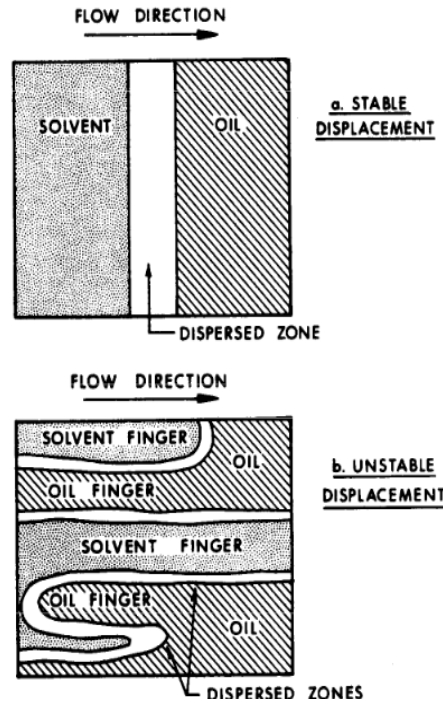


Figure 3.13: Dispersed zone in a grid block displacing oil by solvent [41]

$$\mu_{oe} = \mu_o^{1-\omega} * \mu_m^\omega \quad (3.26)$$

$$\mu_{ge} = \mu_g^{1-\omega} * \mu_m^\omega \quad (3.27)$$

Assuming $\omega=1$ for complete mixture, equation (3.28) can be derived by 1/4 -power fluidity mixing rule. This means effective viscosity for all components are same as the mixture effective viscosity .

$$\mu_m = \mu_o \mu_g / \left(\frac{S_g}{S_n} \cdot \mu_o^{\frac{1}{4}} + \frac{S_o}{S_n} \cdot \mu_g^{\frac{1}{4}} \right)^4 \quad (3.28)$$

In this condition effective density will also be same which can be formulated in equation 3.29

$$\rho_m = \rho_o \frac{S_o}{S_n} + \rho_g \frac{S_g}{S_n} \quad (3.29)$$

M. Todd and W. Longstaff recommended $\omega= 2/3$ to model viscous fingering in secondary gas miscible injection in laboratory setup and $\omega= 1/3$ to heterogenous field application [41].

4 Development of the OLGA/ECLIPSE model

The objective of this study is to simulate the CO₂-WAG enhanced oil recovery (EOR) in a heterogeneous reservoir with specified fluid and rock properties using advanced horizontal and multilateral wells. The EOR process involves four vertical injectors which inject water, gas, and CO₂ simultaneously. Different inflow control devices are used to analyze the performance of oil recovery. The step-by-step approach is described briefly in this chapter.

4.1 Well model in OLGA

A production well model has been designed in OLGA coupled with ECLIPSE to find out the total oil production for specific times. Figure 4.1 illustrates the set-up of a production model with production pipeline, and annulus in a reservoir.

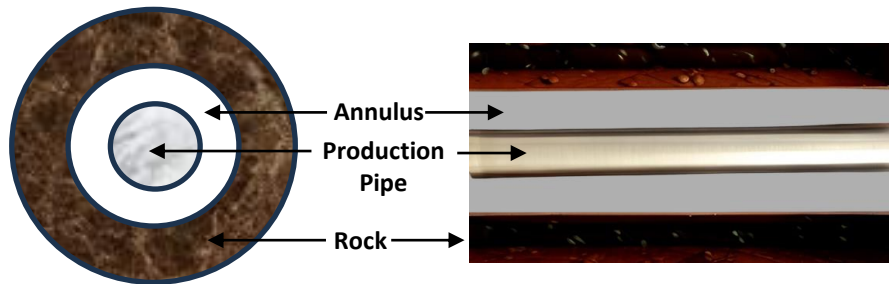


Figure 4.1: Cross sectional and side view of a production pipe in annulus.

Annulus is the gap between the wellbore and the production pipe where oil flows through the inflow control devices. Inflow control devices are generally attached to the production pipe and packers are built within an annulus to separate multiple sections. Figure 4.2 illustrates the flow pattern of the horizontal well, reservoir, and annulus zone. Two different sections are divided with packers [42].

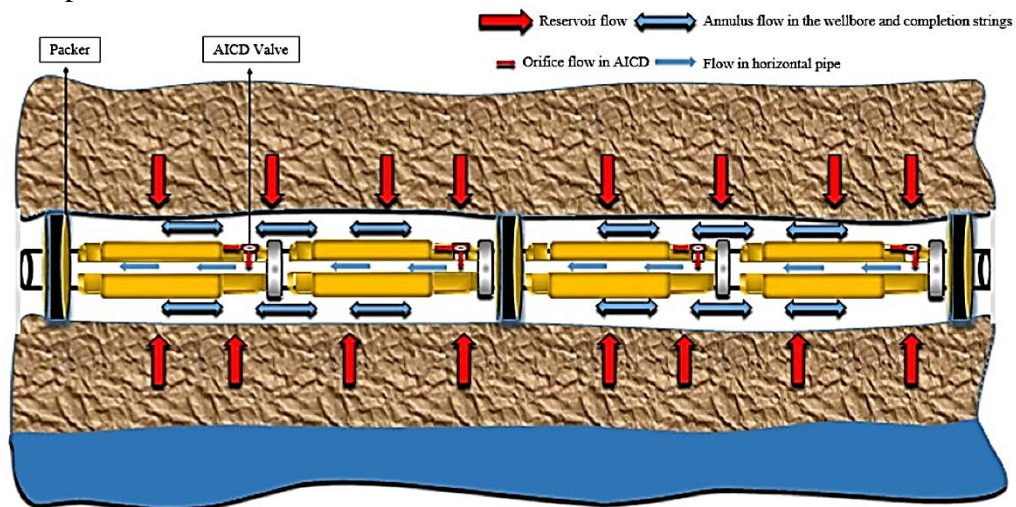


Figure 4.2: Fluid flow path through reservoir and annulus in a packer [42].

4.1.1 Flow component set-up

For the horizontal well model, the length is considered 3240 m. The diameter of the production pipe and the wellbore is considered 0.1397 m and 0.2159 m respectively. The production well has 18 valves to divide the production pipe into 18 zones. Equivalent diameter is taken at 0.0078 m for both ICD and AICD considering the discharge coefficient (CD) as 0.85. Table 4.1 shows the technical data for the wellbore and production pipe.

Table 4.1: Technical data of the wellbore and the production pipe.

Pipe name	Length (m)	Diameter (m)	Roughness (mm)	Sections (m)
Wellbore	3240	0.2159	1	36
Production pipe	3240	0.1397	1	

The whole production pipe is sectioned into 18 zones assuming 18 near-well sources which contain 36 hypothetical sections divided of 90m each. Figure 4.3 shows a simplified sketch of a single production zone in a production pipe containing the packers, fluid flow path, and inflow control device. Packers prevent fluid flow from an adjacent zone through the annulus. Near-well source is the connecting component between OLGA and ECLIPSE. Through section I fluid enters into the wellbore and then passes through inflow control devices. After that fluid passes through the Leak into the production pipe in section II. This method was proposed by Haavard Akre in 2012 and is much used in research [43].

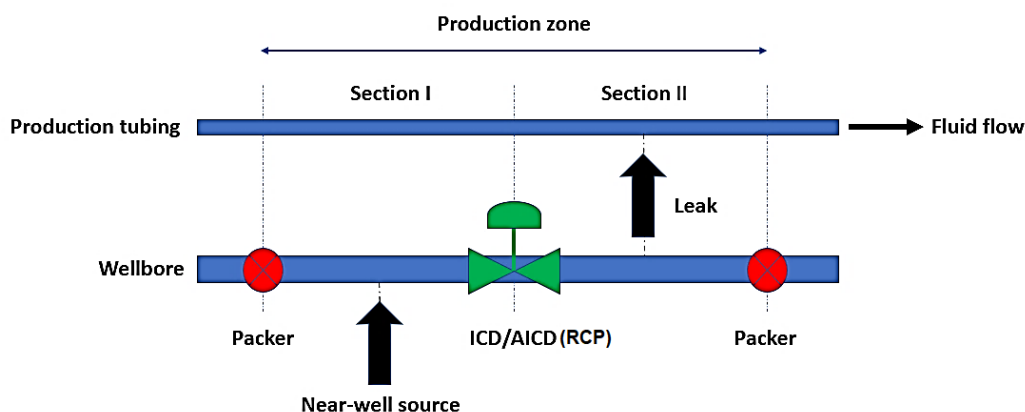


Figure 4.3: Schematic of a single zone in a production pipe [43].

If there is no use of any flow control devices in the simulation, then it can be considered an OPENHOLE case. For simulation with ICD and AICD, a fully open valve with a specified diameter is taken in OLGA. Figure 4.4 is the schematic for the OPENHOLE, ICD, and AICD set up in a single production zone. Full production pipe design is provided in Appendix D. For AICD, an algebraic controller is used to control the valve opening according to the equation (3.22).

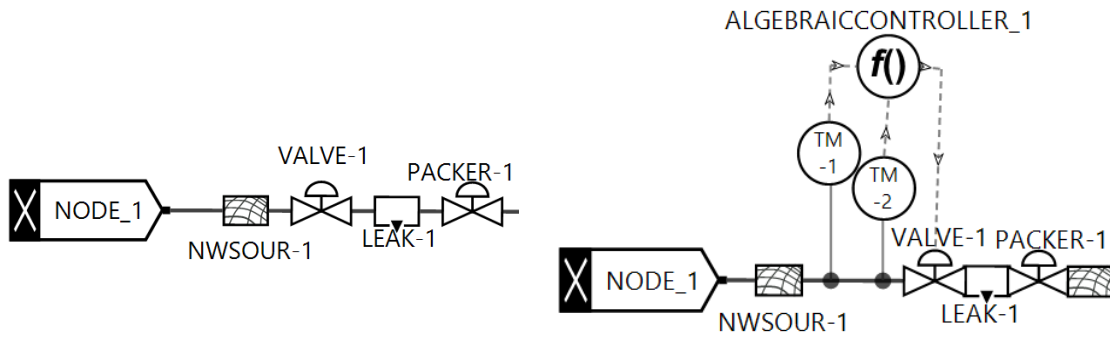


Figure 4.4: OPENHOLE/ICD (left) and AICD (right) setup in OLGA for a single production zone.

In an algebraic controller, two input signals are taken by two transmitters which contain water volume fraction and oil volume fraction. Table 4.2 shows the specifications for OPENHOLE, ICD, and AICD in OLGA.

Table 4.2: Technical data for OPENHOLE, ICD, and AICD.

Component	Flow control device	Diameter (m)	CD	Opening control	Connection
Valve	OPENHOLE	0.12	0.85	Fully open	Wellbore
	ICD	0.0078	0.85	Fully open	Wellbore
	AICD	0.0078	0.85	Algebraic controller	Wellbore

4.1.2 Case definition

Analysis of the oil production for OPENHOLE, ICD, and AICD total simulation was done for specified days by providing the maximum time step (MAXDT) and minimum time step (MINDT). Table 4.3 shows integration data for the simulation cases.

Table 4.3: Integration data for simulation in OLGA for OPENHOLE, ICD, and AICD.

Days	3500
MAXDT (d)	1
MINDT (s)	0.00001

4.1.3 Compositional setup

Oil, water, and gas are used as the black oil components. Table 4.4 shows the compositional data for all three feeds.

Table 4.4: Compositional setup in OLGA.

Feed	Gas fraction	Water cut
Oil	74 Sm ³ / Sm ³ (GOR)	0.0001
Water_drive	0.0001 Sm ³ /Sm ³ (GLR)	0.99
Gas_drive	0.99 Sm ³ /Sm ³ (GLR)	0.0001

4.2 Reservoir model in ECLIPSE

For the simulation of the reservoir, the ECLIPSE 100 facility is used, and a script file is added as the input data which contains all descriptions of the reservoir model such as reservoir rock and fluid properties. The data file contains below mentioned sections-

- RUNSPEC
- GRID
- PROPS
- SOLUTION
- SUMMARY
- SCHEDULE

Among these sections, RUNSPEC, GRID, PROPS, SOLUTION, and SCHEDULE sections are required sections. ECLIPSE reads the data file section by section. RUNSPEC includes a description of different parameters and titles to run the simulation, such as grid size, table sizes, number of wells, and liquid phases. GRID section includes petrophysics-related terms such as permeability and porosity of each grid with different data files. The PROPS section provides the rock and fluid properties like relative permeability and capillary pressure with PVT data. The SOLUTION section includes the compositional data like initial pressure, temperature, and saturation. The SUMMARY section generates the output file defined in the data file. The SCHEDULE section contains all the geometrical data for injectors and pipes [44].

Tecplot is used for the visual representation of the outputs. The ECLIPSE data file is given in Appendix B.

4.2.1 PUNQ-S3 reservoir model construction

For this study, the PUNQ-S3 (Production forecasting with Uncertainty Quantification, variant 3) synthetic reservoir model is used which was implemented in a real field study by Elf Exploration Production [45]. This is a three-dimensional dome-shaped heterogeneous reservoir. Figure 4.5 shows the reservoir with initial three-phase saturation in the XY plane.

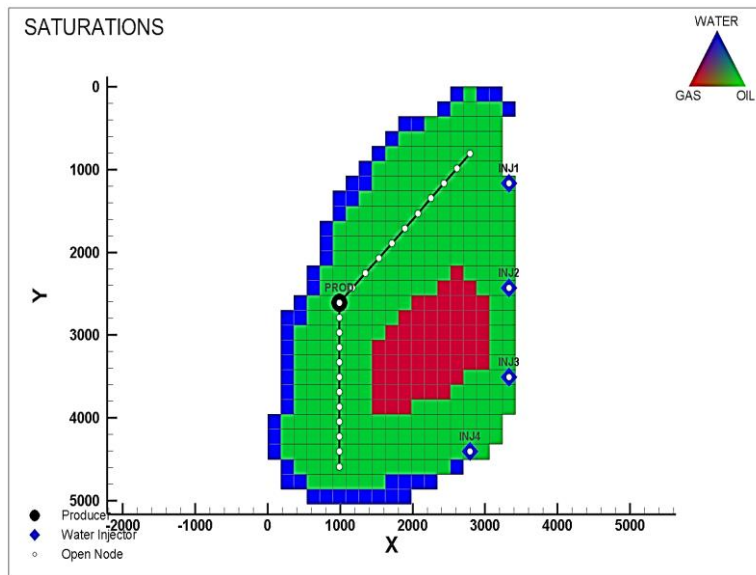


Figure 4.5: PUNQ-S3 reservoir fluid saturation in XY plane [45].

Table 4.5 shows the reservoir grid and the corresponding length of the reservoir. A total of 2660 grid blocks are present in the model and 1761 blocks are active for production.

Table 4.5: PUNQ-S3 reservoir grid dimensions.

Direction	No. of blocks	Length (m)/angle
x	19	19*180
y	28	28*180
z	5	2355/1.5°

4.2.2 PUNQ-S3 reservoir rock and fluid properties

For this study, the Black oil model has been selected with lower viscosity with a value of 2.7cP. Table 4.6 shows the rock and fluid properties of the PUNQ-S3 reservoir model. Table 4.6: PUNQ-S3 rock and fluid properties [45].

Table 4.6: PUNQ-S3 rock and fluid properties [45].

Parameter	Value
Oil density	912 kg/m ³
Water density	1000 kg/m ³
Gas density	0.8266 kg/m ³

GOR	74 Sm ³ / Sm ³
Reservoir Pressure	234.5 bar
Temperature	105 °C
Water viscosity (reservoir condition)	0.5 cP
Oil viscosity (reservoir condition)	1.46 cP
Gas viscosity (reservoir condition)	0.0133 cP
Porosity	0.1 – 0.3
Mean Porosity	0.14
Rock compressibility	0.00045 1/bar

4.2.3 Water and CO₂ injection

Four injectors are designed by trial-and-error method to inject water and CO₂ simultaneously with a regular time interval. Injectors 1, 2, 3, and 4 are placed by the depth of 2390 m, 2375 m, 2370 m, and 2370m respectively. Figure 4.6 represents the positioning of the injectors and production pipe with top face depth.

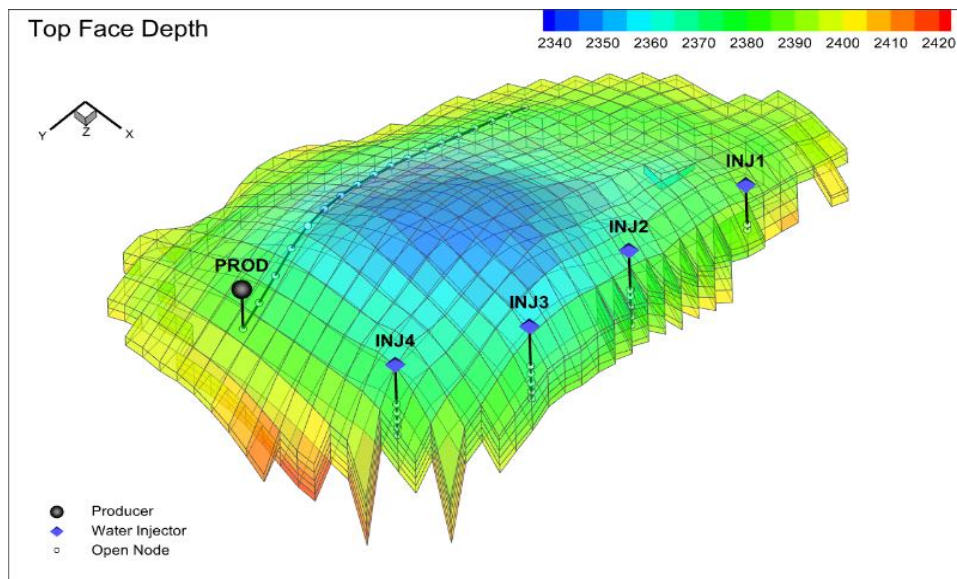


Figure 4.6: Positioning of Production pipe and injectors into reservoir.

4.2.4 PUNQ-S3 reservoir permeability

The reservoir is considered heterogeneous, so different permeability is considered in different directions with a porosity of 0.2. In the horizontal direction, permeability ranges between 0.5 mD to 999 mD with a mean value of 269 mD. On the other hand, permeability ranges between 0.2 mD to 498 mD with a mean value of 122 mD. These two ranges are accountable for uncertainty in the reservoir. It means that absolute permeability in the reservoir cannot be determined but it can be assumed that it can be expected in these ranges. Figure 4.7 is the visual representation of the reservoir grids for porosity and permeability in three directions.

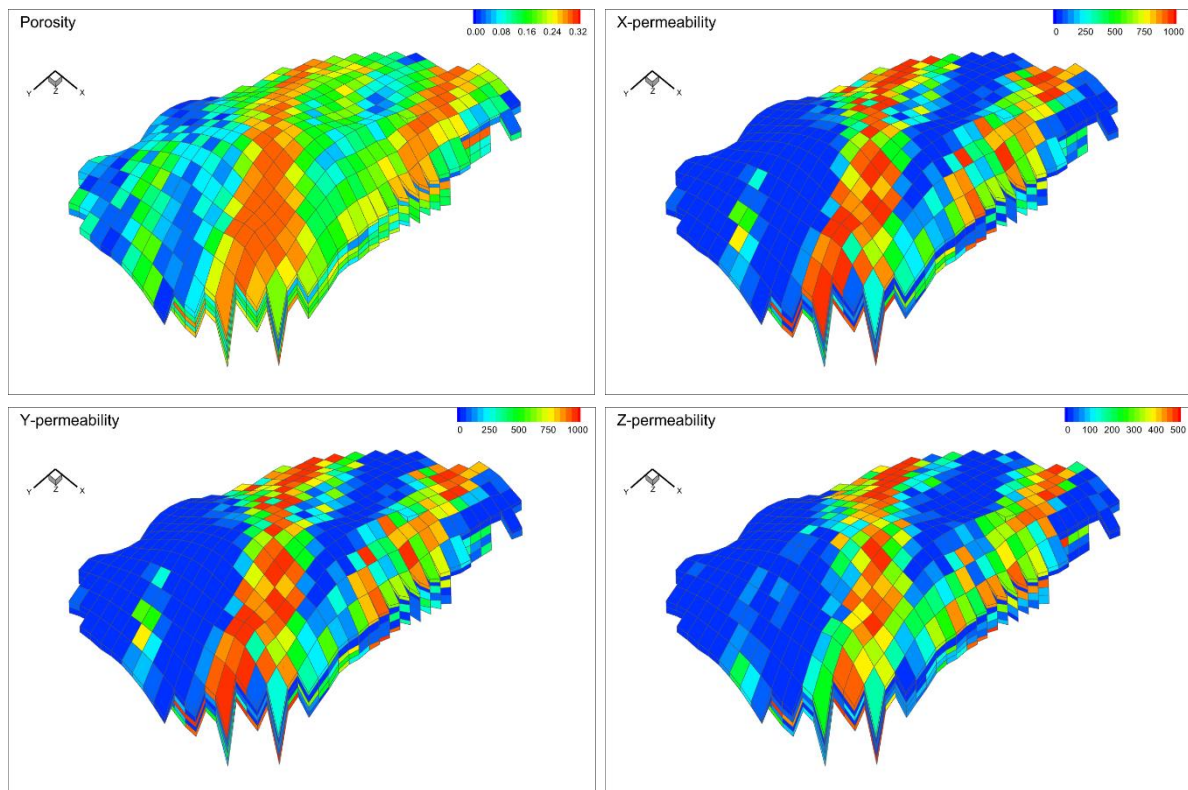


Figure 4.7: Porosity and permeability in X, Y and Z direction.

4.2.5 Initial conditions

Initially, the pressure is 234.5 bar with a datum depth of 2355 m. In ECLIPSE, water-oil contact depth and gas-oil contact depth are considered 2395 m and 2355 m respectively. Figure 4.8 represents the initial saturations of water, oil, and gas. It can be observed that the top part is filled with gas creating a gas cap with a saturation point greater than 0.75 and at the bottom the presence of water creates an aquifer zone. Water cut ranges between 0.2 to 0.9. Most of the amount of oil is distributed in the middle of the reservoir almost at the saturation point of 0.80.

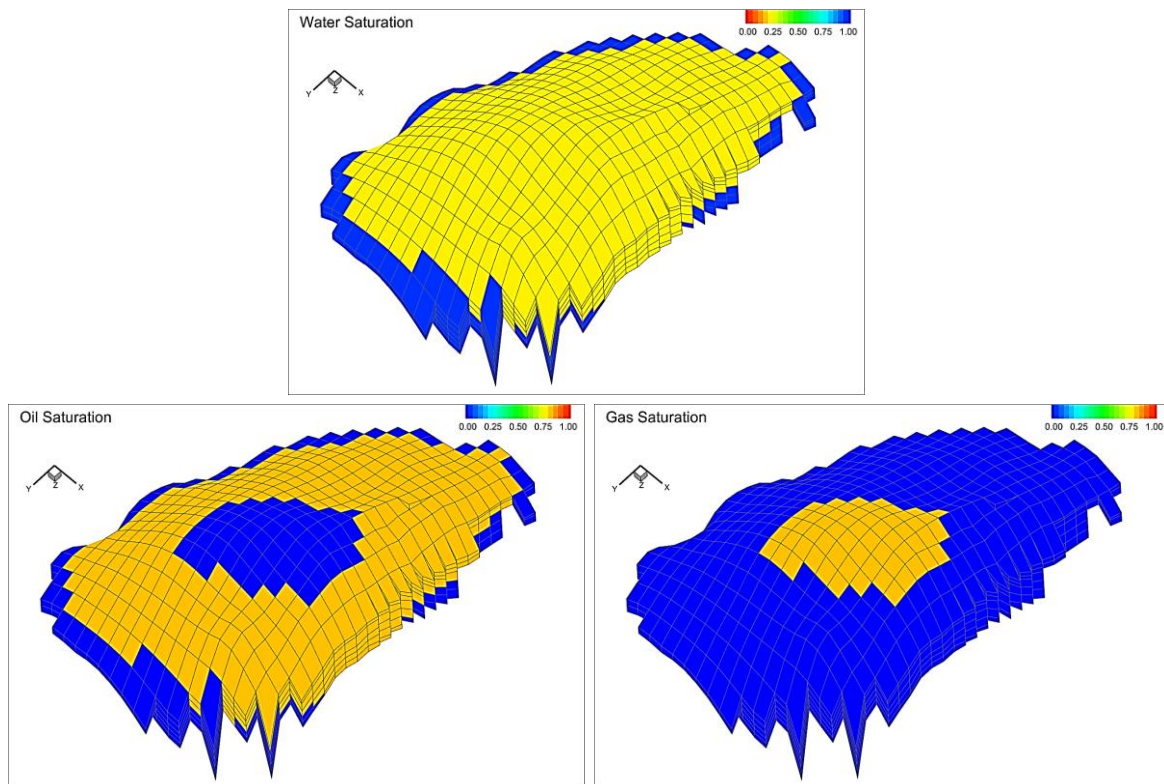


Figure 4.8: Initial water, oil, and gas saturation in the PUNQ-S3 reservoir.

4.3 Multisegment well model in ECLIPSE

To analyze the performance of OPENHOLE, ICD, AICD, and AICV in an advanced multi-lateral well a multisegment well is designed in ECLIPSE for the PUNQ-S3 reservoir. Figure 4.9 shows the multisegment well model with production outlet and injectors. ECLIPSE data file is given for the multi-lateral well with inflow control devices in Appendix B.

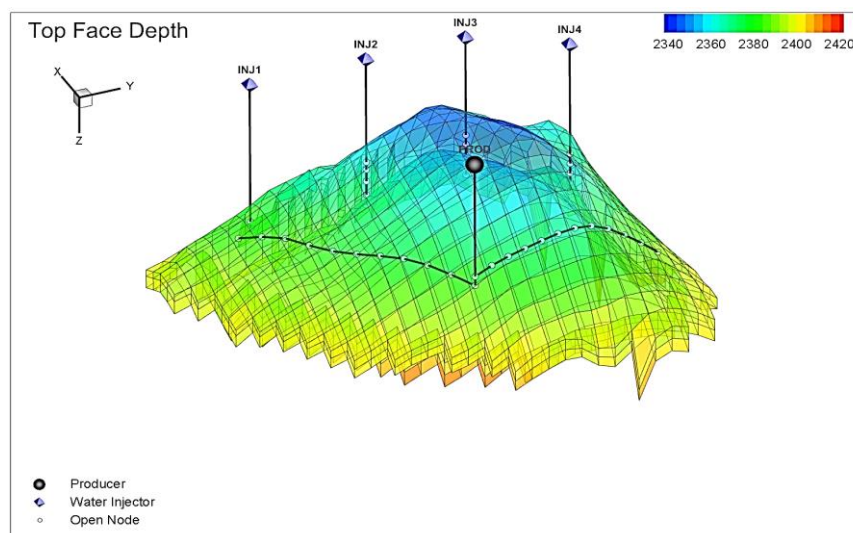


Figure 4.9: Multisegment well model in ECLIPSE.

5 Results and discussion

One of the main tasks of the study is to obtain simulation results in WAF and CO₂-WAG injection for oil recovery on three different FCDs (ICD, AICD, AICV) and compare them. Some of the results obtained through simulation by OLGA coupled with ECLIPSE and the rest obtained by simulation by ECLIPSE are discussed below.

5.1 Horizontal well with FCDs in OLGA and ECLIPSE

5.1.1 Oil production

Figure 5.1 shows the oil production rates for the OPENHOLE, ICD, and AICD simulated for 3500 days. Initially, in all the cases from 0 to 500 days oil production rate was higher. Then in all cases oil production rate decreases. OPENHOLE has an initial oil production rate higher than ICD and AICD. This happens as OPENHOLE is receiving more oil and gas for its bigger cross-sectional area than ICD and AICD. Both ICD and AICD are preventing gas production for initial production. But at the end of the simulation oil production for ICD and AICD is getting more oil production compared to OPENHOLE and if the simulation was continued for more than 3500 days, more oil could be produced with the inflow control devices. This is the benefit of using inflow control devices by optimizing the well design in oil recovery. Figure 5.1 also shows that there are some zig-zag patterns for numerical instabilities

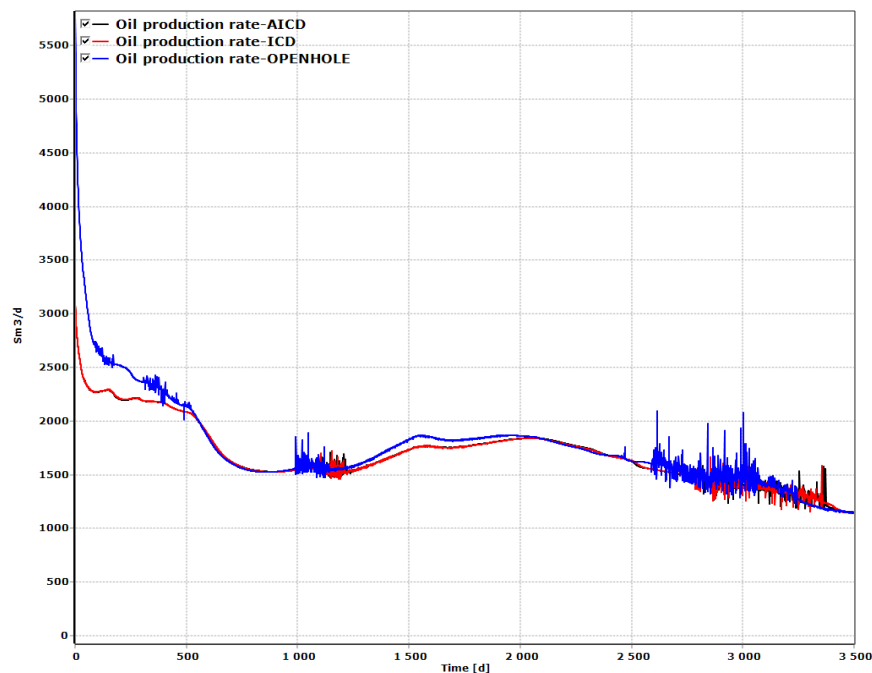


Figure 5.1: Oil production rate for OPENHOLE, ICD, and AICD.

Figure 5.2 shows the accumulated oil production for each device for 3500 days. Both figures show that ICD and AICD have similar rates of oil production. According to the theoretical study, AICD should have more oil production than other flow control devices. So, for 3500 days of production, there is no difference between using ICD and AICD. If the simulation

would run for more than 3500 days, like for 7500 days or more, AICD would produce more oil than ICD.

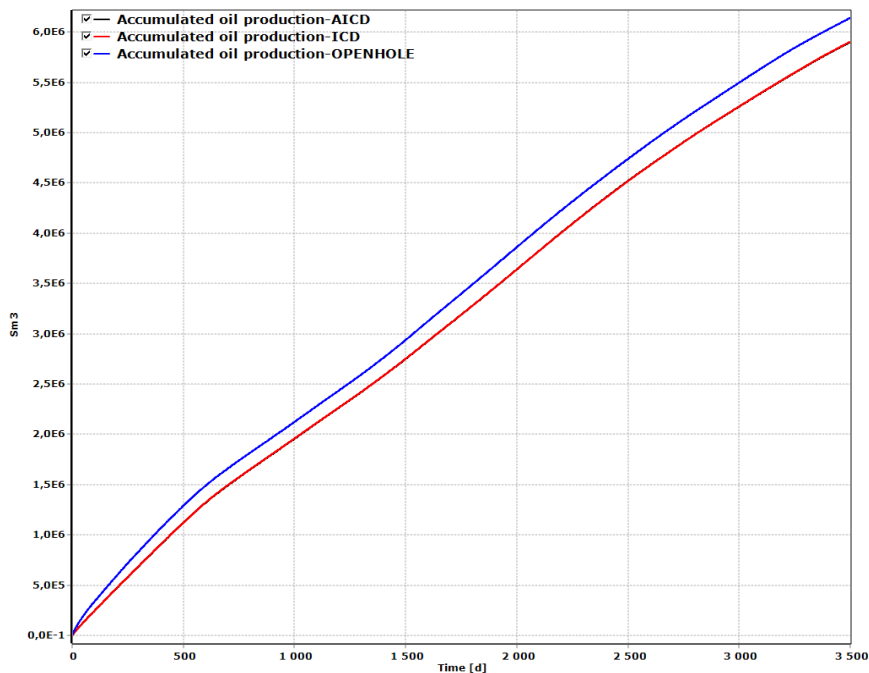


Figure 5.2: Accumulated oil production for OPENHOLE, ICD, and AICD.

5.1.2 Water production

Figure 5.3 shows that the initial water production for all the devices was zero. Water started to be produced for OPENHOLE at around 100 days and for ICD and AICD water started to be produced at around 200 days because these inflow control devices have a choking effect on water. Figure 5.4 shows the accumulated water production for 3500 days for all the devices.

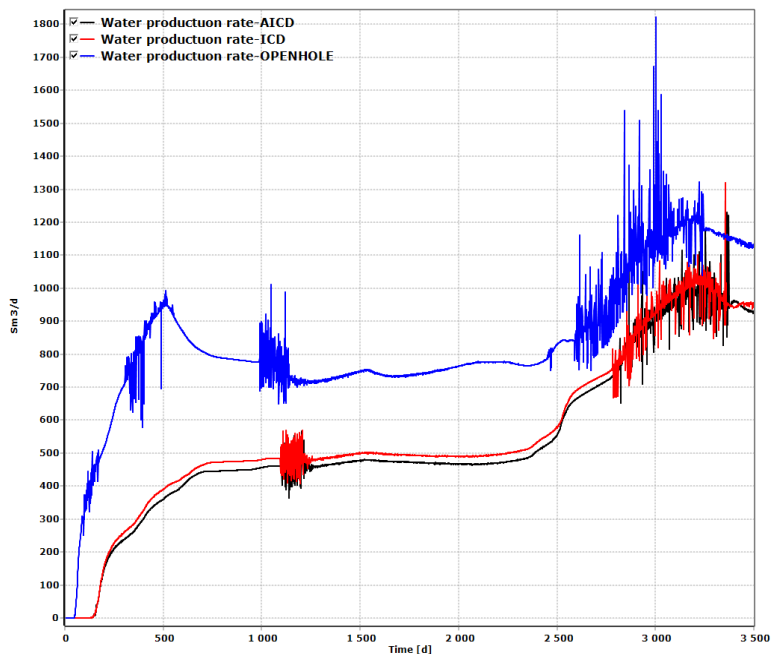


Figure 5.3: Water production rate for OPENHOLE, ICD, and AICD.

Both the figures show that the water production rate is significantly reduced when the inflow control devices are used. ICD and AICD have less water production by 33.8% and 36.3% respectively compared to OPENHOLE. Higher water production harms total production costs. Separating the water from oil is expensive which increases the cost for the overall production process. Besides, disposal of produced water needs special treatment which is also expensive. In this case, inflow control devices play an important role in preventing early water breakthroughs in the production process which has a positive effect on the economy and environment. AICD has less accumulated water production by 3.7% compared to ICD. This indicates that the algebraic controller is performing well for AICD valve opening control in preventing early water breakthrough.

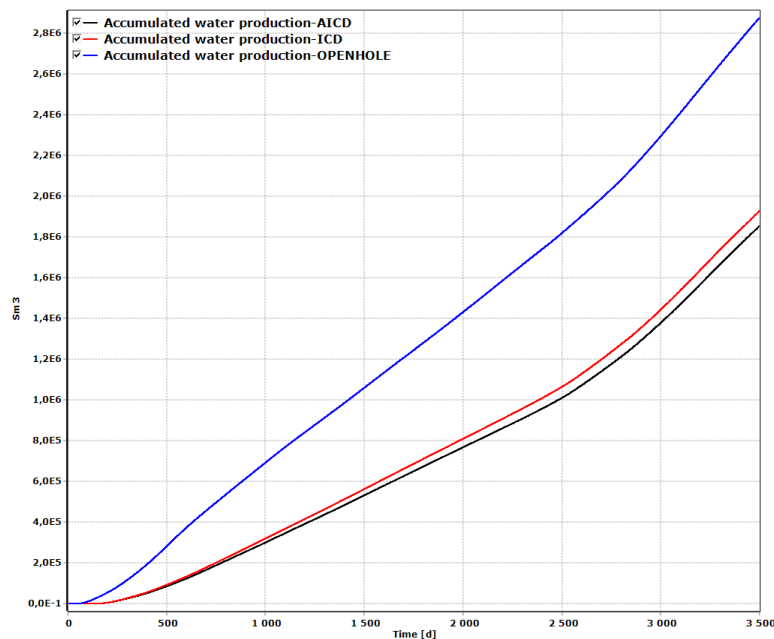


Figure 5.4: Accumulated water production for OPENHOLE, ICD, and AICD.

5.1.3 Liquid production

The limitation of liquid production for simulation was defined at 4000 m³/day. Figure 5.5 shows that all the devices have the same flow pattern for 3500 days of simulation. OPENHOLE setup shows higher liquid production than AICD and ICD because of having a bigger cross-sectional area and there is no choking effect. As a result, more water and oil are produced. ICD has a little higher rate of production than AICD. This is because ICD has a higher rate of water production but both ICD and AICD have the same rate of oil production. The functionality of the algebraic controller is responsible for less water production for AICD.

Figure 5.6 shows the accumulated liquid production for all the devices. Initially, AICD and ICD had the same rate of liquid production till 550 days. After that algebraic controller started to function for AICD and less liquid was produced. It is very important to have lower liquid production. Refining the recovered oil can extract a lot of carbon and using inflow control devices can reduce the carbon footprint by producing less liquid.

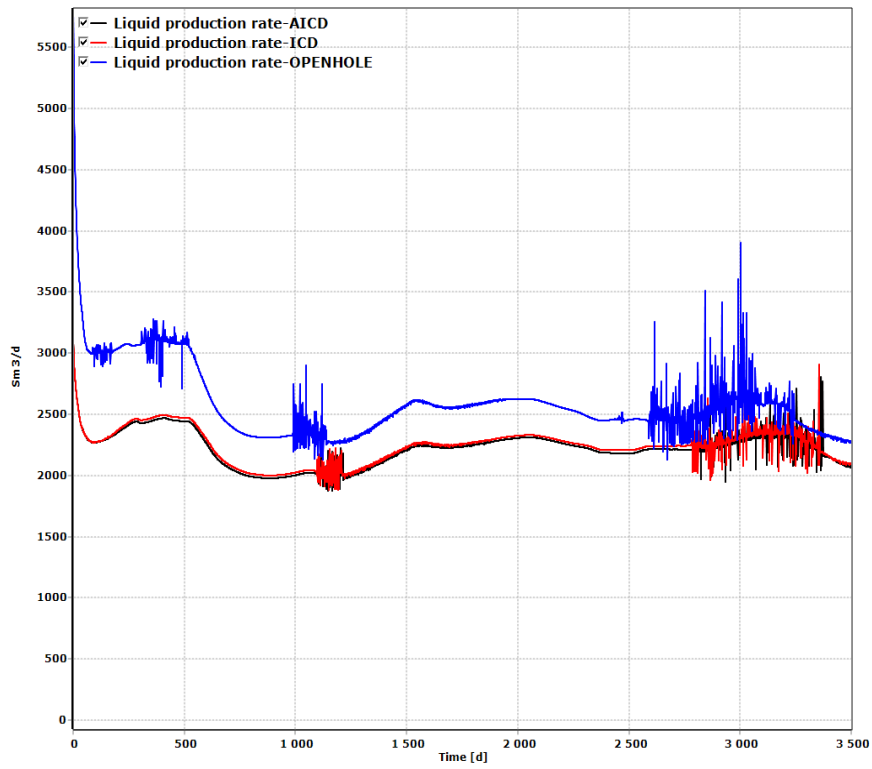


Figure 5.5: Liquid production rate for OPENHOLE, ICD, and AICD.

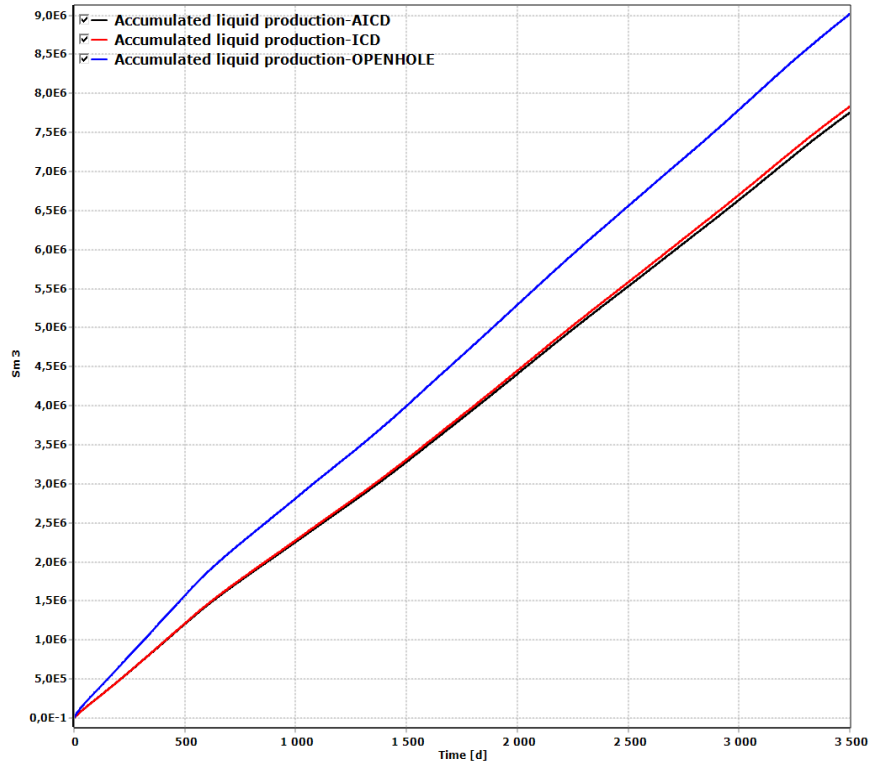


Figure 5.6: Accumulated liquid production for OPENHOLE, ICD, and AICD.

5.1.4 Water cut variations

Water cut in oil production has a greater impact on the economy and sustainability. For this reason, keeping the lower water cut is very important in the operation process. Figure 5.7 shows the water cut variations throughout the production pipe for each flow control device. Water cut increased gradually as there was water injection at regular intervals. OPENHOLE has the highest water cut of 0.442. ICD and AICD have a water cut of 0.408 and 0.399 respectively. This indicates that inflow control devices have more choking effects than OPENHOLE. Water cut is increasing for all the cases which means higher WC can be achieved for extended simulation time. Then it would be possible to observe the true impact of inflow control devices for advanced well technologies and more efficient oil production can be achieved.

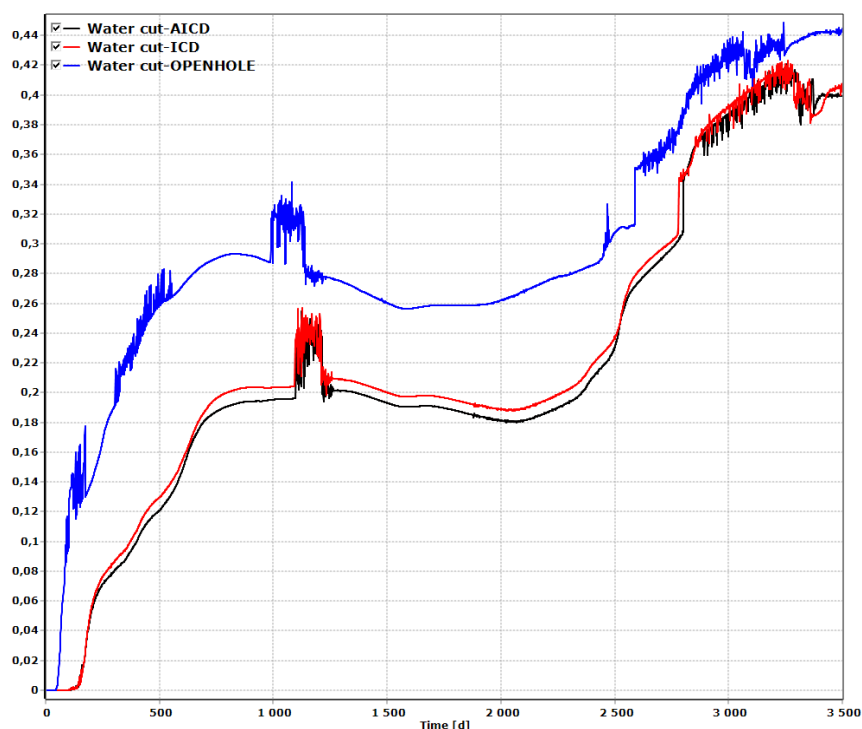


Figure 5.7: Water cut in OPENHOLE, ICD, and AICD.

5.1.5 Performance analysis of algebraic controller for AICD

In this study algebraic controller is used to control the valve opening of AICD. Equation (3.22) is implemented with two variables, water volume fraction and oil volume fraction. These two variables are taken by two transmitters from the production pipe. Appendix C is used for the known input variables. According to the calculation for Equation 3.22, Figure 5.8 shows the valve opening vs oil volume fraction considering no gas, no water, and some mixed phases. The blue solid line indicates the zero gas volume fractions. When the oil volume fraction is 1 the valve is fully opened. For example, if the oil volume fraction is 0.6 and the water cut is 0.4 then the valve opening is up to 0.94. The red solid line indicates the zero water cut and the valve opening is 1 for the oil volume fraction of 1. Like the previous example, considering the oil volume fraction of 0.6 and GVF of 0.4 then the valve opening is up to 0.98. For GVF of 50% valve opening is up to 0.97.

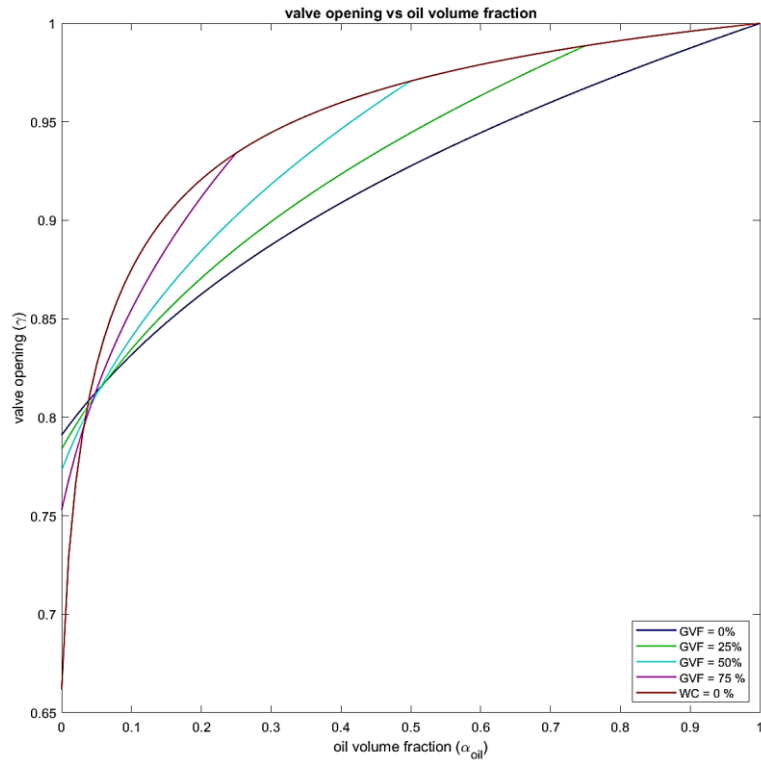


Figure 5.8: Valve opening vs oil volume fraction for the algebraic controller in different phases of fluid.

Figure 5.9 shows the valve opening of AICD for 3500 days of simulation for algebraic controllers 1 and 18 respectively in the toe and heel section.

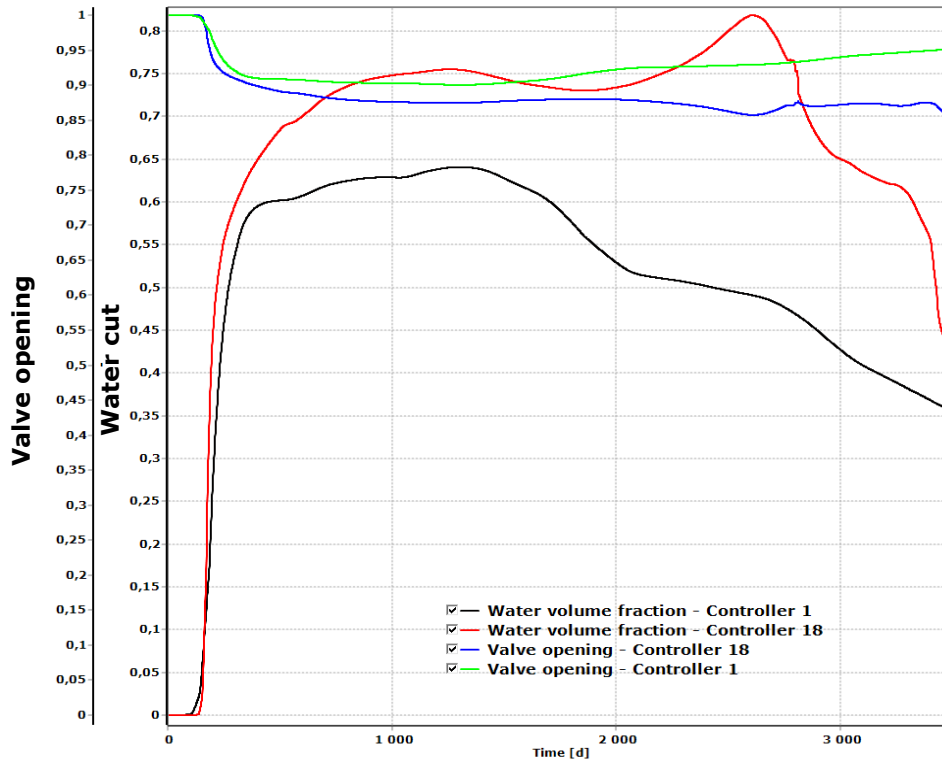


Figure 5.9: Valve opening with algebraic controller in toe (Controller 18) and heel section (Controller 1).

A maximum water cut of 0.64 and 0.82 was found for the toe and heel sections. At the toe section valve opening was up to 0.90 and at the heel section valve opening was up to 0.85. It can be observed that the more water cut increased the more valve opening was getting closed. From this observation, it can be said that the algebraic controller is showing the choking effect on water production.

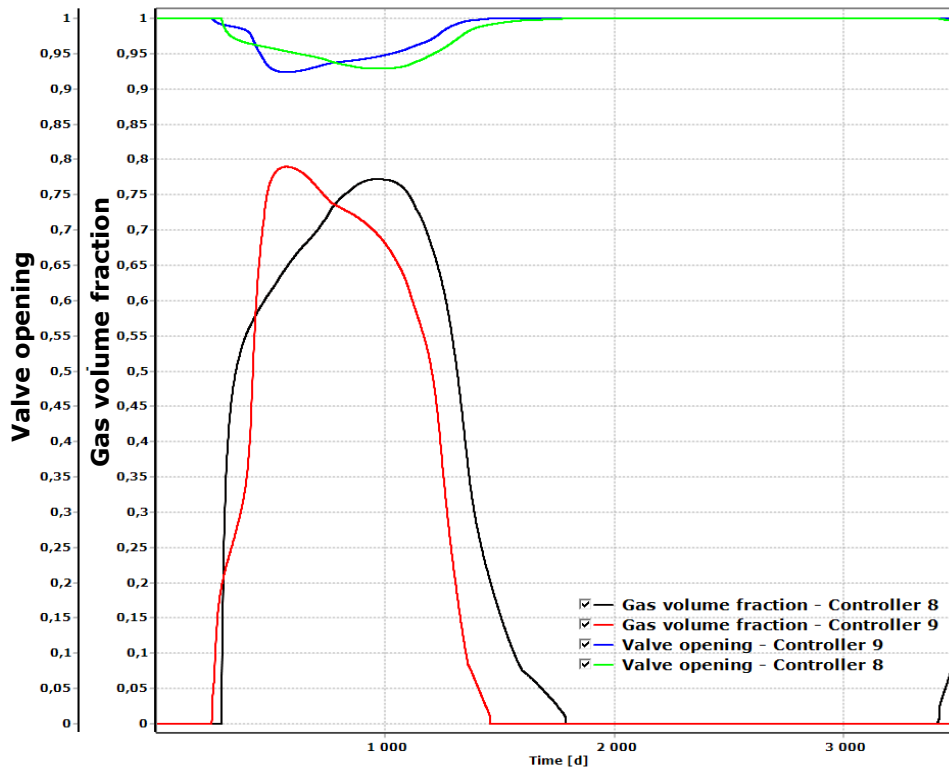


Figure 5.10: Valve opening of the algebraic controller according to GVF.

To observe the functionality of valve opening according to GVF controllers 8 and 9 are selected at the middle of the horizontal well. A maximum GVF of 0.77 and 0.79 was found for the controllers 8 and 9 respectively. For controller 8 valve opening was up to 0.93 and for controller 9 valve opening was up to 0.92. It can be observed that the more GVF was increased the more valve opening was getting closed. From this observation, it can be said that the algebraic controller is showing the choking effect on gas volume fraction.

From the analysis of Figure 5.9 and Figure 5.10, similarities can be observed with the analysis from Figure 5.8. Considering the oil volume fraction of 0.6 valve opening can be found up to 0.94 for water cut and up to 0.98. So, it can be said that the valve opening control for AICD with the algebraic controller is successful in OLGA/ECLIPSE simulation. The performance of the algebraic controller can be observed more for the extended simulation ti.

5.1.6 Fluid and gas saturations

The simulation was carried out in OLGA and ECLIPSE for 3500 days. Saturations of fluid for each device do not show much variation. Figure 5.11 shows the oil saturation in the reservoir after 3500 days.

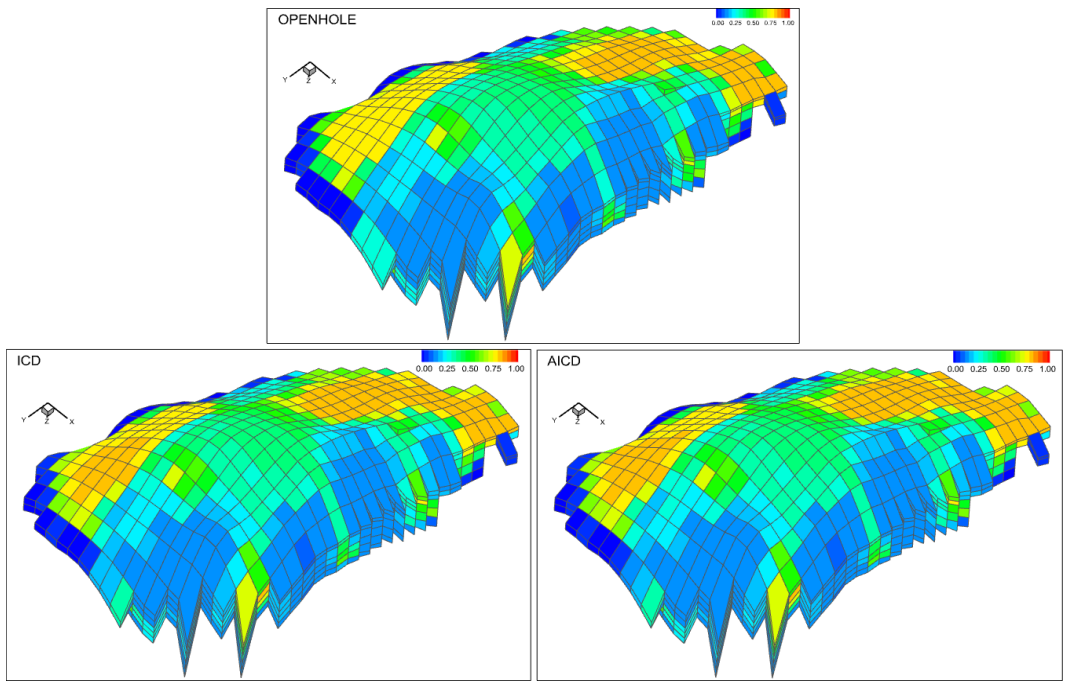


Figure 5 11: Oil saturation for OPENHOLE, ICD, and AICD after 3500 days.

Figure 5.12 and Figure 5.13 shows the water and gas saturation after 3500 days. From all the figures it can be observed that variation in fluid and gas saturation is almost similar. In some grids, residual oil is saturated between 0.50 to 0.75, which means more oil can be recovered from the reservoir for more simulation days. Upper grids are low in water saturation because of WAG injection and bottom grids still have some water because of water injection.

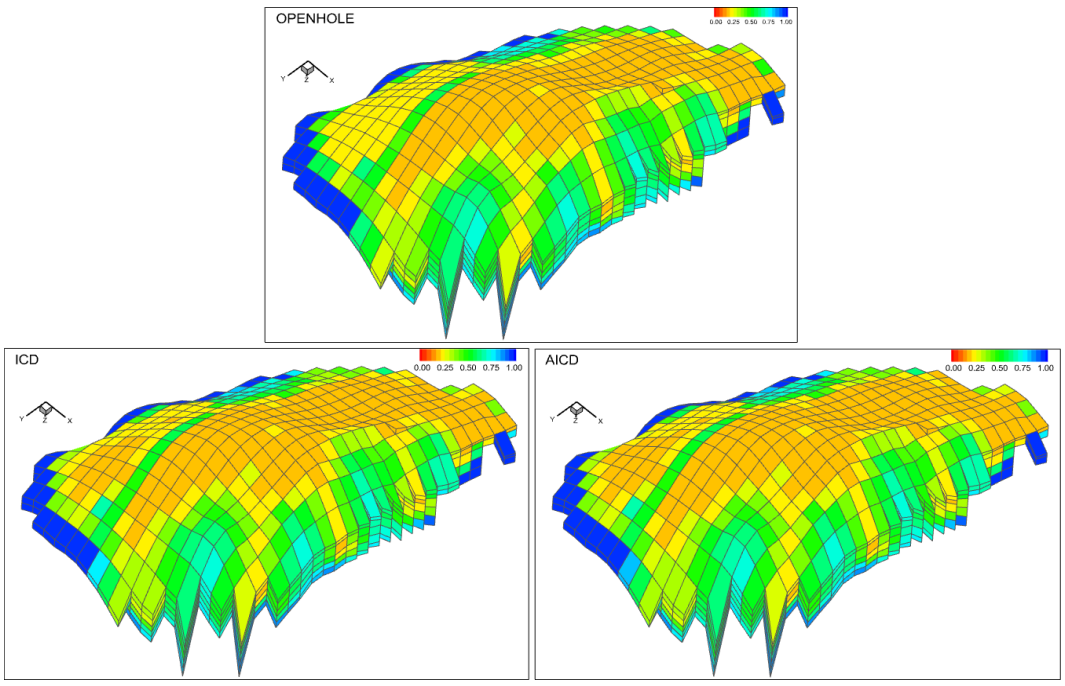


Figure 5.12: Water saturation for OPENHOLE, ICD, and AICD after 3500 days.

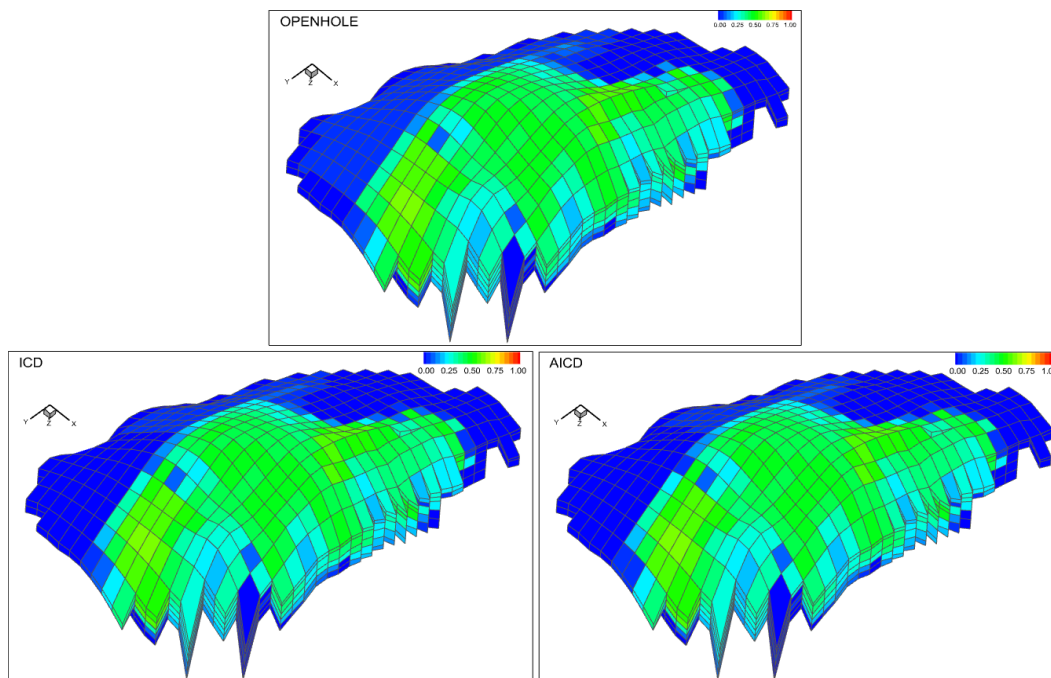


Figure 5.13: Gas saturation for OPENHOLE, ICD, and AICD after 3500 days.

5.2 CO₂-WAG vs WAG

CO₂-WAG injection and WAG injection EOR simulations were carried out for 7500 days for a horizontal well in ECLIPSE. The simulation was implemented only for the OPENHOLE case to find out the performance of CO₂-WAG injection and WAG injection. In this chapter comparison between the CO₂-WAG injection and the WAG injection is shown.

5.2.1 Oil production

Figure 5.14 shows the oil production rate and the total oil production rate for CO₂-WAG injection and WAG injection. In general natural gas is injected for the WAG injection process where heavy components like propane, butane, etc. can be dissolved. For this study, immiscible WAG injection is considered and miscibility is considered for the CO₂-WAG injection. For this reason, it is observed that CO₂-WAG injection has more oil production than the WAG injection process. Because of the miscibility of the CO₂, oil gets more mobility to the production zone and then more oil can be produced. Fluctuations of oil production can be seen for CO₂-WAG injection and this continued for the whole simulation time. Two major fluctuations around 1000 days and 2000 are observed. This higher production rate of oil would not be possible if only the water flooding technique was used. However, after 4500 days of simulation, fluctuations are not observed in oil production for WAG injection. This indicates the immiscible characteristics of the WAG injection process. From the total production of oil, it can be said that CO₂-WAG injection performs better than WAG injection.

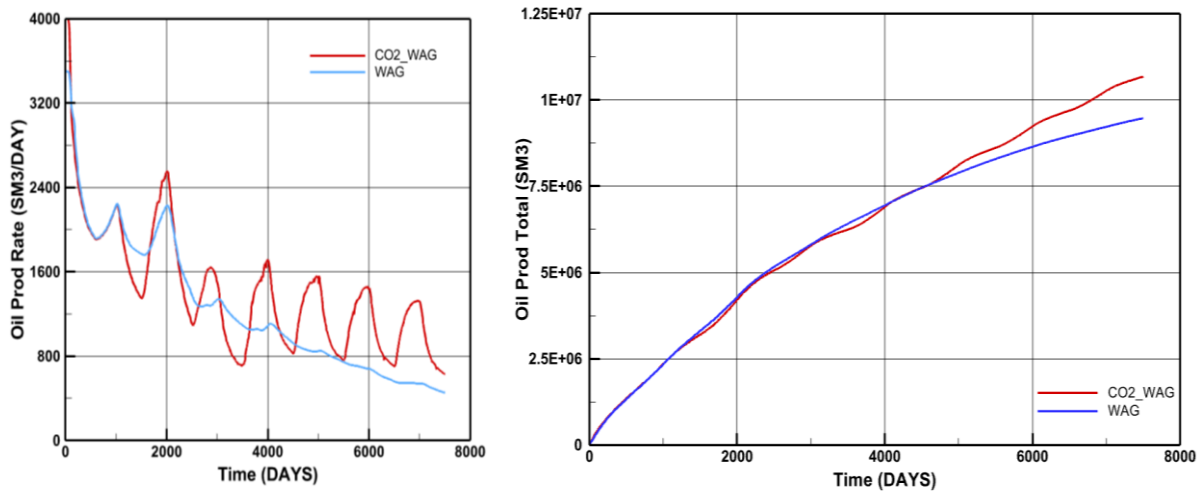


Figure 5.14: Oil production rate and total oil production for CO₂-WAG injection and WAG injection.

5.2.2 Water production

Figure 5.13 shows the water production rate and total water production for CO₂-WAG injection and WAG injection. CO₂-WAG performed better as it has a lower water production rate than WAG injection. Because of the miscible characteristics of CO₂ with residual oil, the mixture viscosity is lower than the water viscosity. For this reason, more oil is pushed to the production zone than water. In the WAG injection process, oil is pushed only by water and gas but is not mixed with the residual oil.

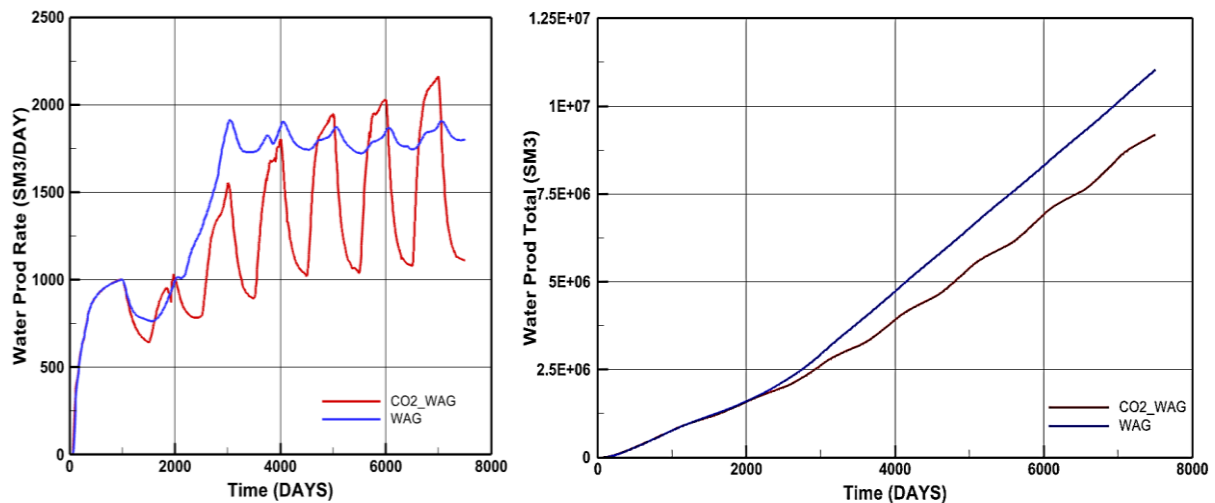


Figure 5.15: Water production rate and total oil production for CO₂-WAG injection and WAG injection.

5.2.3 Water cut and GOR

Figure 5.16 shows the water cut for CO₂-WAG injection and WAG injection. CO₂-WAG has less water cut than WAG injection. CO₂-WAG has a water cut of 0.65 and WAG has 0.80. Figure 5.17 shows the GOR for CO₂-WAG injection and WAG injection. CO₂-WAG injection has lower GOR than WAG injection. In this study, only OPENHOLE was simulated. A lower water cut and lower gas oil ratio would be observed if inflow control devices were used. Better oil production would be observed too using the inflow control devices.

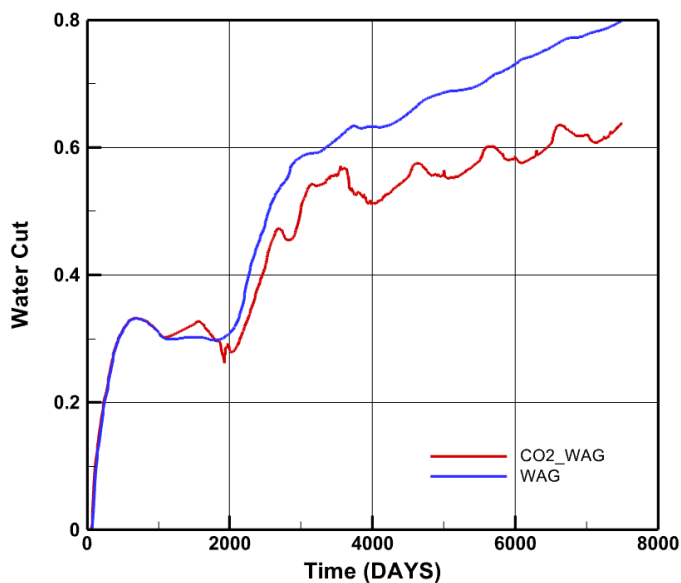


Figure 5.16: Water cut for CO₂-WAG injection and WAG injection.

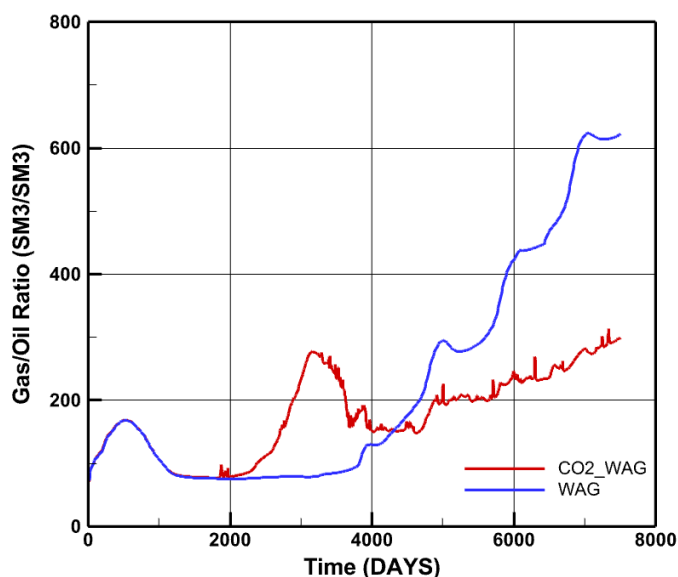


Figure 5.17: GOR for CO₂-WAG injection and WAG injection.

5.3 Multilateral wells with different FCDs

The multilateral lateral well simulation was carried out in ECLIPSE for 11,000 days. Flow control devices such as ICD, AICD, and AICV are used along with the OPENHOLE case for their performance analysis.

5.3.1 Oil production

Figure 5.18 shows the oil production rate and total oil production for all the devices in the multilateral wells. There is no significant change in oil production for all the inflow control devices. All the cases showed almost similar oil production rates. Within this similarity, it can be observed that AICV has a slightly higher production. Also, all the FCDs showed a decreasing manner in production and there are not many fluctuations. With the multi-lateral advanced well model, oil can be produced more from the oil-saturated zone of the reservoir. As a result, oil production efficiency rises. Besides using inflow control devices prevents early water and gas coning. Continuous production of oil is also found because of better sweep efficiency.

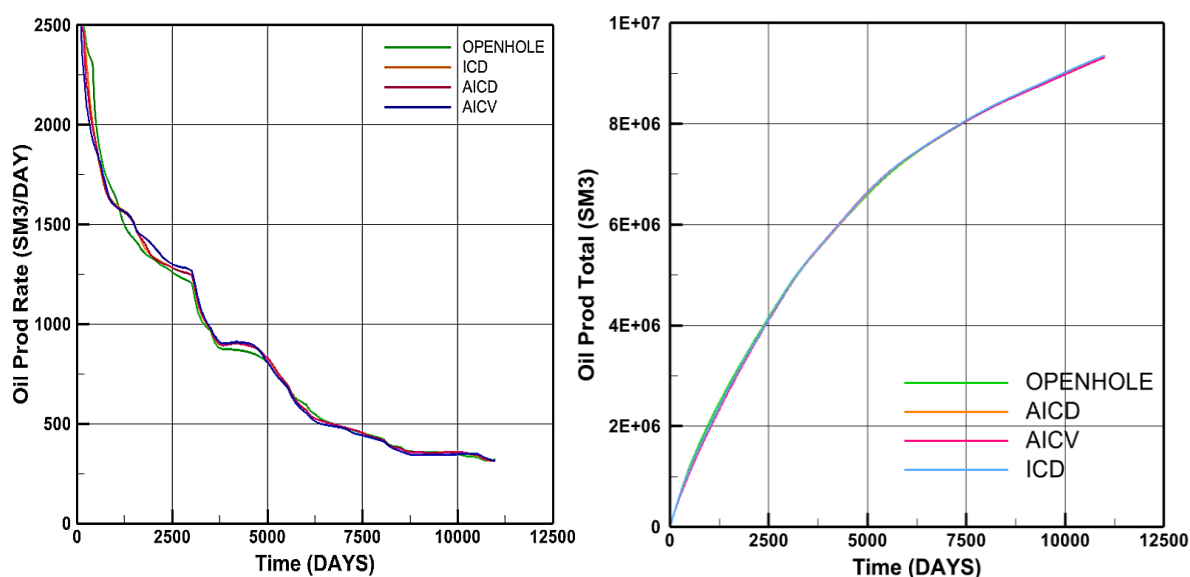


Figure 5.18: Oil production rate and total oil production in multi-lateral well for all the FCDs.

5.3.2 Water production

Figure 5.19 shows the water production rate for all the devices in the multilateral well. Among all the cases OPENHOLE has the most water production because of more production area. Fluid can pass through easily with a bigger cross-sectional area. Using inflow control devices minimized water production. ICD, AICD, and AICV have less water production by 4.5%, 7.2%, and 14% respectively compared to OPENHOLE. AICD and AICV have the best choking effect on low viscous fluid. As already mentioned less water production minimizes the total processing cost of oil production. Inflow control devices help to prevent early water and gas

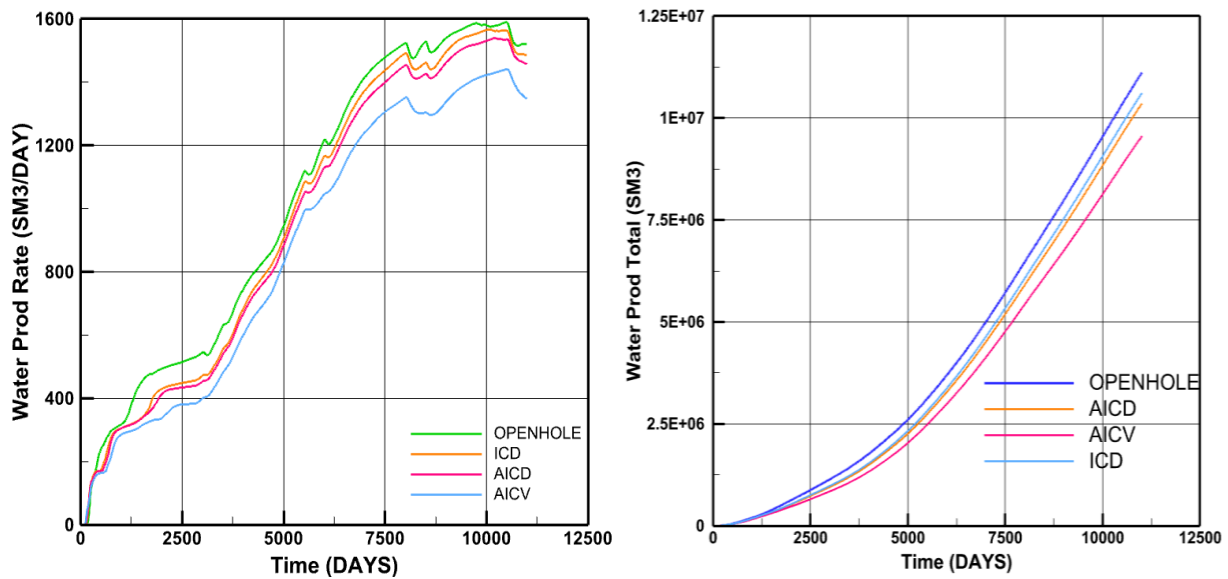


Figure 5.19: Water production rate and total water production in multi-lateral wells for all the FCDs.

breakthroughs in total liquid production. This plays an important role in the economy by reducing water separation and disposal expenses.

5.3.3 Water cut

Figure 5.20 shows the water cut variations for all the FCDs. OPENHOLE, ICD, AICD, and AICV have a water cut of 0.83, 0.825, 0.820, and 0.81 respectively. AICV has less water cut than other inflow control devices. Less water cut means AICV has the best performance in the oil recovery process and has a better choking effect on the water production. If the simulation was run for a more extended period functionality of the inflow control devices would be observed more.

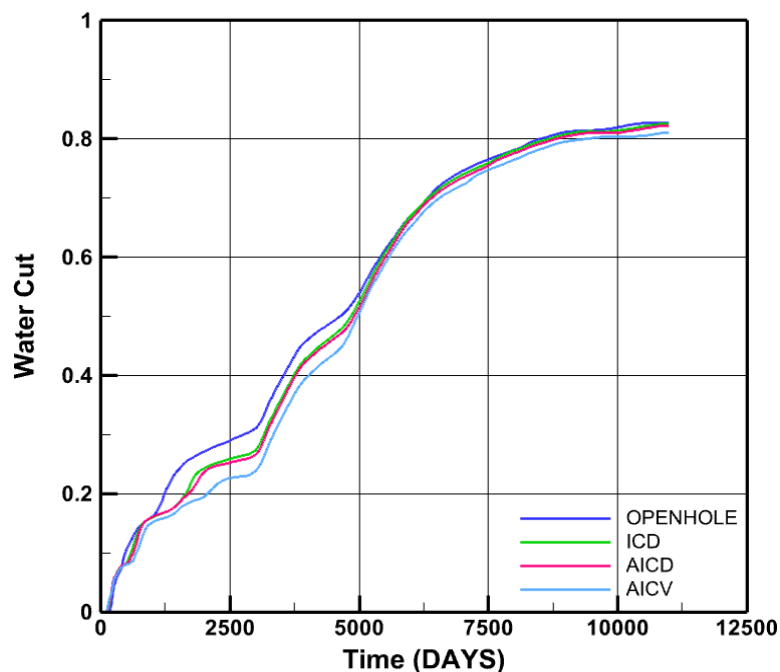


Figure 5.20: Water cut for OPENHOLE, ICD, AICD, and AICV in multi-lateral well.

5.4 Water/CO₂ injection ratio for CO₂-WAG injection

To find out the best water/CO₂ injection ratio simulations were carried out in ECLIPSE for ratios 1, 1.5, 2, 2.5, 3, 3.5, and 4. Figure 5.21 shows the total oil production for all the ratios. For the initial 1000 days, oil production was equal for all the ratios. A water/CO₂ ratio of 1 has the best oil production and a ratio of 4 has the least water production. From ratio 1 to ratio 2 it maintains the production but the ratio of 3.5 has better oil production capacity than the ratios of 2.5, 3, and 4.

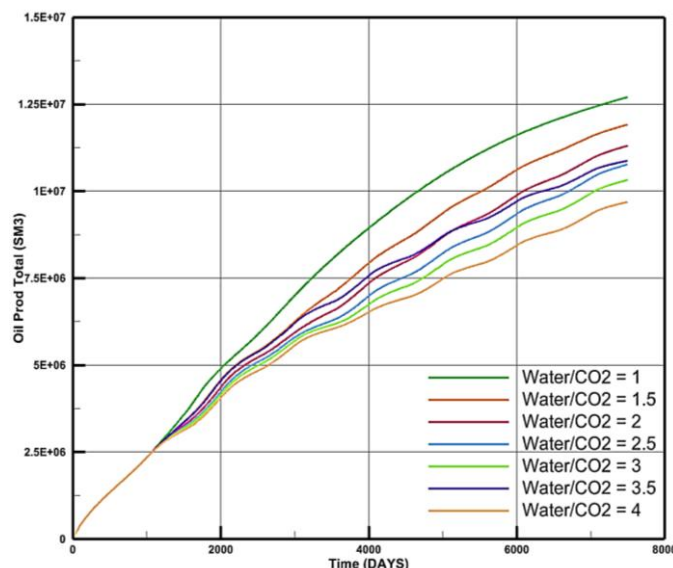


Figure 5.21: Oil production for different water/CO₂ injection ratios.

Figure 5.22 shows the water production for all the mentioned ratios. In terms of water production ratios 4, 3, and 2.5 have the same production patterns. Then ratios 1, 2, 1.5, and 3.5 have different patterns.

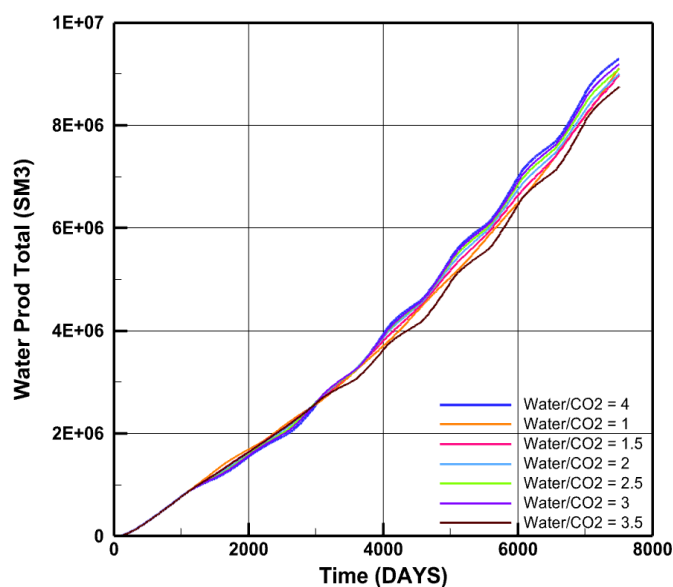


Figure 5.22: Water production for different water/CO₂ injection ratios.

Oil production does not increase if the water/CO₂ injection ratio increases. Ratios 1, 1.5, and 2 have more oil production because injected CO₂ gets mixed with the residual oil and enhances

the mixture's mobility to the production zone. A higher injection ratio means more water injection and comparatively less CO₂ injection. For this, the formation of water channeling is found [46]. This can create a blockage for oil mobility as residual oil can be mixed properly with the injected gas. Formation of water channeling leads the injected gas to store in pores for increasing pressure. When the pressure reaches its limit a flow path is created and more oil recovery can be observed [46]. This can be a possible reason for the water/CO₂ ratio of 3 for not following the sequential pattern in oil production.

From the above-mentioned analysis, it can be said that the water/CO₂ ratio of 1.5 is the best ratio with better oil production considering lower water production. the water/CO₂ ratio of 1 and 2 also showed a better performance than the rest of the ratios.

5.5 Discussion

5.5.1 Simulation in OLGA/ECLIPSE

In this study, the AICD valve opening control was controlled by an algebraic controller for WAG injection. The simulation was carried out for 3500 days. If the simulation time can be extended for 7500 days or 20 years then the efficiency of the AICD can be observed better. The functionality of the algebraic controller for AICD valve opening control can be observed better with extended simulation time. Another observation is that the simulation of an advanced multi-lateral well for the heterogenous reservoir is time-consuming with OLGA/ECLIPSE coupling. For this reason, only the horizontal well was modeled and simulated in OLGA coupled with ECLIPSE.

5.5.2 Simulation in ECLIPSE

To show the comparison between CO₂-WAG injection and WAG injection, a simulation was carried out in ECLIPSE for the horizontal well model. The solvent model was used for the CO₂-WAG injection model. An error message occurred when the simulation case was chosen for the multi-segment well model for CO₂-WAG injection. It is said that the solvent model can not be used for the multi-segment well model for CO₂-WAG injection. But it was not mentioned in any manual of ECLIPSE. Figure 5.23 shows the error message generated during the simulation for the multi-segment well model of CO₂-WAG injection.

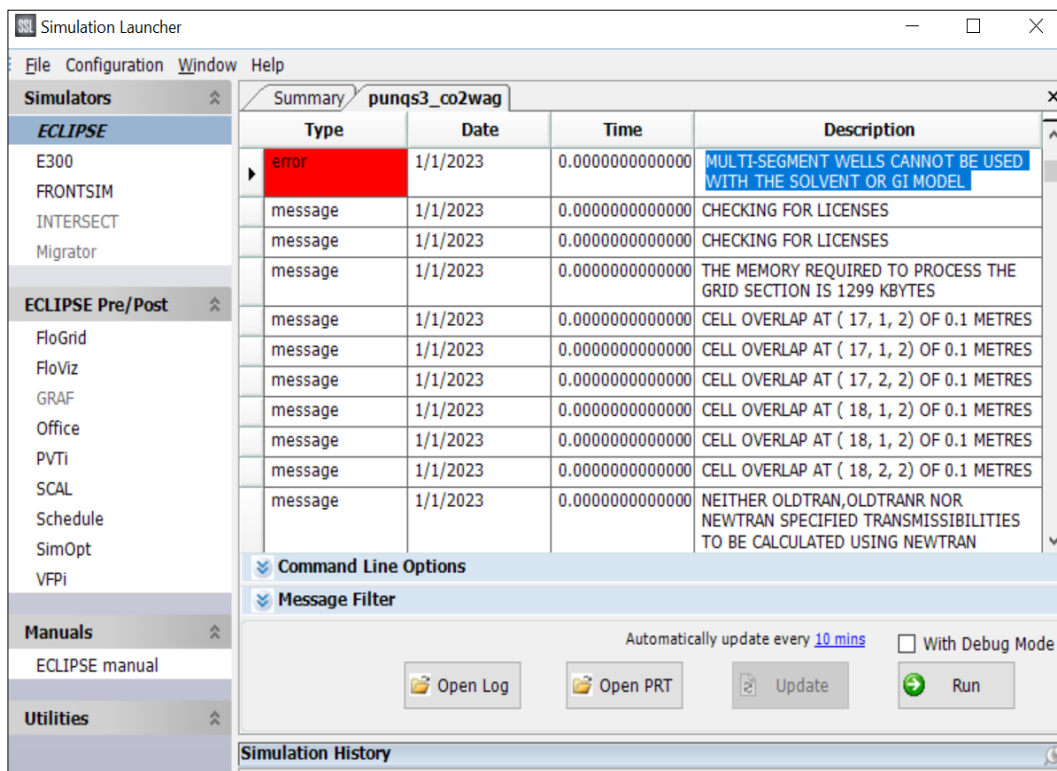


Figure 5.23: Error message generated in ECLIPSE.

5.5.3 Future task recommendation

- Simulation for 7500 days or more to observe the performance of the AICD valve control using the algebraic controller.
- Simulation for the performance analysis of the AICV valve opening control using the algebraic controller.
- Simulation of multi-lateral well models for CO₂-WAG and WAG injection in OLGA coupled with ECLIPSE.
- A compositional model can be used for the simulation of the CO₂-WAG EOR for the multisegment well model in ECLIPSE.

6 Conclusion

The main objective of this thesis is to simulate CO₂-WAG injection, and WAG injection for advanced multi-lateral wells in the heterogeneous PUNQ-S3 reservoir using OLGA and ECLIPSE simulator. OLGA and ECLIPSE were coupled for the simulation of the WAG injection process which can be referred to as a novel approach. Generally, this kind of coupling method is not used. However, simulation and modeling oil models with the coupling of OLGA and ECLIPSE is time-consuming. For this reason, it was needed to simulate only an advanced horizontal well.

A literature review is presented on EOR with CO₂-WAG injection, WAG injection, and advanced multi-lateral wells including inflow control technologies. After that, a theoretical study is presented which is related to reservoir engineering.

Preventing early water and gas breakthroughs is very important in the oil recovery process. Inflow control devices like ICD, AICD, and AICV can prevent this kind of unwanted fluid. From the simulation result, it is observed that AICD and AICV have better choking effects on this unwanted fluid for a long time. ICD is unable to prevent early fluid breakthroughs for a longer time compared to AICD and AICV. This kind of inflow control technology simulated both an advanced horizontal well and an advanced multi-lateral well. In the horizontal case, ICD and AICD have less water production by 33.8% and 36.3% respectively compared to OPENHOLE. In multi-lateral cases, ICD, AICD, and AICV have less water production by 4.5%, 7.2%, and 14% respectively compared to OPENHOLE.

A novel approach was to control the AICD valve opening by using the algebraic controller feature in OLGA. Considering the water and gas volume fractions a mathematical model is implemented for the algebraic controller which has successfully lowered the water production. Both AICD and ICD had the same oil production but AICD had less accumulated water production by 3.7% compared to ICD by using the algebraic controller.

Performance comparison was shown in this study for CO₂-WAG injection, and WAG injection process where CO₂-WAG injection had the higher oil production. CO₂-WAG injection has lower water production than WAG injection with a water cut of 0.65 and 0.80 respectively.

Using the solvent model for the CO₂-WAG injection process with multi-lateral wells is not possible to simulate, which can be referred to as a significant finding from this study. This finding can be an insight for future studies in the oil recovery process.

Using the better water/CO₂ injection ratio is important for EOR with CO₂-WAG injection. Seven ratios from 1 to 4 with an interval of 0.5 were selected and simulated to analyze the better ratio for efficient oil recovery. Among them, the water/CO₂ injection ratio of 1.5 has the best production rate.

The difficulties and challenges are also discussed in this study. All the objectives were successfully fulfilled with analysis and several tasks were also recommended for future study.

References

- [1] U. Ali, “The history of the oil and gas industry from 347 AD to today,” Offshore Technology. Accessed: May 03, 2024. [Online]. Available: <https://www.offshore-technology.com/comment/history-oil-gas/?cf-view&cf-closed>
- [2] Our World in Data, “Oil consumption,” Energy Institute - Statistical Review of World Energy. Accessed: May 03, 2024. [Online]. Available: <https://ourworldindata.org/grapher/oil-consumption-by-region-terawatt-hours-twh>
- [3] NORWEGIANPETROLEUM.NO, “PRODUCTION FORECASTS,” Ministry of Energy and the Norwegian Offshore Directorate.
- [4] Aakre Haavard, Halvorsen Britt, Werswick Bjørnar, and Mathiesen Vidar, “Smart Well With Autonomous Inflow Control Valve Technology ,” *SPE Middle East Oil and Gas Show and Conference*, Mar. 2013, doi: <https://doi.org/10.2118/164348-MS>.
- [5] PetroWiki, “Multilateral wells,” SPE International. Accessed: May 03, 2024. [Online]. Available: https://petrowiki.spe.org/Multilateral_wells
- [6] V. Vishnyakov, B. Suleimanov, A. Salmanov, and E. Zeynalov, “7 - Oil recovery stages and methods,” in *Primer on Enhanced Oil Recovery*, V. Vishnyakov, B. Suleimanov, A. Salmanov, and E. Zeynalov, Eds., Gulf Professional Publishing, 2020, pp. 53–63. doi: <https://doi.org/10.1016/B978-0-12-817632-0.00007-4>.
- [7] Office of FOSSIL ENERGY AND CARBON MANAGEMENT, “Enhanced Oil Recovery.” Accessed: Oct. 17, 2023. [Online]. Available: [https://www.energy.gov/fecm/enhanced-oil-recovery#:~:text=Crude%20oil%20development%20and%20production,tertiary%20\(or%20enhanced\)%20recovery.](https://www.energy.gov/fecm/enhanced-oil-recovery#:~:text=Crude%20oil%20development%20and%20production,tertiary%20(or%20enhanced)%20recovery.)
- [8] P. Kalita, V. Sharma, L. Pandey, and P. Tiwari, “Secondary and Tertiary Oil Recovery Processes,” in *Microbial Enhanced Oil Recovery: Principles and Potential*, L. Pandey and P. Tiwari, Eds., Singapore: Springer Singapore, 2022, pp. 23–50. doi: [10.1007/978-981-16-5465-7_2](https://doi.org/10.1007/978-981-16-5465-7_2).
- [9] S. Afzali, N. Rezaei, and S. Zendejboudi, “A comprehensive review on Enhanced Oil Recovery by Water Alternating Gas (WAG) injection,” *Fuel*, vol. 227, pp. 218–246, 2018, doi: <https://doi.org/10.1016/j.fuel.2018.04.015>.
- [10] F. Luis, A.-H. Khaled, B.-A. Khaled, and A.-A. Fatema, “Performance Review and Field Measurements of an EOR-WAG Project in Tight Oil Carbonate Reservoir-Abu Dhabi Onshore Field Experience,” 2014. doi: doi.org/10.2118/171871-MS.
- [11] National Energy Technology Laboratory, “Commercial Carbon Dioxide Uses: Carbon Dioxide Enhanced Oil Recovery.”
- [12] M. Al-Shargabi, S. Davoodi, D. A. Wood, V. S. Rukavishnikov, and K. M. Minaev, “Carbon Dioxide Applications for Enhanced Oil Recovery Assisted by Nanoparticles: Recent Developments,” *ACS Omega*, vol. 7, no. 12, pp. 9984–9994, Mar. 2022, doi: [10.1021/acsomega.1c07123](https://doi.org/10.1021/acsomega.1c07123).
- [13] National Energy Technology Laboratory, “Carbon Dioxide Enhanced Oil Recovery - Untapped Domestic Energy Supply and Long Term Carbon Storage Solution.”

- [14] D. S. Whittaker and D. E. Perkins, “Technical aspects of CO₂ enhanced oil recovery and associated carbon storage,” *Global CCS Institute*, 2013.
- [15] O. M. Mathiassen, “CO₂ as Injection Gas for Enhanced Oil Recovery and Estimation of the Potential on the Norwegian Continental Shelf,” Trondheim/Stavanger, 2003.
- [16] L. B. J. Chaturangani and B. M. Halvorsen, “Near well simulation of CO₂ injection for Enhanced Oil Recovery (EOR).”
- [17] S. Fakher and A. Imqam, “A data analysis of immiscible carbon dioxide injection applications for enhanced oil recovery based on an updated database,” *SN Appl Sci*, vol. 2, no. 3, p. 448, 2020, doi: 10.1007/s42452-020-2242-1.
- [18] A. Hashemi Fath and A.-R. Pouranfard, “Evaluation of miscible and immiscible CO₂ injection in one of the Iranian oil fields,” *Egyptian Journal of Petroleum*, vol. 23, no. 3, pp. 255–270, 2014, doi: <https://doi.org/10.1016/j.ejpe.2014.08.002>.
- [19] Rick von Flatern, “The Defining Series: Multilateral Wells,” *Oilfield Review*. Accessed: Oct. 29, 2023. [Online]. Available: <https://www.slb.com/resource-library/oilfield-review/defining-series/defining-multilateral-wells>
- [20] F. T. Al-Khelaiwi and D. D.R., “Inflow Control Devices: Application and Value Quantification of a Developing Technology,” *International Oil Conference and Exhibition*, 2007, doi: <https://doi.org/10.2118/108700-MS>.
- [21] L.-B. Ouyang, “SPE 124154 Practical Consideration of an Inflow Control Device Application for Reducing Water Production,” *SPE Annual Technical Conference and Exhibition*, pp. 4–7, 2009, doi: <https://doi.org/10.2118/124154-MS>.
- [22] Fripp Michael, Zhao Liang, and Least Brandon, “The Theory of a Fluidic Diode Autonomous Inflow Control Device,” *SPE Middle East Intelligent Energy Conference and Exhibition*, Oct. 2013, doi: <https://doi.org/10.2118/167415-MS>.
- [23] Halvorsen Martin, Madsen Martin, Vikøren Mo Mathias, Isma Mohd Ismail, and Green Annabel, “Enhanced Oil Recovery On Troll Field By Implementing Autonomous Inflow Control Device ,” *Annabel* , Apr. 2016, doi: <https://doi.org/10.2118/180037-MS>.
- [24] S. Taghavi, H. Aakre, S. Amin Tahami, and B. M. E. Moldestad, “The Impact of Autonomous Inflow Control Valve on Improved Oil Recovery in a Thin-Oil-Rim Reservoir,” *SPE Journal*, 2024, [Online]. Available: <http://onepetro.org/SJ/article-pdf/29/04/1989/3388553/spe-218393-pa.pdf/1>
- [25] X. Huang, “Petrophysics.” Accessed: Mar. 17, 2024. [Online]. Available: <https://petgeo.weebly.com/petrophysics.html>
- [26] D. Tiab and E. C. Donaldson, *Petrophysics: Theory and Practice of Measuring Reservoir Rock and Fluid Transport Properties*, 4th ed. Elsevier: Gulf Professional Publishing, 2015.
- [27] A. Y. Dandekar, *Petroleum reservoir rock and fluid properties*, 2nd ed. Taylor & Francis Group, 2013.
- [28] M. A. Sattar, “Effective and Relative Permeability,” AONG manager.
- [29] S&P, “Relative Permeability,” Energy Portal. Accessed: Apr. 22, 2024. [Online]. Available:

- https://www.ihsenergy.ca/support/documentation_ca/Harmony/content/html_files/reference_material/general_concepts/relative_permeability.htm
- [30] R. Nolen-Hoeksema, “The Defining Series: Wettability,” Schlumberger NV - Oilfield Review. Accessed: Mar. 21, 2024. [Online]. Available: <https://www.slb.com/resource-library/oilfield-review/defining-series/defining-wettability>
- [31] Reservoir Engineering Online, “Capillary Pressure.” Accessed: May 06, 2024. [Online]. Available: <https://reservoironline.blogspot.com/2014/08/capillary-pressure.html>
- [32] C. Team, “Crude Oil Overview,” CFI. Accessed: Apr. 07, 2024. [Online]. Available: <https://corporatefinanceinstitute.com/resources/economics/crude-oil-overview/>
- [33] P. Luna and A. Hidalgo, “MATHEMATICAL MODELING AND NUMERICAL SIMULATION OF TWO-PHASE FLOW PROBLEMS AT PORE SCALE,” *ResearchGate*, vol. 22, pp. 79–97, Jan. 2015.
- [34] B. Tolbert, “Types of Reservoir Fluids,” Top Dog Engineer. Accessed: Apr. 08, 2024. [Online]. Available: <https://topdogengineer.com/types-of-reservoir-fluids/>
- [35] B. Guo, K. Sun, and A. Ghalambor, “Well Productivity Handbook: Vertical, Fractured, Horizontal, Multilateral, and Intelligent Wells,” Houston, Texas, 2008.
- [36] SLB, “water cut,” Energy Glossary. Accessed: Apr. 09, 2024. [Online]. Available: https://glossary.slb.com/en/Terms/w/water_cut.aspx
- [37] A. Moradi, N. A. Samani, A. S. Kumara, and B. M. E. Moldestad, “Evaluating the performance of advanced wells in heavy oil reservoirs under uncertainty in permeability parameters,” *Energy Reports*, vol. 8, pp. 8605–8617, Nov. 2022, doi: 10.1016/j.egy.2022.06.077.
- [38] A. F. Rasmussen *et al.*, “The Open Porous Media Flow reservoir simulator,” *Computers and Mathematics with Applications*, vol. 81, pp. 159–185, Jan. 2021, doi: 10.1016/j.camwa.2020.05.014.
- [39] M. H. Raoufi, A. Farasat, and M. Mohammadifard, “Application of simulated annealing optimization algorithm to optimal operation of intelligent well completions in an offshore oil reservoir,” *J Pet Explor Prod Technol*, vol. 5, no. 3, pp. 327–338, Sep. 2015, doi: 10.1007/s13202-014-0142-x.
- [40] Schlumberger, *ECLIPSE Technical Description*. 2020.
- [41] M. R. Todd and W. J. Longstaff, “The Development, Testing, and Application Of a Numerical Simulator for Predicting Miscible Flood Performance,” *Journal of Petroleum Technology*, vol. 24, no. 7, Jul. 1972, doi: <https://doi.org/10.2118/3484-PA>.
- [42] N. Zhang, Y. An, and R. Huo, “Research on Production Performance Prediction Model of Horizontal Wells Completed with AICDs in Bottom Water Reservoirs,” *Energies (Basel)*, vol. 16, no. 6, Mar. 2023, doi: 10.3390/en16062602.
- [43] A. Moradi and B. M. E. Moldestad, “Near-well simulation of oil production from a horizontal well with ICD and AICD completions in the Johan Sverdrup field using OLGA/ROCX,” in *Proceedings of The 61st SIMS Conference on Simulation and Modelling SIMS 2020, September 22-24, Virtual Conference, Finland*, Linköping University Electronic Press, Mar. 2021, pp. 249–256. doi: 10.3384/ecp20176249.

- [44] Petrofaq, "Eclipse Input Data," Petrofaq. Accessed: Apr. 21, 2024. [Online]. Available: http://petrofaq.org/wiki/Eclipse_Input_Data
- [45] A. Moradi, A. S. Kumara, and B. M. E. Moldestad, "DEVELOPMENT OF DYNAMIC FULLY INTEGRATED WELL-RESERVOIR MODELS FOR SIMULATION OF OIL RECOVERY THROUGH ADVANCED WELLS."
- [46] P. Pourafshary, I. Al Khanbashi, and N. Mosavat, "Effect of Water/CO₂ Ratio on Performance of CO-Based EOR in a Sandstone Reservoir –Insights from Core Flood Tests and Simulations," in *SPE Gas & Oil Technology Showcase and Conference*, Dubai: Society of Petroleum Engineers, Oct. 2019. doi: <https://doi.org/10.2118/198624-MS>.
- [47] T. Ellis *et al.*, "Inflow control devices - Raising profiles," *ResearchGate*, vol. 21, pp. 30–37, Dec. 2009.
- [48] Minulina Polina, Al-Sharif Shahin, Zeito George, and Bouchard Michel, "The Design, Implementation and Use of Inflow Control Devices for Improving the Production Performance of Horizontal Wells," May 2012, doi: <https://doi.org/10.2118/157453-MS>.
- [49] Inflow Control, *InflowControl's Autonomous Inflow Control Valve - AICV®*. Accessed: May 06, 2024. [Online Video]. Available: <https://www.youtube.com/watch?v=7vmSTix9uiQ>

Appendices

Appendix A: Thesis task description

Appendix B: ECLIPSE data file for PUNQ-S3 reservoir model

Appendix C: Known variables for algebraic controller

Appendix D: OLGA model with OPENHOLE/ICD and AICD

Appendix A: Thesis task description



Faculty of Technology, Natural Sciences and Maritime Sciences, Campus Porsgrunn

FMH606 Master's Thesis

Title: Modeling and simulation of oil recovery through advanced multilateral wells with CO₂-WAG injection

USN supervisor: Prof. Britt M. E. Moldestad and Ali Moradi

External partner: Equinor and SINTEF

Task background:

Norwegian Continental Shelf (NCS) is one of the most technologically advanced petroleum regions in the world and has great potential to supply petroleum to the global market. To secure the competitiveness of the NCS in the international market, OG21 (Oil and gas for the 21st century) has developed a national technology strategy for guiding research efforts in the field of petroleum technology. The main strategic objective of OG21 is to obtain efficient, secure, and environmentally friendly value creation from the Norwegian oil and gas resources for several generations.

In line with the OG21 strategy, in collaboration with Equinor and SINTEF, there is an ongoing research project called *DigiWell* (*digital wells for optimal production and drainage*) at USN. The project aims at developing new methods, algorithms, and tools for the prediction of oil production under uncertain conditions in order to maximize profit margins by minimizing production costs. As part of this project, it is of great interest to model and evaluate the performance of advanced multilateral wells with the goal of improving oil recovery.

Extraction of oil from a reservoir starts by drilling a well into the oil zone. If the initial pressure inside the reservoir is sufficiently high, it will push oil up to the surface which is referred as primary production (see Figure 1 for further details). As the oleic phase is produced, the pressure inside the reservoir will decline. Therefore, other mechanisms like gas or water injection are used for maintaining pressure and producing more oil from the reservoir. This production method is called secondary production (see Figure 2 for further details).



Figure 1. Primary oil production

Figure 2. Secondary oil production

Enhanced oil recovery (EOR) or tertiary recovery, is the extraction of crude oil from an oil field by increasing the mobility of the oil. Miscible water alternating gas injection with CO₂ (CO₂-WAG injection) can be used as an effective EOR method. By dissolving oil and CO₂ in each other, a single-phase fluid with lower viscosity is formed. This can help the oil to be displaced more easily from the reservoir pore to the surface. Besides, by alternating injection of CO₂ and water, the CO₂ consumption can be reduced while also the benefits of water injection

like displacement and pressure support are provided. From an environmental point of view, this method can be combined with carbon capture projects as an effective solution for preserving the environment. Figure 3 illustrates the improvement in the sweeping efficiency with miscible WAG injection compared to the gas injection.

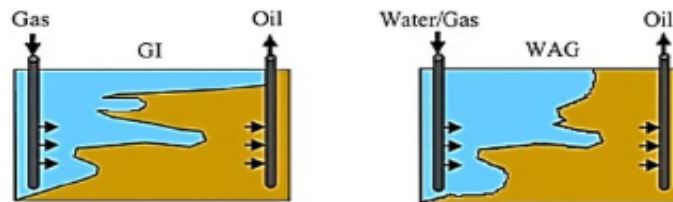


Figure 3: Comparison of oil displacement by gas injection and water alternating gas injection.

One of the main principles for achieving cost-effective and efficient oil recovery is maximizing the well-reservoir contact by using long horizontal wells. One of the main challenges of using such wells is early gas and/or water breakthrough due to the heel-toe effect and heterogeneity along the horizontal wells after applying EOR methods. To tackle this problem, Advanced (smart or intelligent) Multilateral Wells (AMWs) are widely applied today. The term “advanced” refers to horizontal wells completed with downhole Flow Control Devices (FCDs), Sand Control Screens (SCSs), Annular Flow Isolation (AFI), as well as other equipment such as sensors, downhole pumps and separators, etc. Figure 4 illustrates the schematic of AMW completions.

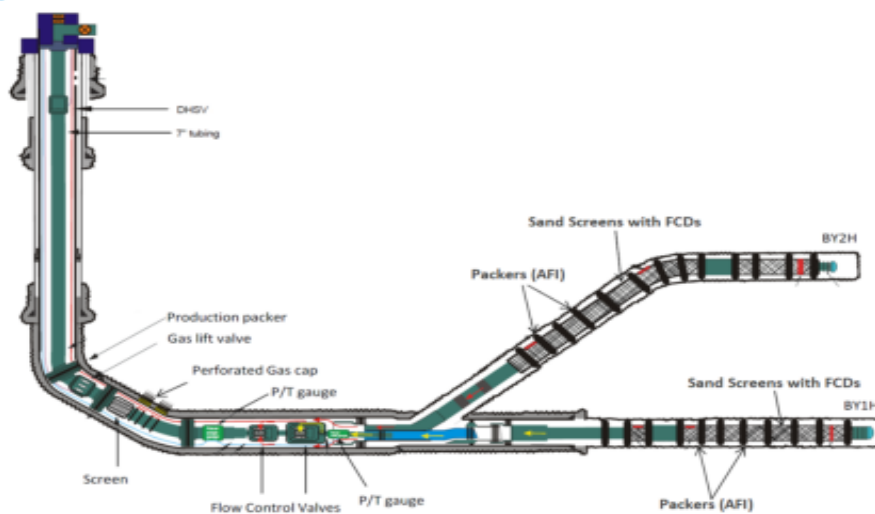


Figure 4. Schematic of advanced multilateral well completions.

The drilling and completion costs of AMWs are much higher compared to those of conventional wells. As a result, a significant improvement in economic recovery is required to justify their utilization. The results of reservoir simulations are crucial to making this judgment. The simulation model needs to reliably predict the performance of AMWs across the lifespan of the reservoir in order to deliver meaningful results. The goal of this project is to generate more insight into the long-term performance of AMWs in EOR with CO₂-WAG injection by developing accurate dynamic simulation models.

Task description:

The objective of this research project can be achieved by completing the following tasks:

1. Literature study

- Enhanced oil recovery with CO₂-WAG injection
 - Advanced multilateral wells
2. Developing suitable models for the simulation of oil recovery through AMWs
 - OLGA which is a dynamic multiphase flow simulator in combination with ECLIPSE which is a reservoir simulator should be used for this purpose.
 3. Evaluating the performance of AMWs
 - The performance of AMWs completed with different types of FCDs as well as AFI in the PUNQ-S3 reservoir with CO₂-WAG injection should be analyzed.
 4. If time permits, preparing a paper based on the results for the next SIMS conference is highly appreciated.

Student category: EET and PT students

Is the task suitable for online students (not present at the campus)? No

Practical arrangements: Necessary software will be provided by USN.

Supervision:

As a general rule, the student is entitled to 15-20 hours of supervision. This includes necessary time for the supervisor to prepare for supervision meetings (reading material to be discussed, etc).

Signatures:

Supervisor (date and signature):

Student (write clearly in all capitalized letters):

Student (date and signature):

Appendix B: ECLIPSE data file for PUNQ-S3 reservoir model

MESSAGES

3* 10000 5* 10000 /

WELLDIMS

20 40 2 20 /

--WSEGDIMS

-- 2 50 50 50 /

AQUDIMS

2 2 2 50 2 200 /

TABDIMS

1* 1* 40 40 /

NUPCOL

100 /

NSTACK

100 /

--NOSIM

UNIFIN

UNIFOUT

GRID

=====

INIT

-- put in your PORO, PERMX and PERMZ

INCLUDE

'PUNQS3.PRP'

/

COPY

'PERMX' 'PERMY' /

/

-- get corner point geometry

INCLUDE

'PUNQS3.GEO'

/

PROPS

=====

-- RELATIVE PERMEABILITY AND CAPPILARY PRESSURE CURVES

SWFN

0.2 0.0 0.0

0.3 0.00024 0.0

0.4 0.0039 0.0

0.5 0.02 0.0

0.6 0.062 0.0

0.7 0.152 0.0

0.8 0.316 0.0

0.9 0.585 0.0

1.0 1.0 0.0

/

SOF2

0.1 0.0

0.2 0.018

0.3 0.073

0.4 0.165

0.5 0.294

0.6 0.459

0.7 0.661

0.8 0.9

/

SOF3

0.1 0.0 0.0

0.2 0.018 0.0

0.3 0.073 0.025

0.4 0.165 0.1

0.5 0.294 0.225

0.6 0.459 0.4

0.7 0.661 0.625

0.8 0.9 0.9

/

SGFN

0.0 0.0 0.0

0.1 0.00000077 0.0

0.2 0.000049 0.0

0.3 0.00056 0.0

0.4 0.0032 0.0

0.5 0.012 0.0

0.6 0.036 0.0

0.7 0.091 0.0

0.8 0.2 0.0

/

-- This part is for keywords related to CO2-miscible flooding

-- From SPE9_CP_SOLVENT_CO2: This keyword to treat gas-solvent fraction for permeability

SSFN

0.0 0.0 0.0

0.5 0.4 0.8

1.0 1.0 1.0

/

-- This keyword is added for defining the transition algorithm from miscible to immiscible

-- and the values is obtained for Eclipse reference manual

MISC

0.0 0.0

0.1 0.5

0.3 1.0

1.0 1.0 /

TLMIXPAR

1 /

-- This value is taken from the SPE9_CP_SOLVENT_CO2

SDENSITY

2 /

-- This values is taken from the SPE9_CP_SOLVENT_CO2

PVDS

80 0.00550 0.0265

87 0.00326 0.0460

95 0.00296 0.0529

102 0.00282 0.0572

109 0.00273 0.0605

117 0.00266 0.0632

124 0.00261 0.0656

131 0.00256 0.0678

139 0.00252 0.0698

146	0.00249	0.0716
153	0.00246	0.0733
161	0.00243	0.0750
168	0.00241	0.0765
175	0.00238	0.0780
183	0.00236	0.0795
190	0.00235	0.0808
197	0.00233	0.0822
205	0.00231	0.0835
212	0.00230	0.0847
219	0.00228	0.0860
227	0.00227	0.0872
234	0.00225	0.0883
241	0.00224	0.0895
249	0.00223	0.0906
256	0.00222	0.0917
263	0.00221	0.0928
271	0.00220	0.0939
278	0.00219	0.0949
285	0.00218	0.0960
293	0.00217	0.0970
300	0.00216	0.0980 /

-- PVT DATA

PVTO

11.460	40.000	1.064	4.338 /
17.890	60.000	1.078	3.878 /
24.320	80.000	1.092	3.467 /
30.760	100.000	1.106	3.100 /
37.190	120.000	1.120	2.771 /
43.620	140.000	1.134	2.478 /

46.840	150.000	1.141	2.343	/
50.050	160.000	1.148	2.215	/
53.270	170.000	1.155	2.095	/
56.490	180.000	1.162	1.981	/
59.700	190.000	1.169	1.873	/
62.920	200.000	1.176	1.771	/
66.130	210.000	1.183	1.674	/
69.350	220.000	1.190	1.583	/
72.570	230.000	1.197	1.497	/
74.000	234.460	1.200	1.460	
	250.000	1.198	1.541	
	300.000	1.194	1.787	/
80.000	245.000	1.220	1.400	
	300.000	1.215	1.700	/

/

PVDG

40.00	0.02908	0.00880	
60.00	0.01886	0.00920	
80.00	0.01387	0.00960	
100.00	0.01093	0.01000	
120.00	0.00899	0.01040	
140.00	0.00763	0.01090	
150.00	0.00709	0.01110	
160.00	0.00662	0.01140	
170.00	0.00620	0.01160	
180.00	0.00583	0.01190	
190.00	0.00551	0.01210	
200.00	0.00521	0.01240	
210.00	0.00495	0.01260	
220.00	0.00471	0.01290	
230.00	0.00449	0.01320	
234.46	0.00440	0.01330	

/

DENSITY

912.0 1000.0 0.8266

/

PVTW

234.46 1.0042 5.43E-05 0.5 1.11E-04 /

-- ROCK COMPRESSIBILITY

--

-- REF. PRES COMPRESSIBILITY

ROCK

235 0.00045 /

STONE1

ECHO

SOLUTION

=====

AQUCT

1 2355 234 137.5 0.2125 3.5E-05 3000 19.6 95 1 1 /

2 2355 234 137.5 0.2125 3.5E-05 3200 6.0 95 1 1 /

/

AQUANCON

1 14 14 4 4 5 5 'I-' 1180.7 /

1 15 15 4 4 5 5 'J-' 1186.7 /

1 16 16 4 4 5 5 'J-' 1189.7 /

1 17 17 4 4 5 5 'J-' 1197.7 /

1 18 18 4 4 5 5 'I-' 1204.3 /

1 12 12 5 5 5 5 'I+' 1094.6 /

1 13 13 5 5 5 5 'I-' 1115.7 /

1 11 11 6 6 5 5 'J-' 1031.0 /

1 10 10 7 7 5 5 'I-' 999.6 /

1 9 9 8 8 5 5 'I-' 983.6 /

1 8 8 9 9 5 5 'I-' 987.8 /
 1 7 7 10 10 5 5 'I-' 1001.5 /
 1 6 6 11 11 5 5 'I-' 1005.3 /
 1 6 6 12 12 5 5 'I-' 966.6 /
 1 5 5 13 13 5 5 'I-' 911.7 /
 1 5 5 14 14 5 5 'I-' 877.4 /
 1 4 4 15 15 5 5 'I-' 835.6 /
 1 4 4 16 16 5 5 'I-' 819.1 /
 1 3 3 17 17 5 5 'I-' 755.5 /
 1 3 3 18 18 5 5 'I-' 720.2 /
 1 3 3 19 19 5 5 'I-' 673.3 /
 1 3 3 20 20 5 5 'I-' 633.9 /
 1 3 3 21 21 5 5 'I-' 596.0 /
 1 3 3 22 22 5 5 'I-' 607.8 /
 1 3 3 23 23 5 5 'I-' 614.3 /
 1 3 3 24 24 5 5 'I-' 598.3 /
 1 3 3 25 25 5 5 'I-' 460.6 /
 1 4 4 26 26 5 5 'I-' 153.2 /
 1 5 5 26 26 5 5 'J+' 256.8 /
 1 6 6 27 27 5 5 'I-' 251.4 /
 1 7 7 27 27 5 5 'J+' 255.2 /
 1 8 8 27 27 5 5 'J+' 247.2 /
 1 9 9 27 27 5 5 'J+' 232.8 /
 1 10 10 27 27 5 5 'J+' 227.4 /
 1 11 11 27 27 5 5 'J+' 222.8 /
 1 12 12 27 27 5 5 'I+' 223.2 /

 1 14 14 4 4 4 4 'I-' 1180.7 /
 1 15 15 4 4 4 4 'J-' 1186.7 /
 1 16 16 4 4 4 4 'J-' 1189.7 /
 1 17 17 4 4 4 4 'J-' 1197.7 /
 1 18 18 4 4 4 4 'I-' 1204.3 /
 1 12 12 5 5 4 4 'I+' 1094.6 /
 1 13 13 5 5 4 4 'I-' 1115.7 /

1 11 11 6 6 4 4 'J-' 1031.0 /
 1 10 10 7 7 4 4 'I-' 999.6 /
 1 9 9 8 8 4 4 'I-' 983.6 /
 1 8 8 9 9 4 4 'I-' 987.8 /
 1 7 7 10 10 4 4 'I-' 1001.5 /
 1 6 6 11 11 4 4 'I-' 1005.3 /
 1 6 6 12 12 4 4 'I-' 966.6 /
 1 5 5 13 13 4 4 'I-' 911.7 /
 1 5 5 14 14 4 4 'I-' 877.4 /
 1 4 4 15 15 4 4 'I-' 835.6 /
 1 4 4 16 16 4 4 'I-' 819.1 /
 1 3 3 17 17 4 4 'I-' 755.5 /
 1 3 3 18 18 4 4 'I-' 720.2 /
 1 3 3 19 19 4 4 'I-' 673.3 /
 1 3 3 20 20 4 4 'I-' 633.9 /
 1 3 3 21 21 4 4 'I-' 596.0 /
 1 3 3 22 22 4 4 'I-' 607.8 /
 1 3 3 23 23 4 4 'I-' 614.3 /
 1 3 3 24 24 4 4 'I-' 598.3 /
 1 3 3 25 25 4 4 'I-' 733.9 /
 1 4 4 26 26 4 4 'I-' 303.9 /
 1 5 5 26 26 4 4 'J+' 256.8 /
 1 6 6 27 27 4 4 'I-' 251.4 /
 1 7 7 27 27 4 4 'J+' 255.2 /
 1 8 8 27 27 4 4 'J+' 247.2 /
 1 9 9 27 27 4 4 'J+' 232.8 /
 1 10 10 27 27 4 4 'J+' 227.4 /
 1 11 11 27 27 4 4 'J+' 222.8 /
 1 12 12 27 27 4 4 'I+' 223.2 /

 1 14 14 4 4 3 3 'I-' 1180.7 /
 1 15 15 4 4 3 3 'J-' 1186.7 /
 1 16 16 4 4 3 3 'J-' 1189.7 /
 1 17 17 4 4 3 3 'J-' 1197.7 /

1 18 18 4 4 3 3 'I-' 1204.3 /
 1 12 12 5 5 3 3 'I+' 1094.6 /
 1 13 13 5 5 3 3 'I-' 1115.7 /
 1 11 11 6 6 3 3 'J-' 1031.0 /
 1 10 10 7 7 3 3 'I-' 999.6 /
 1 9 9 8 8 3 3 'I-' 983.6 /
 1 8 8 9 9 3 3 'I-' 987.8 /
 1 7 7 10 10 3 3 'I-' 1001.5 /
 1 6 6 11 11 3 3 'I-' 1005.3 /
 1 6 6 12 12 3 3 'I-' 966.6 /
 1 5 5 13 13 3 3 'I-' 911.7 /
 1 5 5 14 14 3 3 'I-' 877.4 /
 1 4 4 15 15 3 3 'I-' 835.6 /
 1 4 4 16 16 3 3 'I-' 819.1 /
 1 3 3 17 17 3 3 'I-' 755.5 /
 1 3 3 18 18 3 3 'I-' 720.2 /
 1 3 3 19 19 3 3 'I-' 673.3 /
 1 3 3 20 20 3 3 'I-' 633.9 /
 1 3 3 21 21 3 3 'I-' 596.0 /
 1 3 3 22 22 3 3 'I-' 607.8 /
 1 3 3 23 23 3 3 'I-' 614.3 /
 1 3 3 24 24 3 3 'I-' 598.3 /
 1 3 3 25 25 3 3 'I-' 733.9 /
 1 4 4 26 26 3 3 'I-' 303.9 /
 1 5 5 26 26 3 3 'J+' 256.8 /
 1 6 6 27 27 3 3 'I-' 251.4 /
 1 7 7 27 27 3 3 'J+' 255.2 /
 1 8 8 27 27 3 3 'J+' 247.2 /
 1 9 9 27 27 3 3 'J+' 232.8 /
 1 10 10 27 27 3 3 'J+' 227.4 /
 1 11 11 27 27 3 3 'J+' 222.8 /
 1 12 12 27 27 3 3 'I+' 223.2 /

 2 15 15 1 1 2 2 'I-' 979.0 /

2 16 16 1 1 2 2 'J-' 963.7 /
 2 17 17 1 1 2 2 'J-' 940.0 /
 2 18 18 1 1 2 2 'I+' 904.5 /
 2 14 14 2 2 2 2 'I-' 860.9 /
 2 11 11 3 3 2 2 'I-' 665.4 /
 2 12 12 3 3 2 2 'J-' 657.5 /
 2 13 13 3 3 2 2 'J-' 652.0 /
 2 10 10 4 4 2 2 'I-' 586.0 /
 2 9 9 5 5 2 2 'I-' 620.4 /
 2 8 8 6 6 2 2 'I-' 743.0 /
 2 7 7 7 7 2 2 'I-' 213.5 /
 2 6 6 8 8 2 2 'I-' 284.7 /
 2 6 6 9 9 2 2 'I-' 366.6 /
 2 5 5 10 10 2 2 'I-' 395.4 /
 2 5 5 11 11 2 2 'I-' 464.4 /
 2 5 5 12 12 2 2 'I-' 504.3 /
 2 4 4 13 13 2 2 'I-' 553.3 /
 2 4 4 14 14 2 2 'I-' 595.7 /
 2 3 3 15 15 2 2 'I-' 716.9 /
 2 2 2 16 16 2 2 'I-' 583.6 /
 2 2 2 17 17 2 2 'I-' 576.6 /
 2 2 2 18 18 2 2 'I-' 518.7 /
 2 1 1 23 23 2 2 'I-' 750.1 /
 2 1 1 24 24 2 2 'I-' 767.4 /
 2 1 1 25 25 2 2 'I-' 698.9 /
 2 2 2 26 26 2 2 'I-' 721.1 /
 2 3 3 27 27 2 2 'I-' 666.0 /
 2 4 4 28 28 2 2 'I-' 644.2 /
 2 5 5 28 28 2 2 'J+' 743.7 /

 2 15 15 1 1 1 1 'I-' 1958.0 /
 2 16 16 1 1 1 1 'J-' 1927.4 /
 2 17 17 1 1 1 1 'J-' 1880.5 /
 2 18 18 1 1 1 1 'I+' 1809.0 /

2 14 14 2 2 1 1 'I-' 1721.9 /
 2 11 11 3 3 1 1 'I-' 1330.8 /
 2 12 12 3 3 1 1 'J-' 1315.0 /
 2 13 13 3 3 1 1 'J-' 1303.9 /
 2 10 10 4 4 1 1 'I-' 1172.1 /
 2 9 9 5 5 1 1 'I-' 1240.8 /
 2 8 8 6 6 1 1 'I-' 1486.0 /
 2 7 7 7 7 1 1 'I-' 1222.1 /
 2 6 6 8 8 1 1 'I-' 1242.7 /
 2 6 6 9 9 1 1 'I-' 1171.9 /
 2 5 5 10 10 1 1 'I-' 988.7 /
 2 5 5 11 11 1 1 'I-' 961.8 /
 2 5 5 12 12 1 1 'I-' 1022.0 /
 2 4 4 13 13 1 1 'I-' 1110.6 /
 2 4 4 14 14 1 1 'I-' 1189.5 /
 2 3 3 15 15 1 1 'I-' 1131.3 /
 2 2 2 16 16 1 1 'I-' 1350.2 /
 2 2 2 17 17 1 1 'I-' 1491.5 /
 2 2 2 18 18 1 1 'I-' 1442.2 /
 2 1 1 23 23 1 1 'I-' 1167.1 /
 2 1 1 24 24 1 1 'I-' 1253.7 /
 2 1 1 25 25 1 1 'I-' 1306.9 /
 2 2 2 26 26 1 1 'I-' 1183.3 /
 2 3 3 27 27 1 1 'I-' 1070.9 /
 2 4 4 28 28 1 1 'I-' 1179.4 /
 2 5 5 28 28 1 1 'J+' 1260.5 /
 /

-- DATUM DATUM OWC OWC GOC GOC RSVD RVVD SOLN
 -- DEPTH PRESS DEPTH PCOW DEPTH PCOG TABLE TABLE METH
 EQUIL
 2355.00 234.46 2395.0 0.00 2355.0 0.000 1 1* 0 /

RSVD

2175 74.00
2496 74.00 /

RPTRST

PRE SWAT SGAS SOIL SSOL RS DEN

VISC

BO BG BW

KRG KRO KRW

PCOW PCOG /

RPTSOL

PRE SWAT SGAS SOIL SSOL RS DEN

VISC

BO BG BW

KRG KRO KRW

PCOW PCOG /

SUMMARY

FOE

FOPR

FWPR

FGPR

FLPR

FWIR

FOPT

FWPT

FGPT

FLPT

FWIT

FWCT

FGOR

FGIR

FGIT

WBHP

'PROD'

'INJ1'

'INJ2'

'INJ3'

'INJ4'

/

WOPR

'PROD' /

WWPR

'PROD' /

WGPR

'PROD' /

WWCT

'PROD' /

WOPT

'PROD' /

WWPT

'PROD' /

WGPT

'PROD' /

WLPR

'PROD' /

WLPT

'PROD' /

WGOR

'PROD' /

WGOT

'PROD' /

FNPR

'PROD' /

FNPT

'PROD' /

WWIR

'INJ1'

'INJ2'

'INJ3'

'INJ4'

/

WGIR

'INJ1'

'INJ2'

'INJ3'

'INJ4'

/

FNIR

'INJ1'

'INJ2'

'INJ3'

'INJ4'

/

RUNSUM

SEPARATE

SCHEDULE

RPTSCHED

'PRES' 'SWAT' 'SGAS' 'RESTART=1' 'RS' 'WELLS=2' 'SUMMARY=2'
'CPU=2' 'WELSPECS' 'NEWTON=2' /

----- WELL SPECIFICATION DATA -----

WELSPECS

-- WELL- GROUP- WELLHEAD(HEEL) REF. DEPTH- PREFERRED- DRAINAGE-
-- NAME NAME I LOC. J LOC. FOR BHP PHASE WELL REDIUS
'PROD' 'G' 8 26 2380 'OIL' 0.0 'STD' 'STOP' 'YES' 0 'AVG' 0 /
'INJ1' 'G_INJ' 19 7 2390 'WAT' 0.0 'STD' 'STOP' 'YES' 0 'AVG' 0 /
'INJ2' 'G_INJ' 19 14 2375 'WAT' 0.0 'STD' 'STOP' 'YES' 0 'AVG' 0 /
'INJ3' 'G_INJ' 19 20 2370 'WAT' 0.0 'STD' 'STOP' 'YES' 0 'AVG' 0 /
'INJ4' 'G_INJ' 16 25 2370 'WAT' 0.0 'STD' 'STOP' 'YES' 0 'AVG' 0 /
/

COMPDAT

-- CONNECTIONS TO ANNULUS

'PROD' 8 26 1 1 3* 0.216 3* 'Y' /
'PROD' 8 25 1 1 3* 0.216 3* 'Y' /
'PROD' 8 24 1 1 3* 0.216 3* 'Y' /
'PROD' 8 23 1 1 3* 0.216 3* 'Y' /
'PROD' 8 22 1 1 3* 0.216 3* 'Y' /
'PROD' 8 21 1 1 3* 0.216 3* 'Y' /
'PROD' 8 20 1 1 3* 0.216 3* 'Y' /
'PROD' 8 19 1 1 3* 0.216 3* 'Y' /
'PROD' 8 18 1 1 3* 0.216 3* 'Y' /
'PROD' 8 17 1 1 3* 0.216 3* 'Y' /
'PROD' 8 16 1 1 3* 0.216 3* 'Y' /
'PROD' 8 15 1 1 3* 0.216 3* 'Y' /
'PROD' 8 14 1 1 3* 0.216 3* 'Y' /
'PROD' 8 13 1 1 3* 0.216 3* 'Y' /
'PROD' 8 12 1 1 3* 0.216 3* 'Y' /
'PROD' 8 11 1 1 3* 0.216 3* 'Y' /
'PROD' 8 10 1 1 3* 0.216 3* 'Y' /

'PROD' 8 9 1 1 3* 0.216 3* 'Y' /

'INJ1' 19 7 1 2 3* 0.216 3* 'Z' /

'INJ2' 19 14 1 5 3* 0.216 3* 'Z' /

'INJ3' 19 20 1 5 3* 0.216 3* 'Z' /

'INJ4' 16 25 1 5 3* 0.216 3* 'Z' /

/

WEFAC

'*' 1.0 /

/

WCONPROD

-- WELL- OPEN- CONTROL- OIL RATE- WAT. RATE- GAS RATE- LIQ.
RATE- RES. FLUID- BHP- THP-

-- NAME SHUT FLAG MODE TARGET TARGET TARGET TARGET
RATE TARGET TARGET TARGET

'PROD' 'OPEN' 'BHP' 1* 1* 1* 4000 1* 210 1*/

/

WCONINJE

'INJ1' 'WAT' 'OPEN' 'RATE' 250 1* 400 /

'INJ2' 'WAT' 'OPEN' 'RATE' 1250 1* 400 /

'INJ3' 'WAT' 'OPEN' 'RATE' 1250 1* 400 /

'INJ4' 'WAT' 'OPEN' 'RATE' 1250 1* 400 /

/

TSTEP

100*10 /

WCONINJE

'INJ1'	'GAS'	'OPEN'	'RATE'	80000	1*	400 /
'INJ2'	'GAS'	'OPEN'	'RATE'	200000	1*	400 /
'INJ3'	'GAS'	'OPEN'	'RATE'	200000	1*	400 /
'INJ4'	'GAS'	'OPEN'	'RATE'	200000	1*	400 /

/

WSOLVENT

'INJ1' 1/

'INJ2' 1/

'INJ3' 1/

'INJ4' 1/

/

TSTEP

50*10 /

WCONINJE

'INJ1'	'WAT'	'OPEN'	'RATE'	250	1*	400 /
'INJ2'	'WAT'	'OPEN'	'RATE'	1250	1*	400 /
'INJ3'	'WAT'	'OPEN'	'RATE'	1250	1*	400 /
'INJ4'	'WAT'	'OPEN'	'RATE'	1250	1*	400 /

/

TSTEP

50*10 /

WCONINJE

'INJ1'	'GAS'	'OPEN'	'RATE'	80000	1*	400 /
--------	-------	--------	--------	-------	----	-------

'INJ2'	'GAS'	'OPEN'	'RATE'	200000	1*	400 /
'INJ3'	'GAS'	'OPEN'	'RATE'	200000	1*	400 /
'INJ4'	'GAS'	'OPEN'	'RATE'	200000	1*	400 /

/

WSOLVENT

'INJ1' 1/

'INJ2' 1/

'INJ3' 1/

'INJ4' 1/

/

TSTEP

50*10 /

WCONINJE

'INJ1'	'WAT'	'OPEN'	'RATE'	250	1*	400 /
'INJ2'	'WAT'	'OPEN'	'RATE'	1250	1*	400 /
'INJ3'	'WAT'	'OPEN'	'RATE'	1250	1*	400 /
'INJ4'	'WAT'	'OPEN'	'RATE'	1250	1*	400 /

/

TSTEP

50*10 /

WCONINJE

'INJ1'	'GAS'	'OPEN'	'RATE'	80000	1*	400 /
'INJ2'	'GAS'	'OPEN'	'RATE'	200000	1*	400 /
'INJ3'	'GAS'	'OPEN'	'RATE'	200000	1*	400 /

'INJ4' 'GAS' 'OPEN' 'RATE' 200000 1* 400 /
/

WSOLVENT

'INJ1' 1/

'INJ2' 1/

'INJ3' 1/

'INJ4' 1/

/

TSTEP

50*10 /

WCONINJE

'INJ1' 'WAT' 'OPEN' 'RATE' 250 1* 400 /

'INJ2' 'WAT' 'OPEN' 'RATE' 1250 1* 400 /

'INJ3' 'WAT' 'OPEN' 'RATE' 1250 1* 400 /

'INJ4' 'WAT' 'OPEN' 'RATE' 1250 1* 400 /

/

TSTEP

50*10 /

WCONINJE

'INJ1' 'GAS' 'OPEN' 'RATE' 80000 1* 400 /

'INJ2' 'GAS' 'OPEN' 'RATE' 200000 1* 400 /

'INJ3' 'GAS' 'OPEN' 'RATE' 200000 1* 400 /

'INJ4' 'GAS' 'OPEN' 'RATE' 200000 1* 400 /

/

WSOLVENT

'INJ1' 1/

'INJ2' 1/

'INJ3' 1/

'INJ4' 1/

/

TSTEP

50*10 /

WCONINJE

'INJ1'	'WAT'	'OPEN'	'RATE'	250	1*	400 /
--------	-------	--------	--------	-----	----	-------

'INJ2'	'WAT'	'OPEN'	'RATE'	1250	1*	400 /
--------	-------	--------	--------	------	----	-------

'INJ3'	'WAT'	'OPEN'	'RATE'	1250	1*	400 /
--------	-------	--------	--------	------	----	-------

'INJ4'	'WAT'	'OPEN'	'RATE'	1250	1*	400 /
--------	-------	--------	--------	------	----	-------

//

TSTEP

50*10 /

WCONINJE

'INJ1'	'GAS'	'OPEN'	'RATE'	80000	1*	400 /
--------	-------	--------	--------	-------	----	-------

'INJ2'	'GAS'	'OPEN'	'RATE'	200000	1*	400 /
--------	-------	--------	--------	--------	----	-------

'INJ3'	'GAS'	'OPEN'	'RATE'	200000	1*	400 /
--------	-------	--------	--------	--------	----	-------

'INJ4'	'GAS'	'OPEN'	'RATE'	200000	1*	400 /
--------	-------	--------	--------	--------	----	-------

/

WSOLVENT

'INJ1' 1/

'INJ2' 1/

'INJ3' 1/

'INJ4' 1/

/

TSTEP

50*10 /

WCONINJE

'INJ1'	'WAT'	'OPEN'	'RATE'	250	1*	400 /
'INJ2'	'WAT'	'OPEN'	'RATE'	1250	1*	400 /
'INJ3'	'WAT'	'OPEN'	'RATE'	1250	1*	400 /
'INJ4'	'WAT'	'OPEN'	'RATE'	1250	1*	400 /

/

TSTEP

50*10 /

WCONINJE

'INJ1'	'GAS'	'OPEN'	'RATE'	80000	1*	400 /
'INJ2'	'GAS'	'OPEN'	'RATE'	200000	1*	400 /
'INJ3'	'GAS'	'OPEN'	'RATE'	200000	1*	400 /
'INJ4'	'GAS'	'OPEN'	'RATE'	200000	1*	400 /

/

WSOLVENT

'INJ1' 1/

'INJ2' 1/

'INJ3' 1/

'INJ4' 1/

/

TSTEP

50*10 /

WCONINJE

'INJ1'	'WAT'	'OPEN'	'RATE'	250	1*	400 /
'INJ2'	'WAT'	'OPEN'	'RATE'	1250	1*	400 /
'INJ3'	'WAT'	'OPEN'	'RATE'	1250	1*	400 /
'INJ4'	'WAT'	'OPEN'	'RATE'	1250	1*	400 /

//

TSTEP

50*10 /

WCONINJE

'INJ1'	'GAS'	'OPEN'	'RATE'	80000	1*	400 /
'INJ2'	'GAS'	'OPEN'	'RATE'	200000	1*	400 /
'INJ3'	'GAS'	'OPEN'	'RATE'	200000	1*	400 /
'INJ4'	'GAS'	'OPEN'	'RATE'	200000	1*	400 /

/

WSOLVENT

'INJ1' 1/

'INJ2' 1/

'INJ3' 1/

'INJ4' 1/

/

TSTEP

50*10 /

-- WSEGITER

-- 25 5 0.1 3.0 /

TUNING

1 1 /

/

2* 100 1* 16 /

END

Appendix C: Known variables for algebraic controller

$$C_D = 0.85, \dot{C}_u = 1.34 \cdot e^{-15}, a_{AICD} = 3.41 \cdot e^{-6}, \Delta P_{mix} = 20 \text{ bar},$$

$$A = \frac{\pi}{4} D^2 = \frac{\pi}{4} (0.002)^2 = 3.2687 \cdot e^{-5}$$

$$x = 3.35, y = 0.4, \mu_{oil} = 2.7, \mu_{water} = 0.45, \mu_{gas} = 0.02,$$

$$\rho_{oil} = 890 \text{ kg/m}^3, \rho_{water} = 1100 \text{ kg/m}^3, \mu_{gas} = 150 \text{ kg/m}^3$$

Appendix D: OLGA model with OPENHOLE/ICD and AICD



OLGA model for ICD (left) and AICD (right)